The CGM around Massive and Dwarf Galaxies in “Zoom-in” Simulations

Sijing Shen
IMPS Fellow, UC Santa Cruz

Higgs Center Workshop on the Intergalactic Medium
June 28, 2013

In collaboration w/: Piero Madau, Javiera Guedes (ETH), Anthony Aguirre, Jason X. Prochaska, James Wadsley (McMaster) & Lucio Mayer (Zurich)

Outline

- The CGM, gas flows and galaxy formation
- Cosmological "zoom-in" simulations of individual galaxies and their environment
- The simulated CGM of a massive galaxy:
  - Detailed comparison at z ~ 2-3 on spatial distribution & kinematics of H I and metal absorbers (Shen+ 2013)
  - The evolution of CGM until z = 0.6 (preliminary)
- The baryon cycle and the CGM of simulated dwarf galaxies
  - The galaxy properties, H I and metal distribution and evolution (Shen+, to be submitted)
  - *The "cusp-core" and "too big to fail" problem in dwarfs (optional)*
- The mixing of metals in galactic outflows (preliminary)

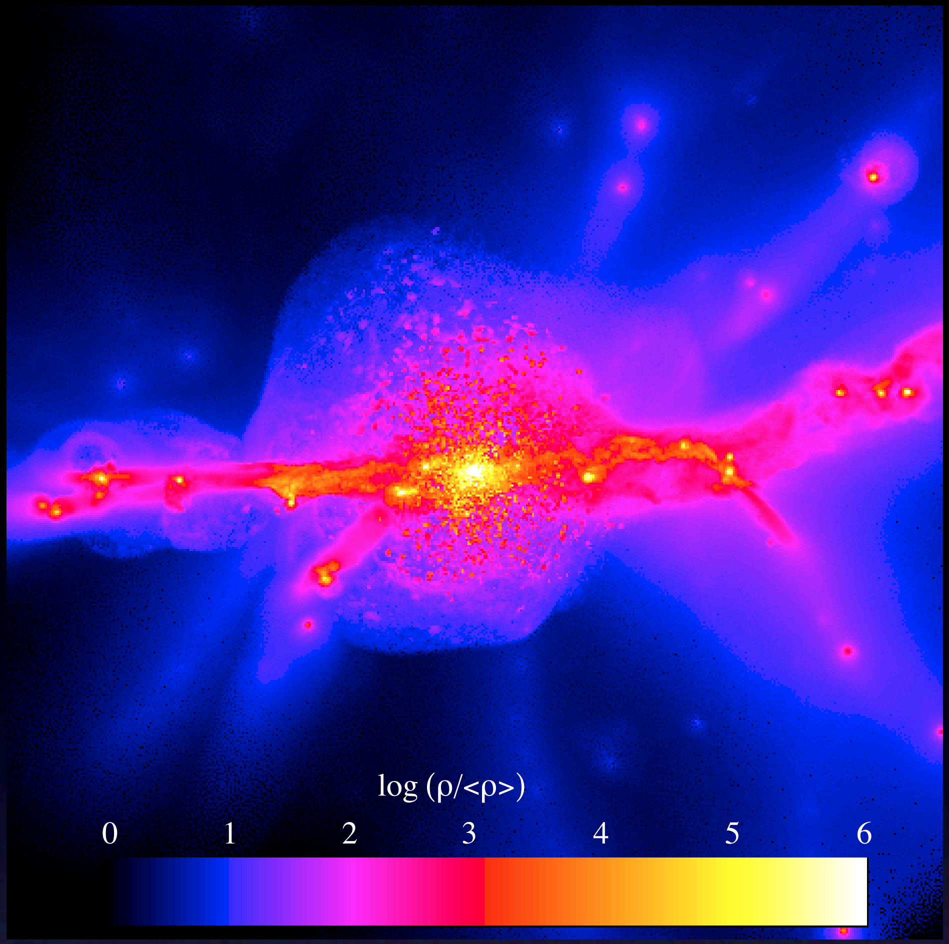
log (ρ/<ρ>)
0
1
2
3
4
5
6

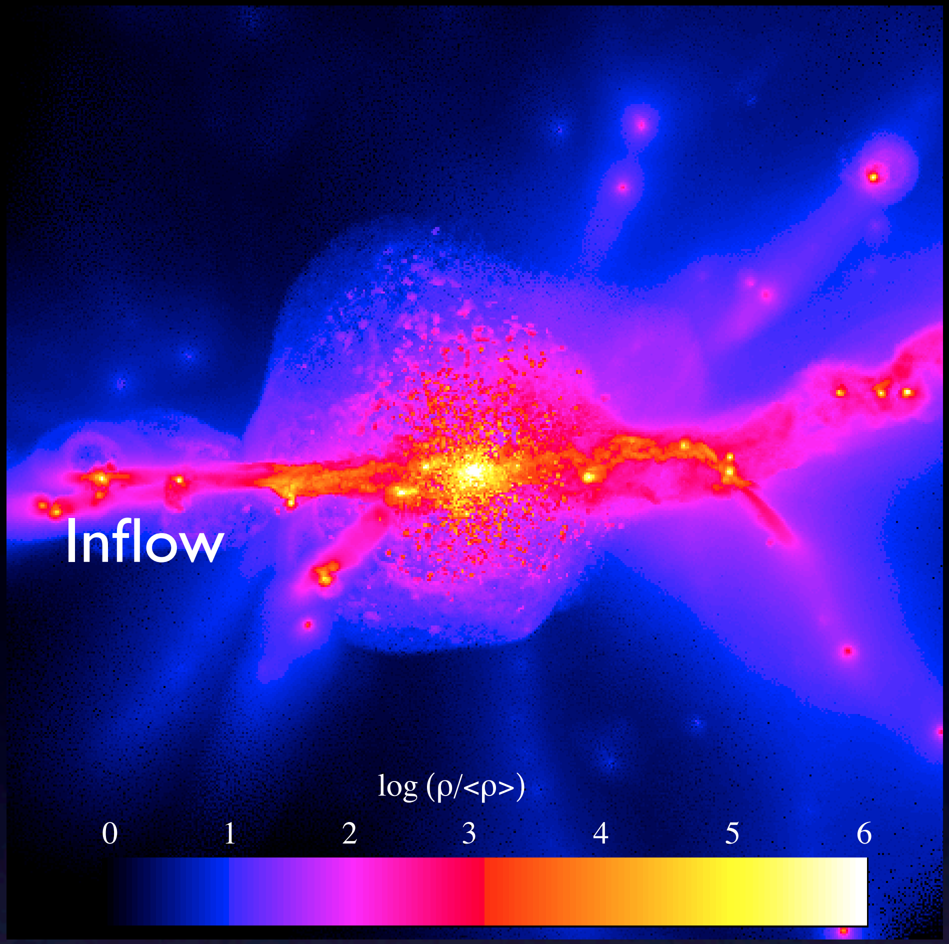
Inflow
log (ρ/<ρ>)
0 1 2 3 4 5 6

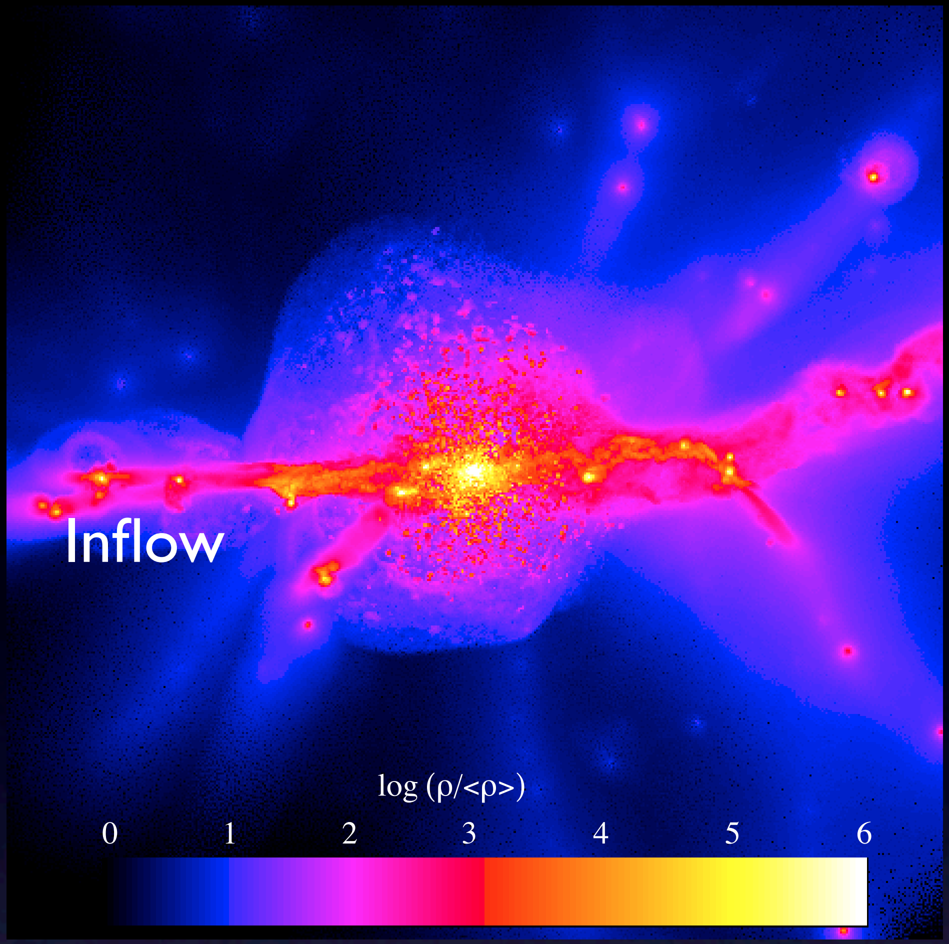

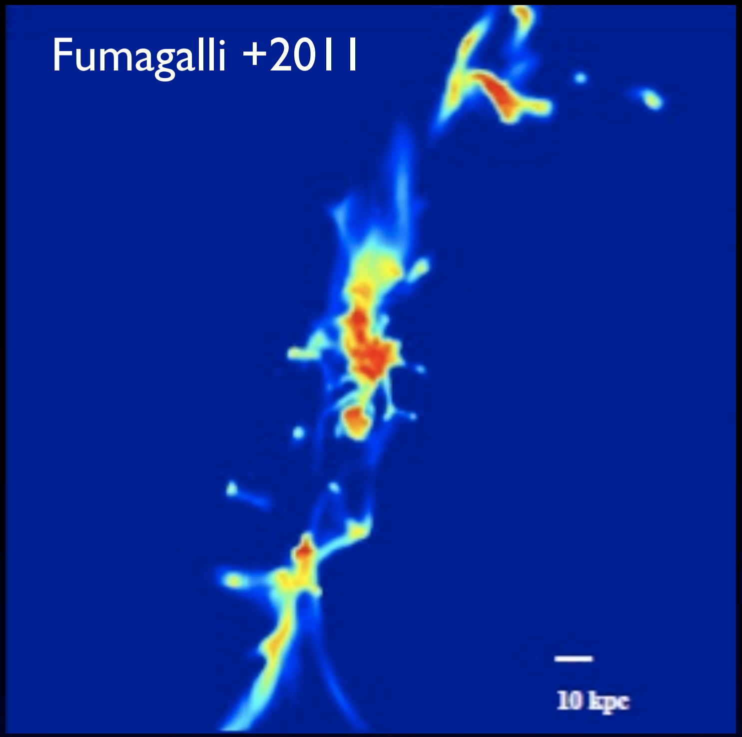

Can cold accretion flow be detected? What's the covering fraction? Are they enriched?

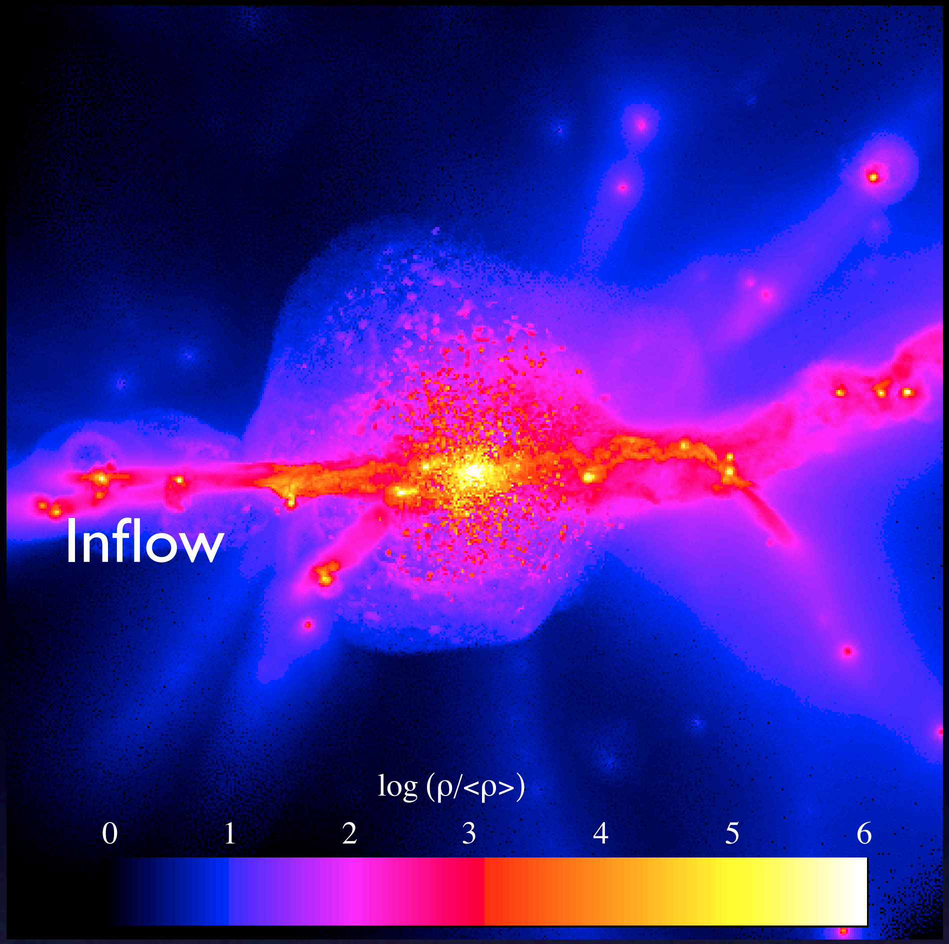

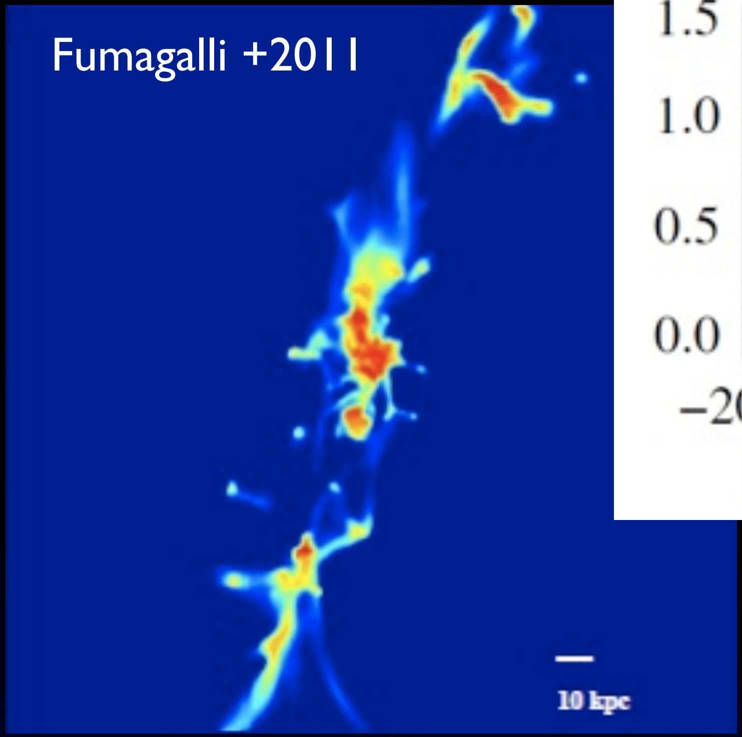

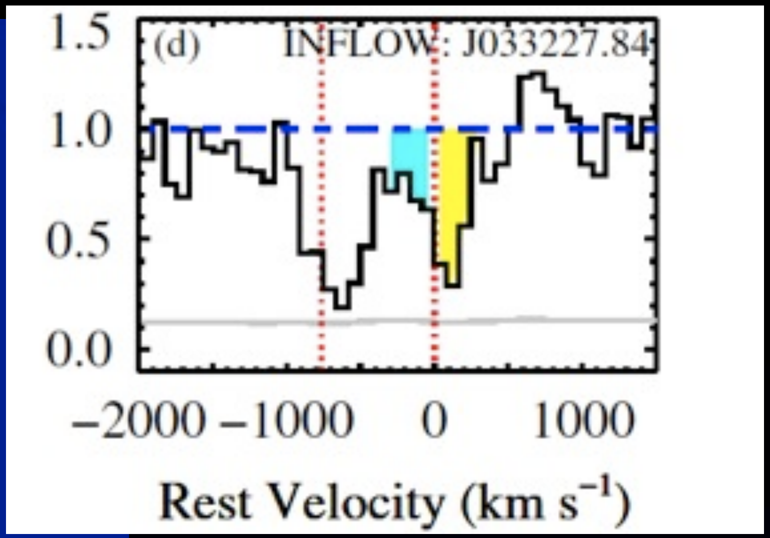

Rubin + 2012

Can cold accretion flow be detected? What's the covering fraction? Are they enriched?

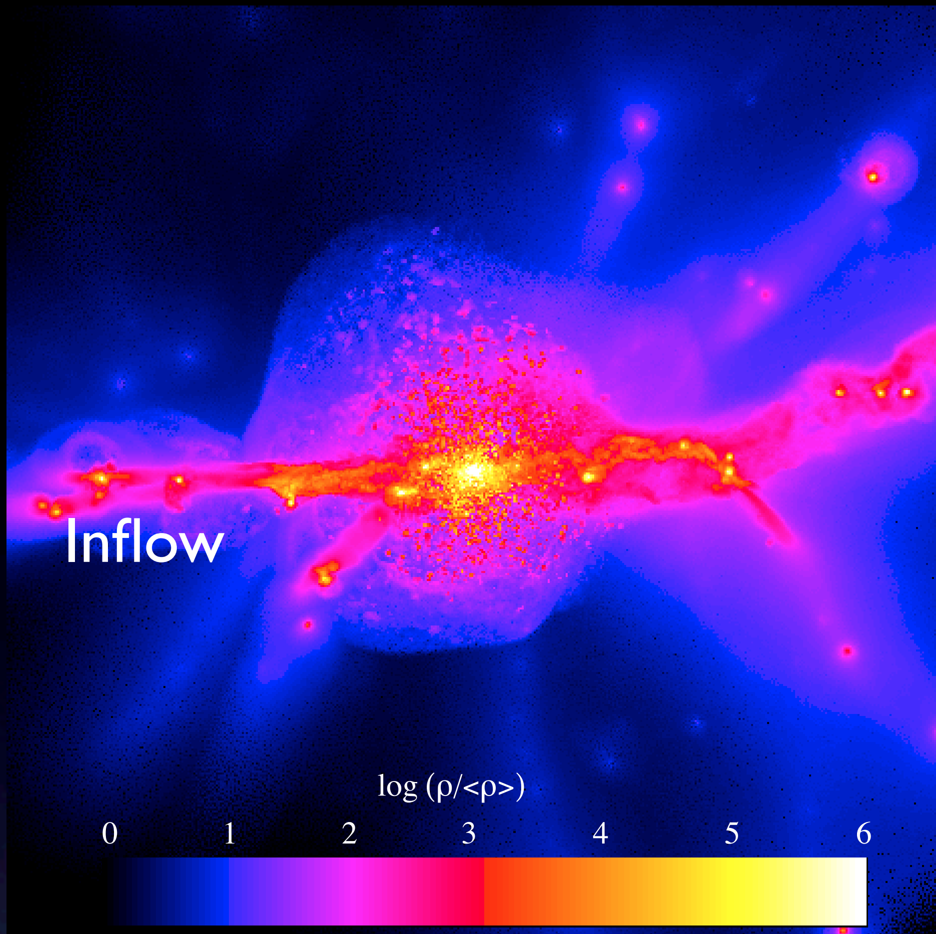

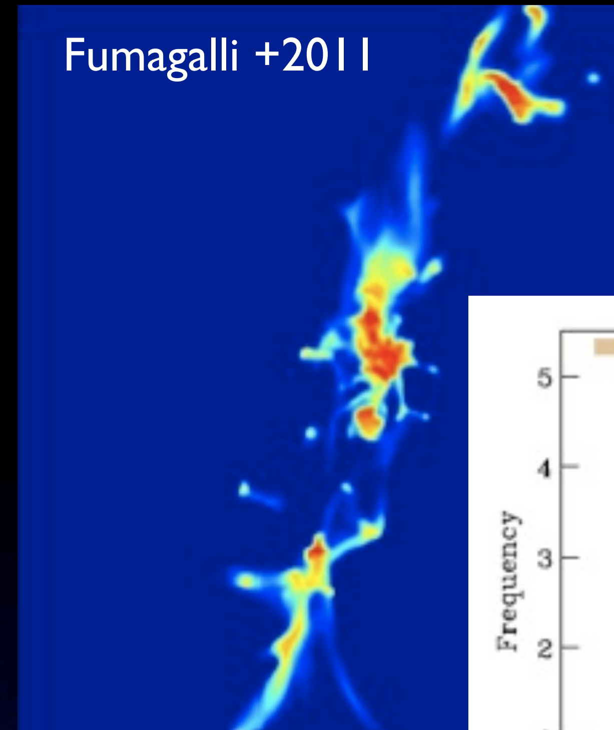

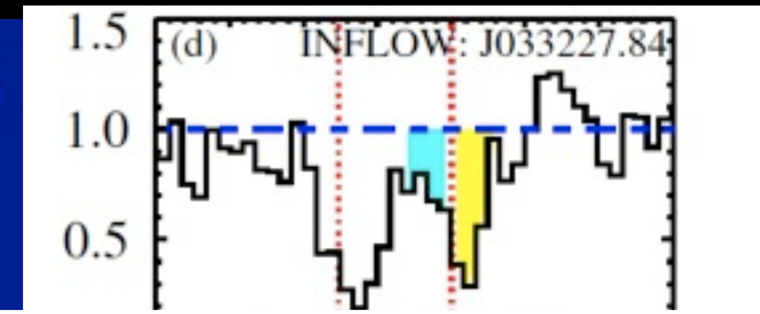

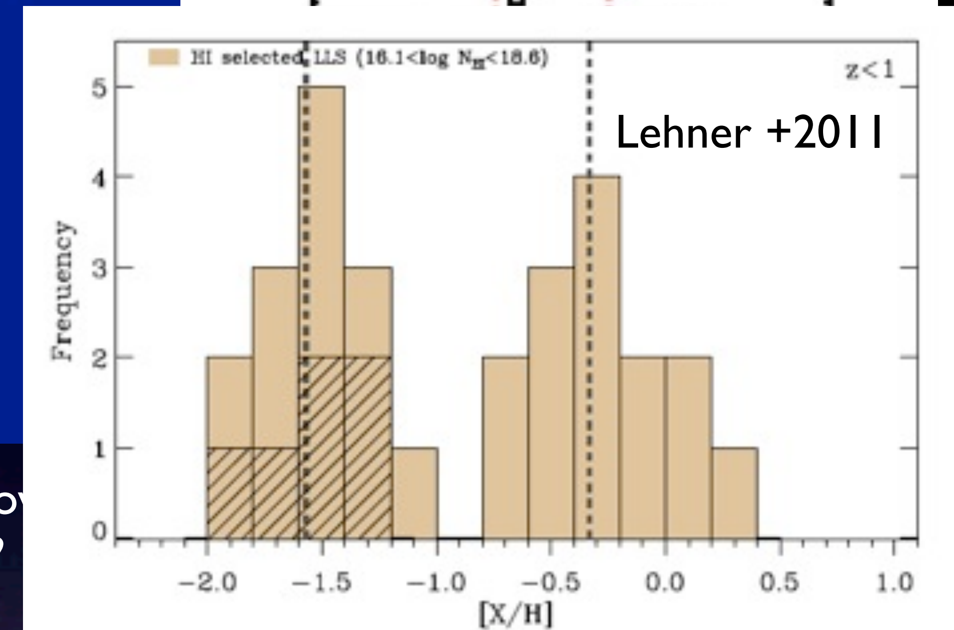

Can cold accretion flo
the covering fraction?

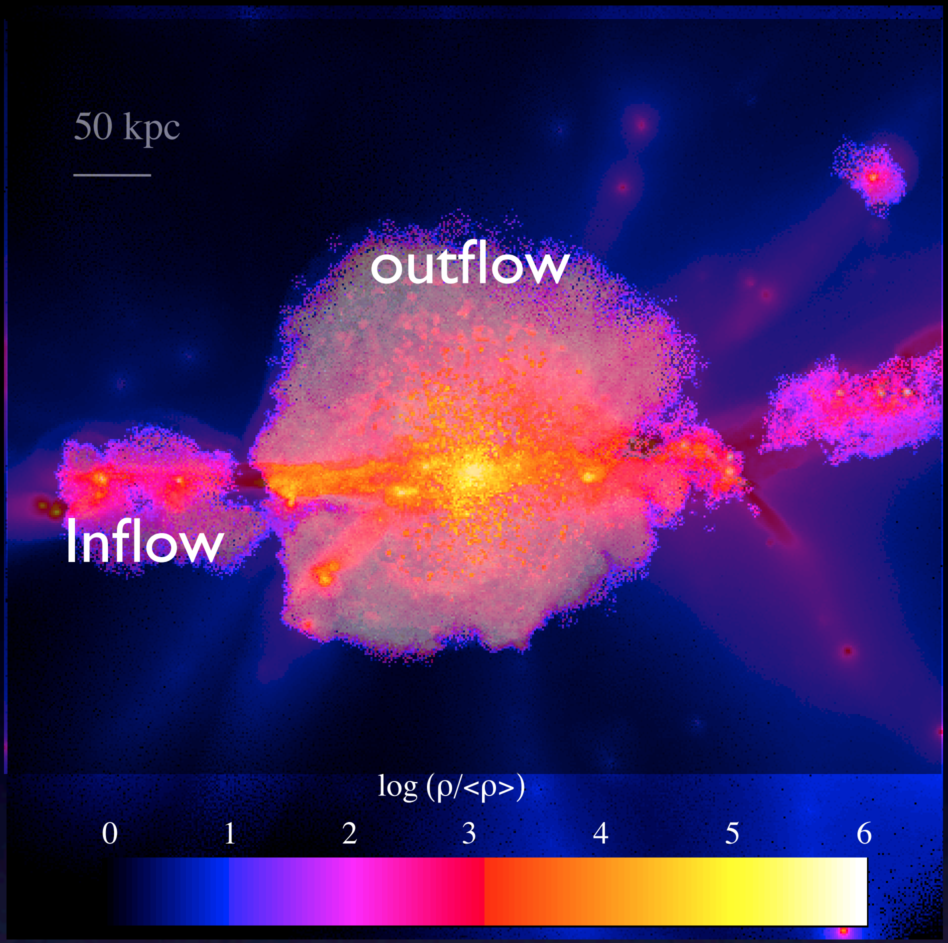

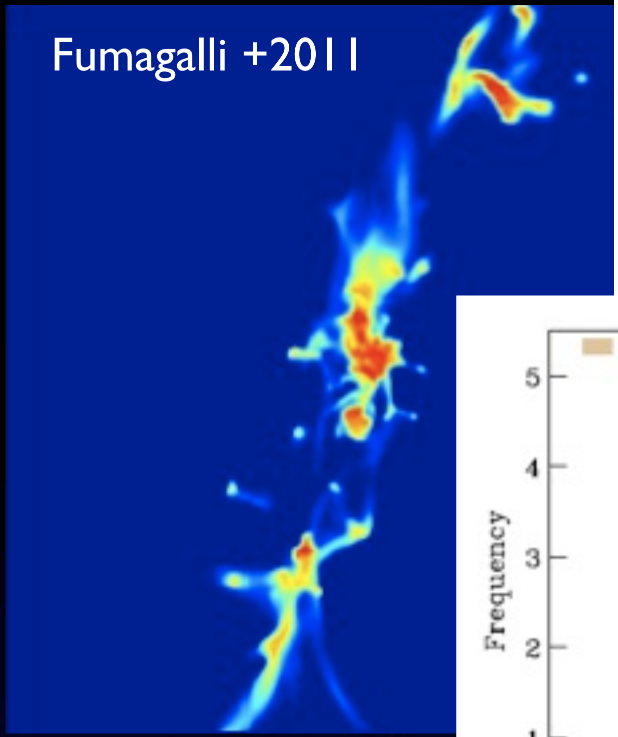

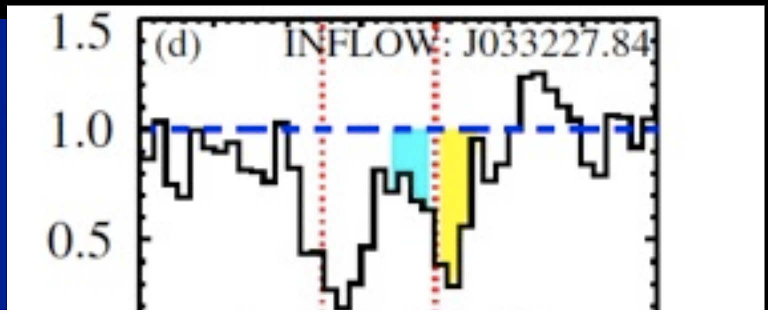

Can cold accretion flo
the covering fraction?

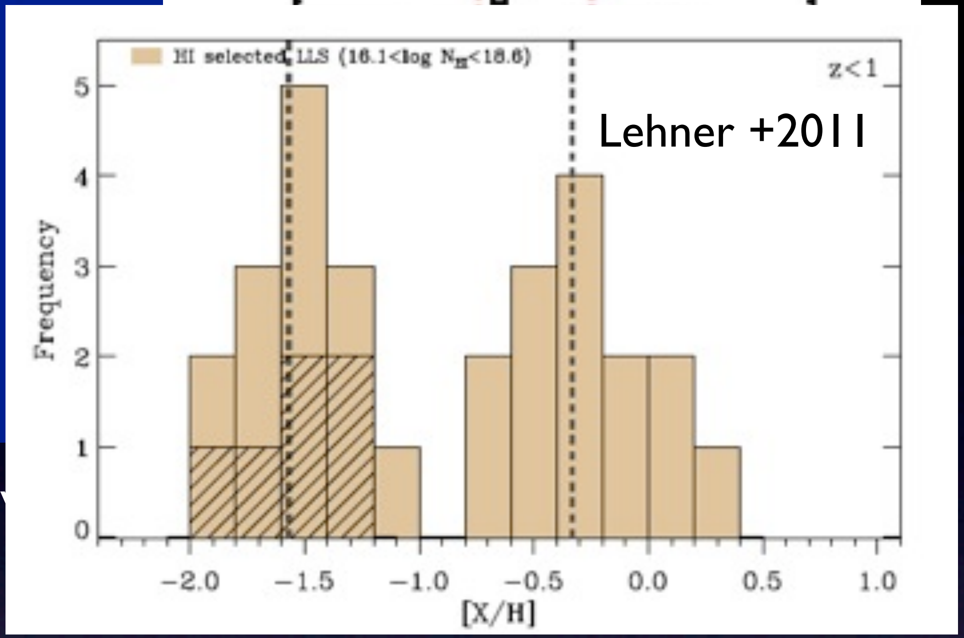

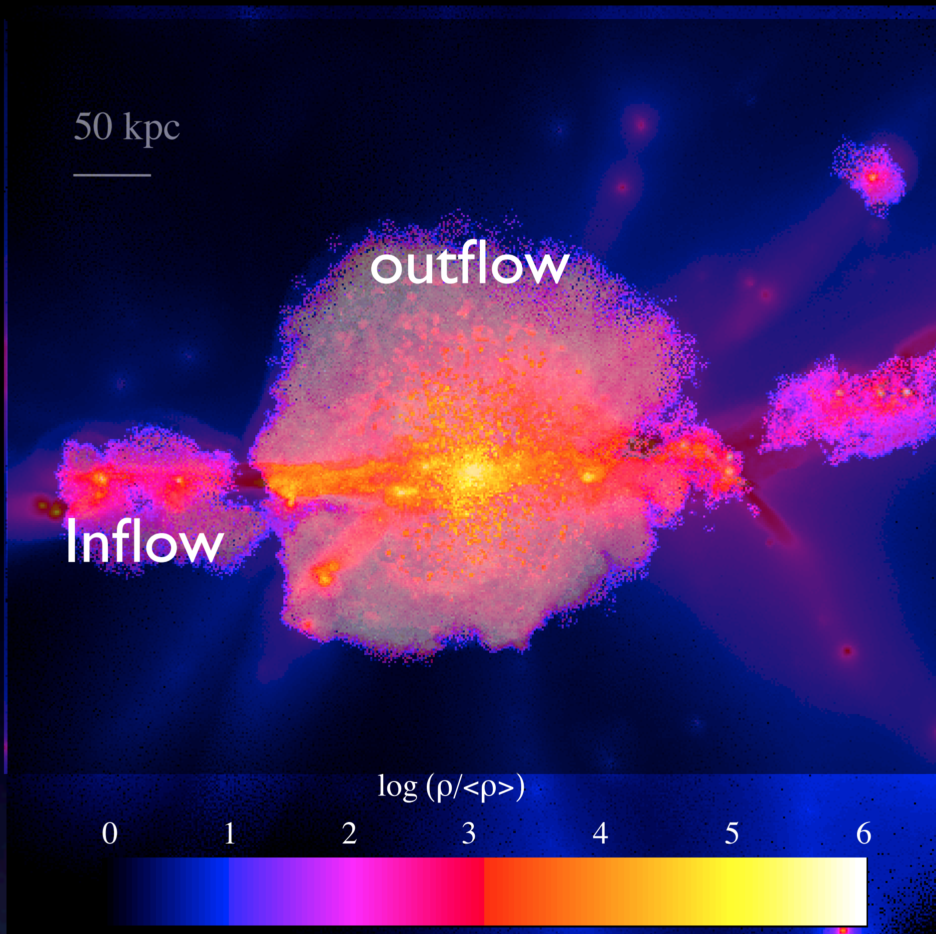

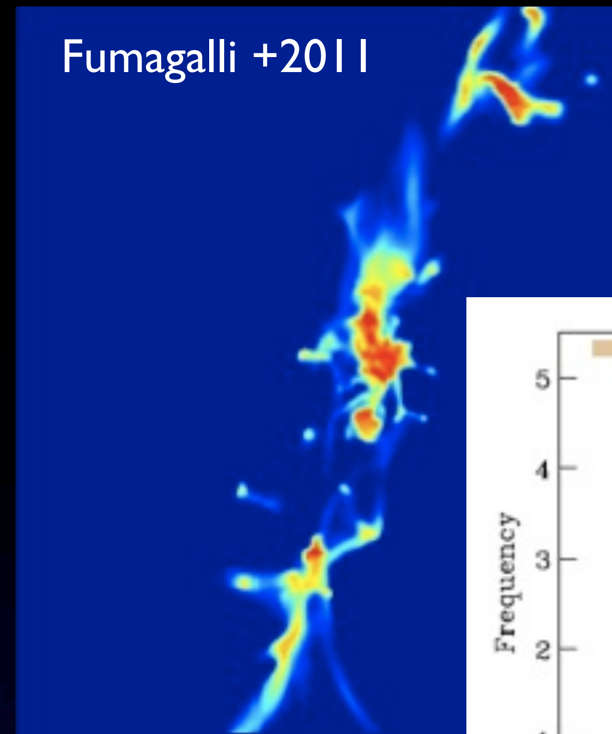

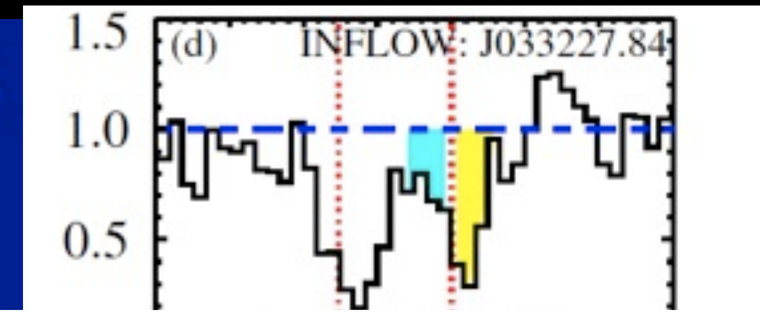

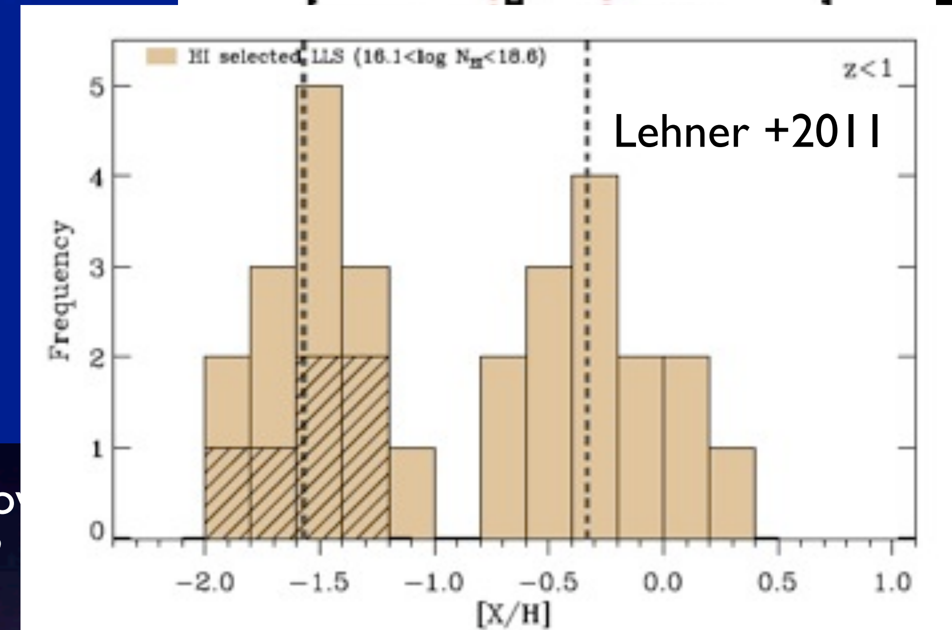

Can cold accretion flo
the covering fraction?

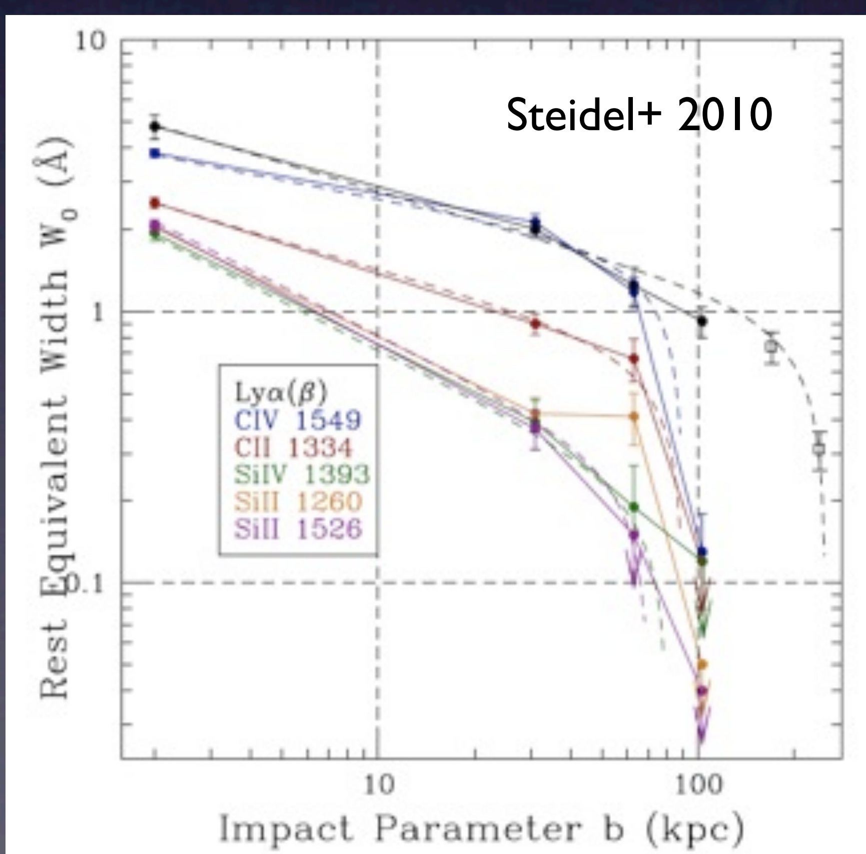

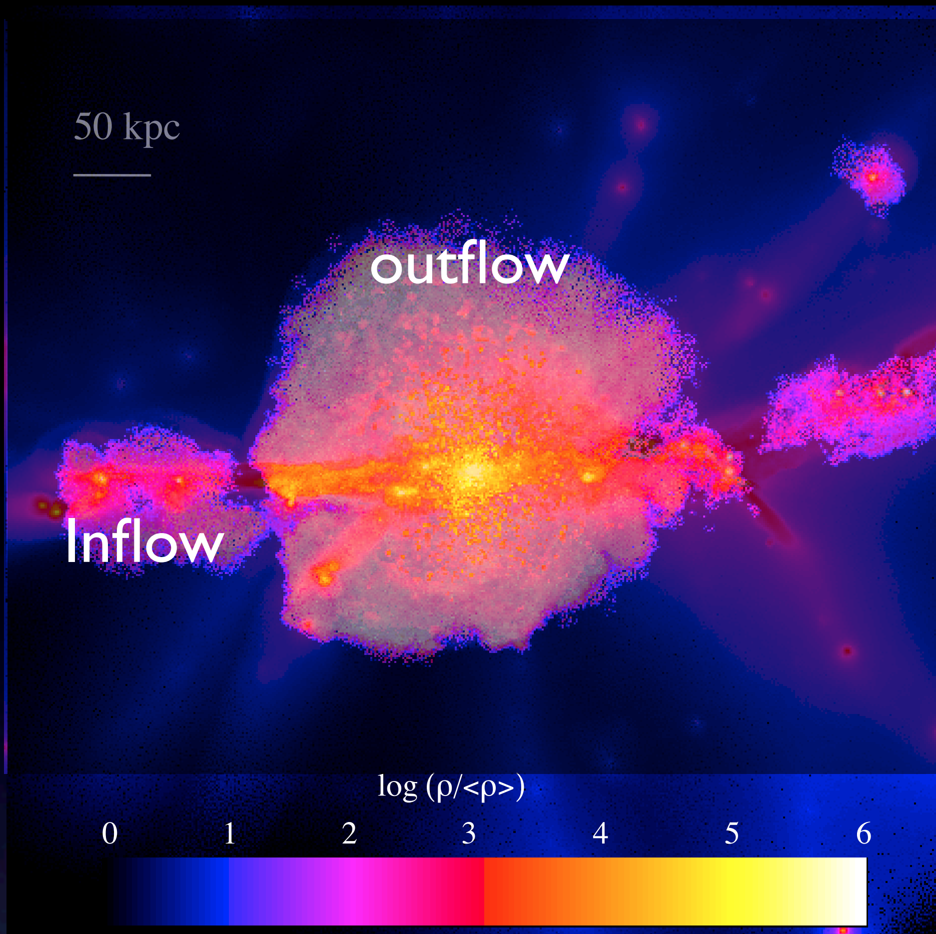

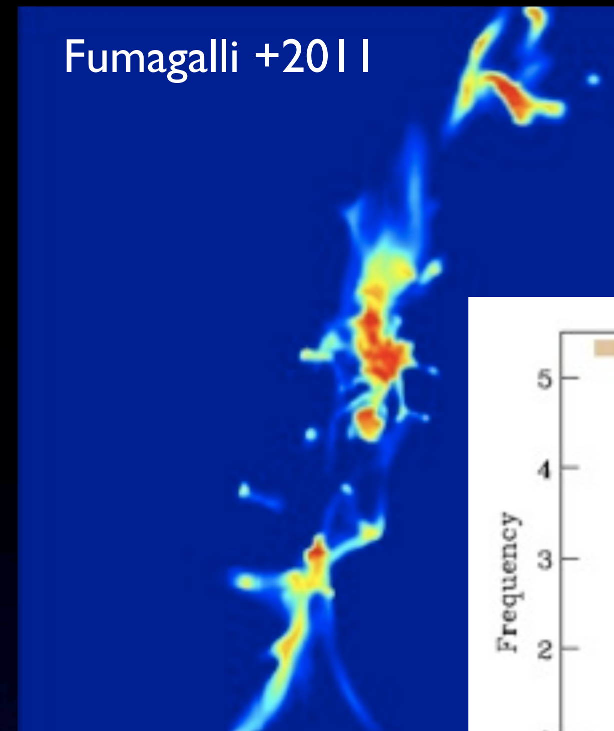

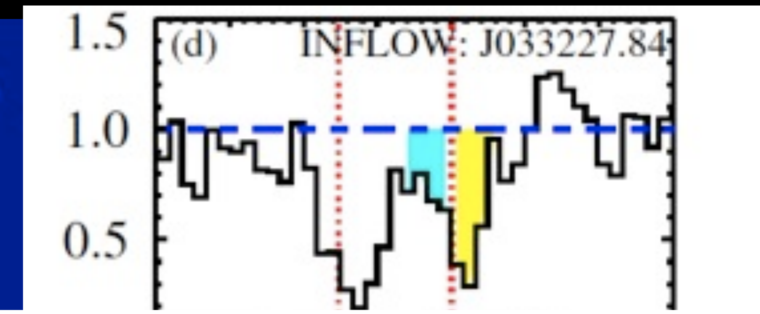

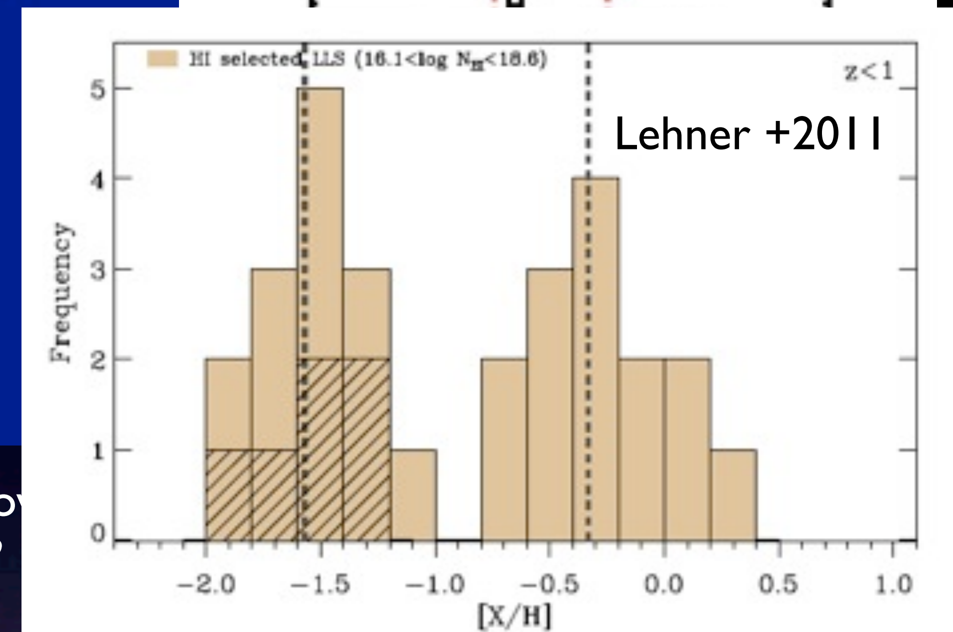

Can cold accretion flo
the covering fraction?

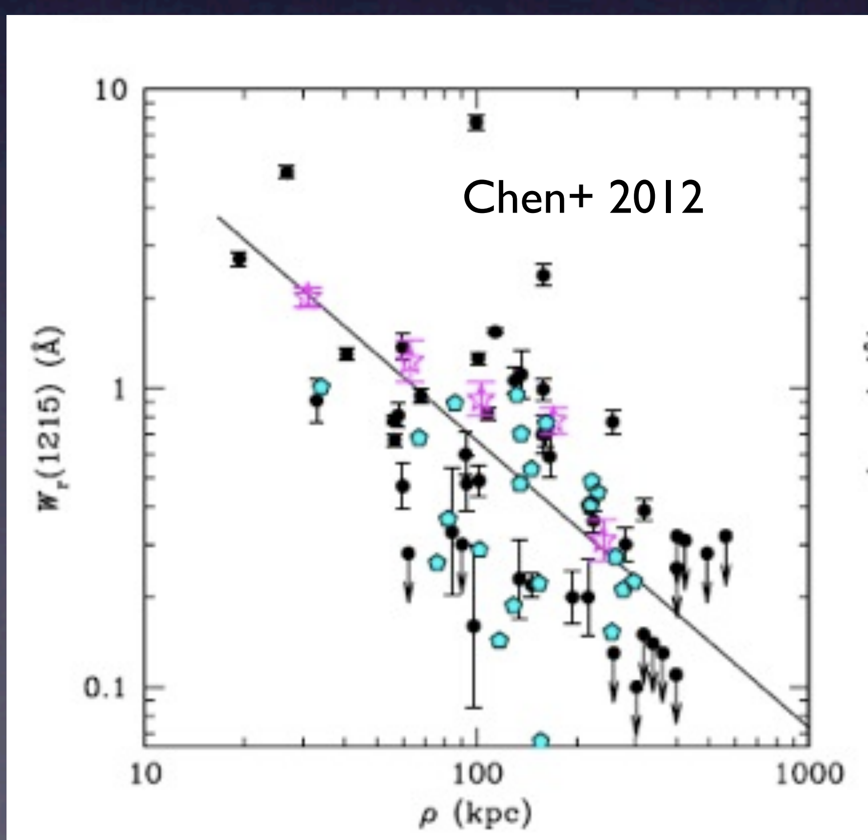

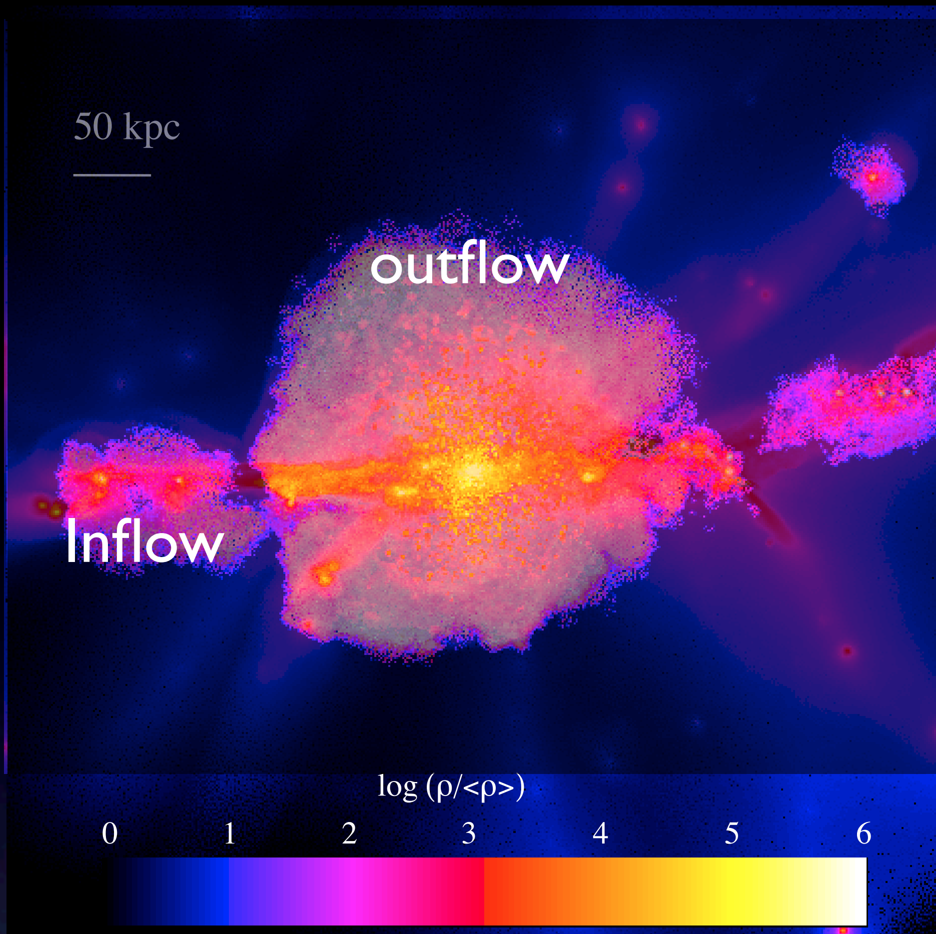

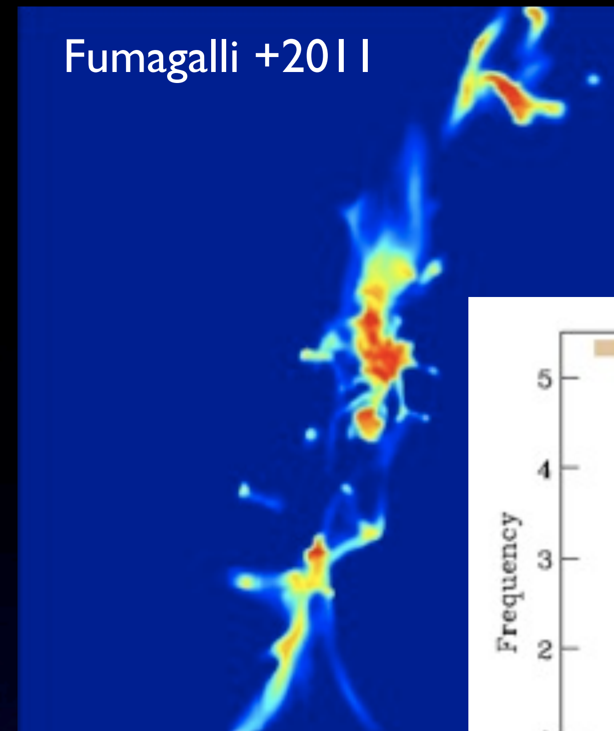

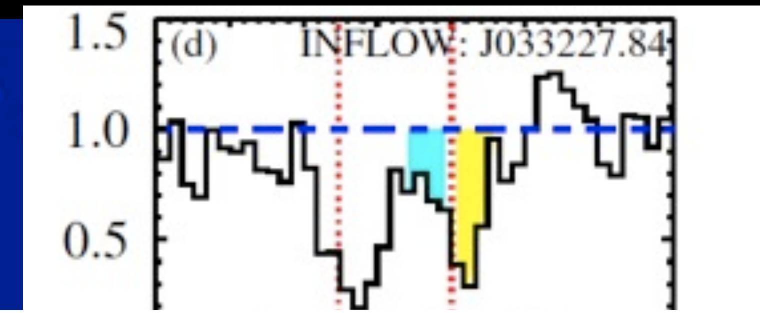

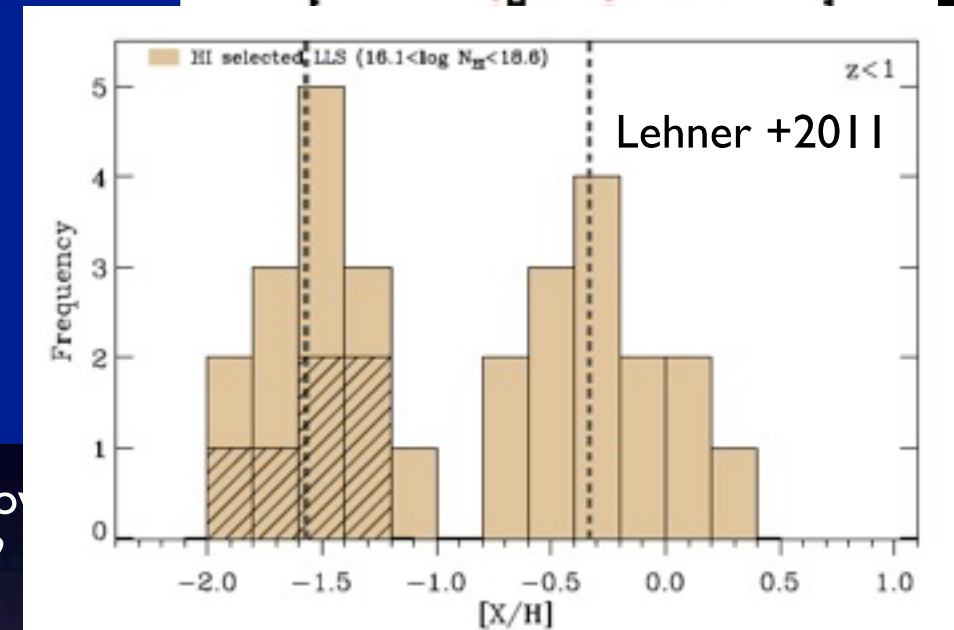

Can cold accretion flo
the covering fraction?

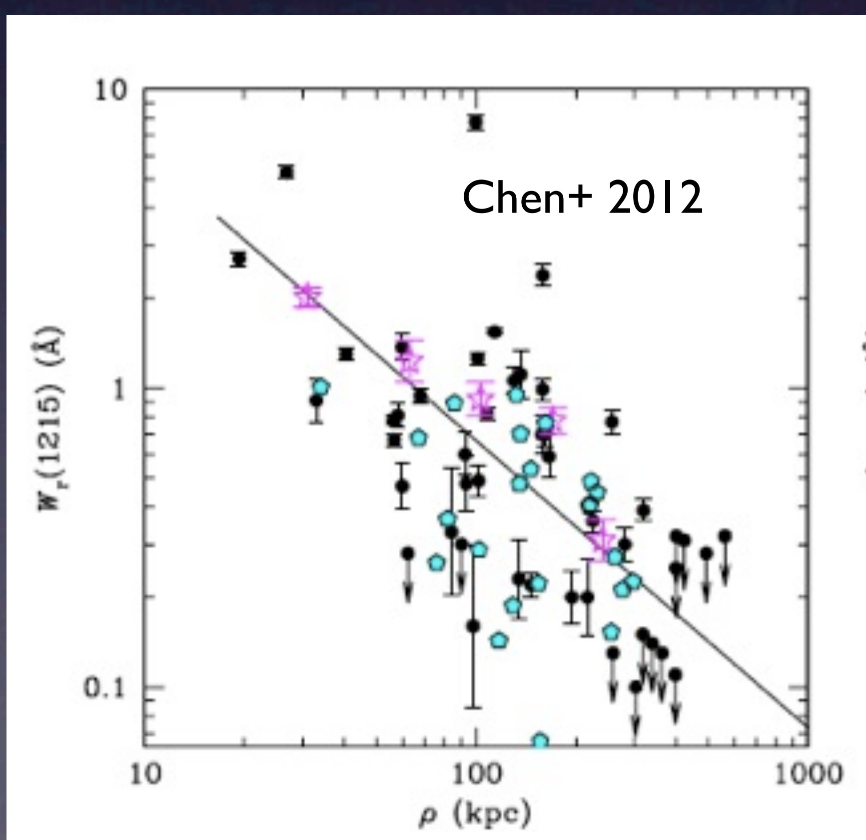

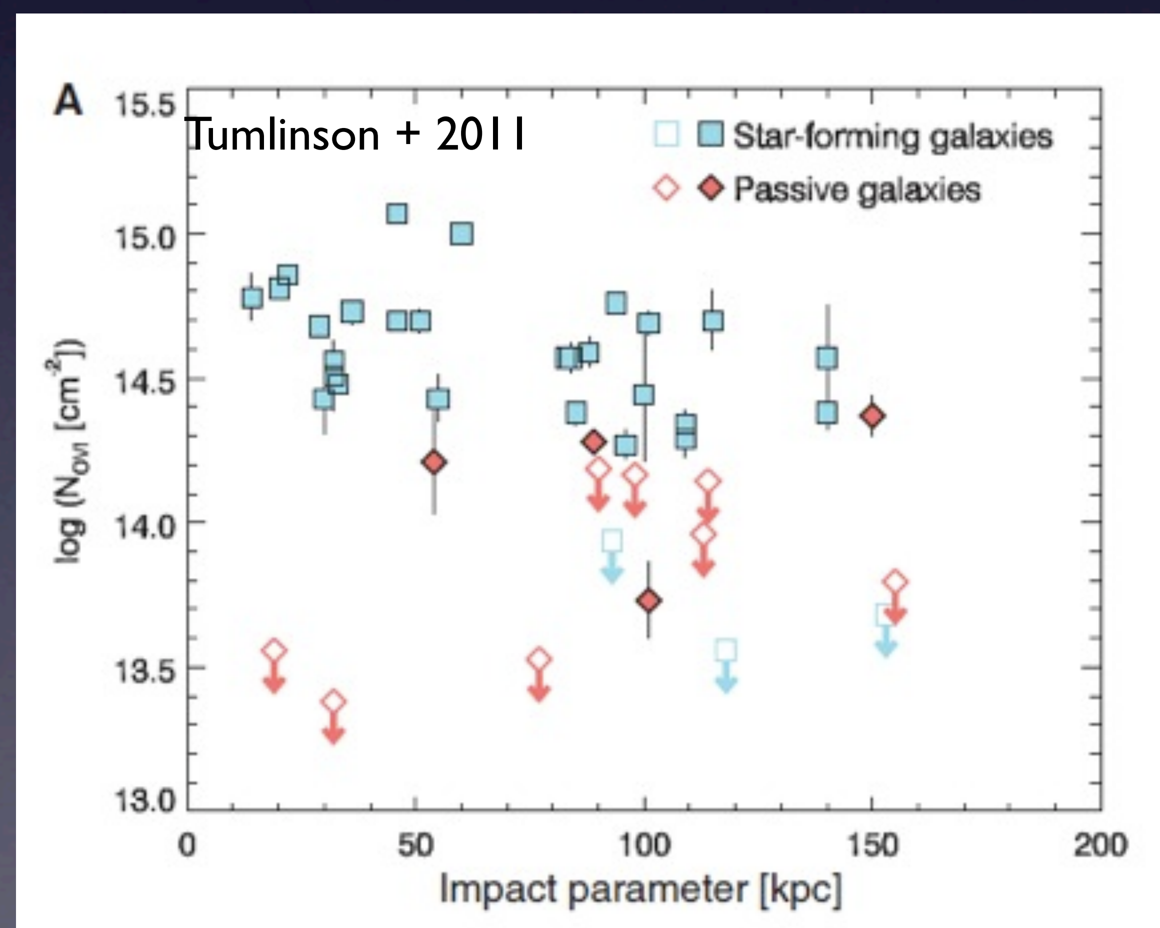

What is the extent of metal enriched CGM?

How does the CGM evolve? How does it correlated with SFR?

Single phase or multi phase gas?

"Feedback", galactic winds & gas accretion: Key components for galaxy formation

Winds are necessary for:

1. Enrich the IGM (e.g., Oppenheimer & Davé 06, 08,10; Wiersma+10; Shen+10)
2. Regulate cosmic SFR (e.g., Schaye+10)
3. M^* - M_h relation (Guedes+11; Brook+12)
4. Produce extended galactic disk in simulations (Agertz+11; Guedes+11; Brook+12;)
5. Create DM cores in dwarf galaxies (Governato+10; Pontzen+12; Tayssier+13)
6. Alleviate "too big to fail" problem (Zolotov +2012)

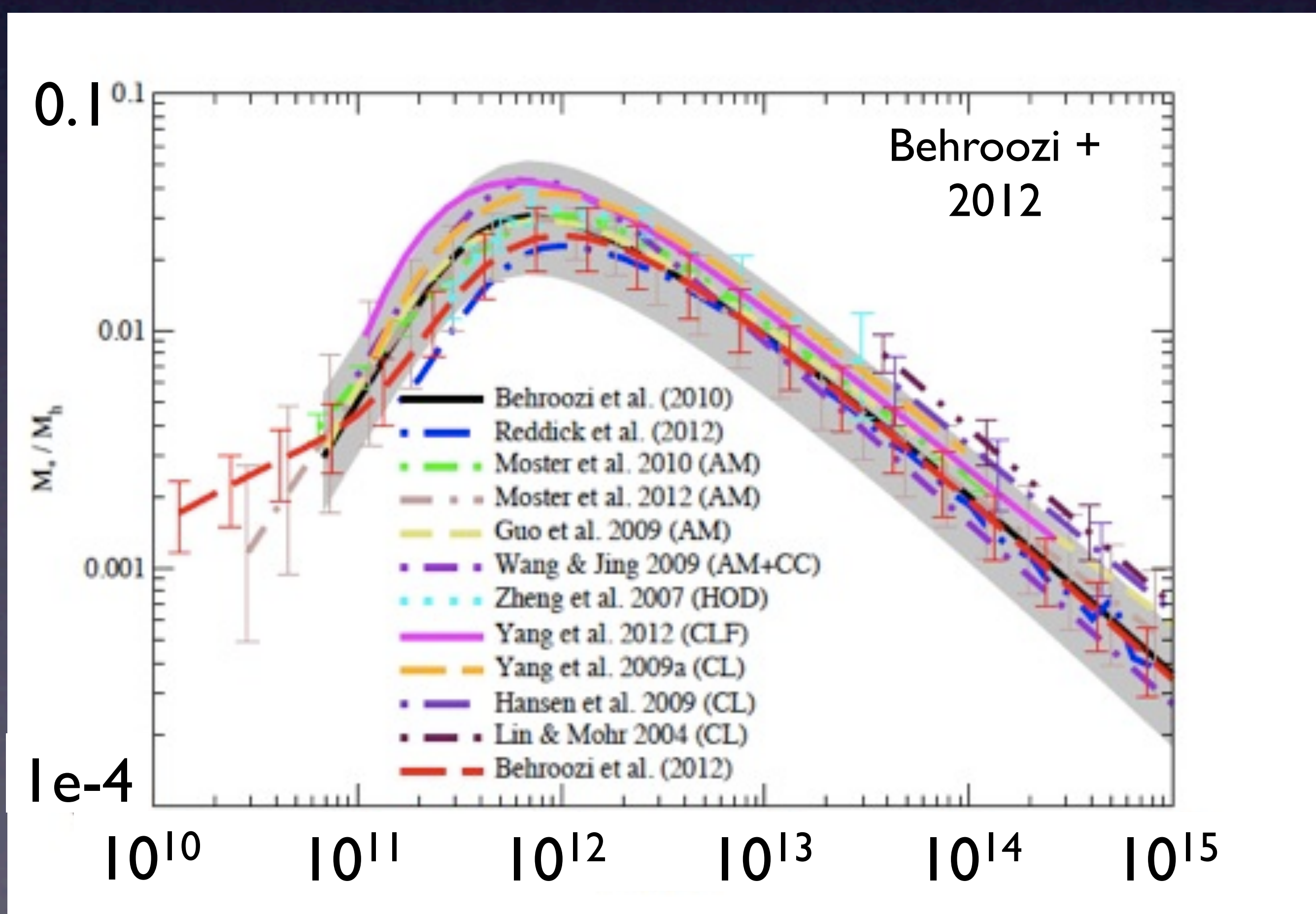

How halos acquire their gas?

1. Photo-heating from the UV background (e.g. Efstathiou+1992; Kravtsov+2004; Madau+2008) suppress dwarf galaxy formation
2. Cold mode vs. Hot mode accretion for large halos (e.g., Birnboim & Dekel 2003; Kereš+2005, 2009; Brooks+2009; Nelson+2013)
   - Halo mass
   - Gas cooling ↔ Metal enrichment & mixing
   - KH instability of gas flows

“Zoom-in” Simulations

Motivation:
1. Computation limit!
2. Correct large scale structure for gas accretion
3. Able to resolve disk structure, constrain feedback from both the galaxy and the CGM

Force resolution down to ~< 100 pc, gas particle mass 10^3-10^4 M_{sun};

1. *Start* to resolve the ISM -- GMC: 10^6 Msun
2. Structure of the streams, winds and the CGM (but not there yet for turbulence)
3. Metal contribution from dwarf satellites: $M_h < 10^9$ M_{sun}

several millions CPU hours
9 months

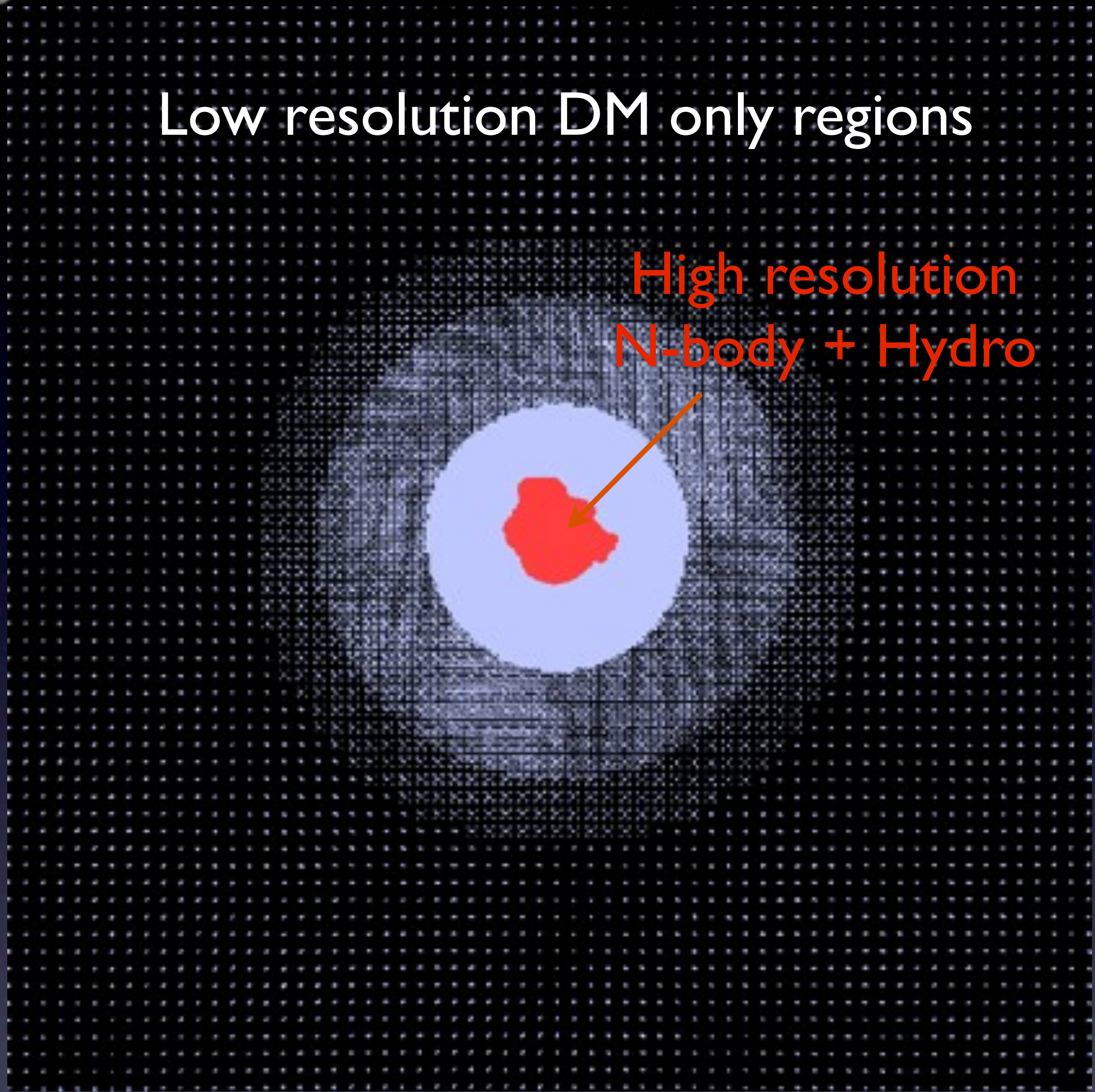

1. Run DM only cosmological box
2. Select one, or several halos and their surrounding regions
3. Track the DM back to the IC, find the Lagrangian region
4. Add resolution and gas dynamics

A Simulated Massive Galaxy: Eris Suite

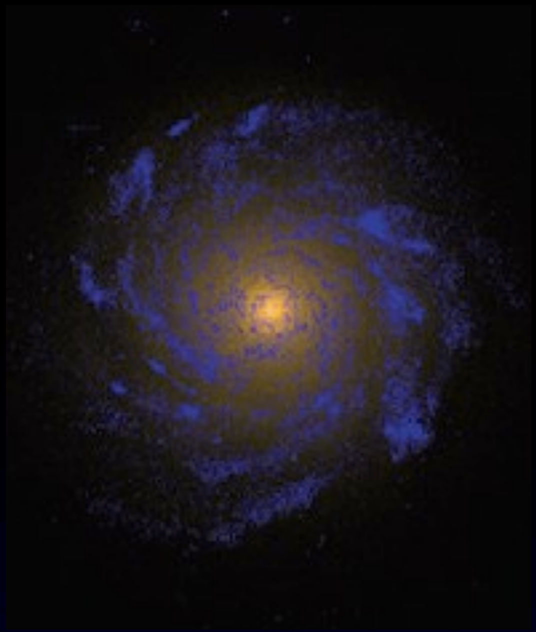

Gasoline

Guedes+11; Shen+12, 13

TreeSPH code Gasoline (Wadsley+ 04)

Star formation & SN feedback (Stinson+ 06); Primordial+metal cooling (Shen+10); Metal mixing (Shen+10);

No AGN feedback

Moster+ 2013

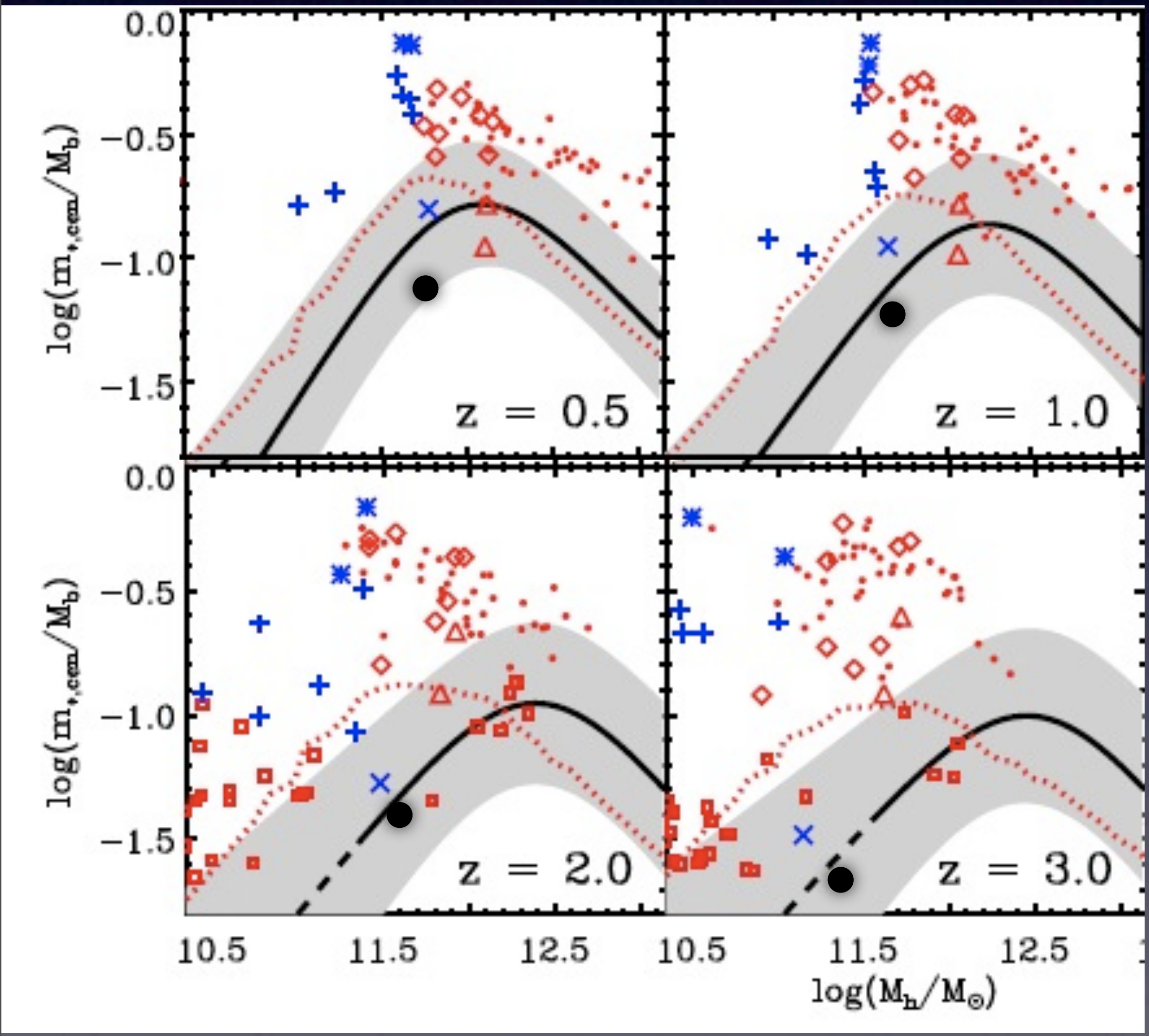

Flat rotation curve: Very small bulge at z ~ 0.6

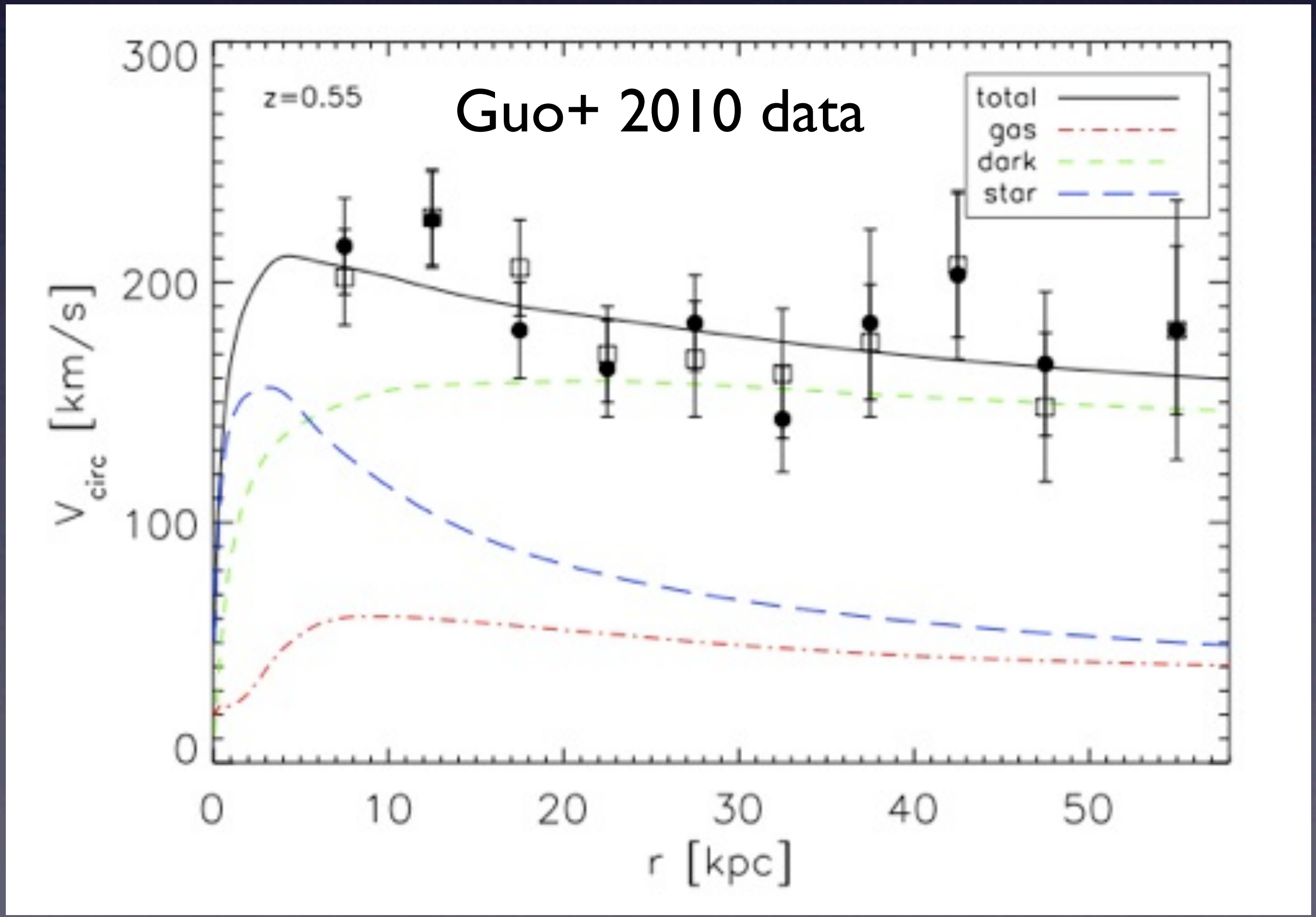

Spatial Distribution & Kinematics of H I and Metal Absorbers at $z \sim 2$-3

Eris2 and Its Metal-Enriched CGM at z = 2.8

Shen et al. (2013)

- At z=2.8, Eris2 has M_{vir} and M_*

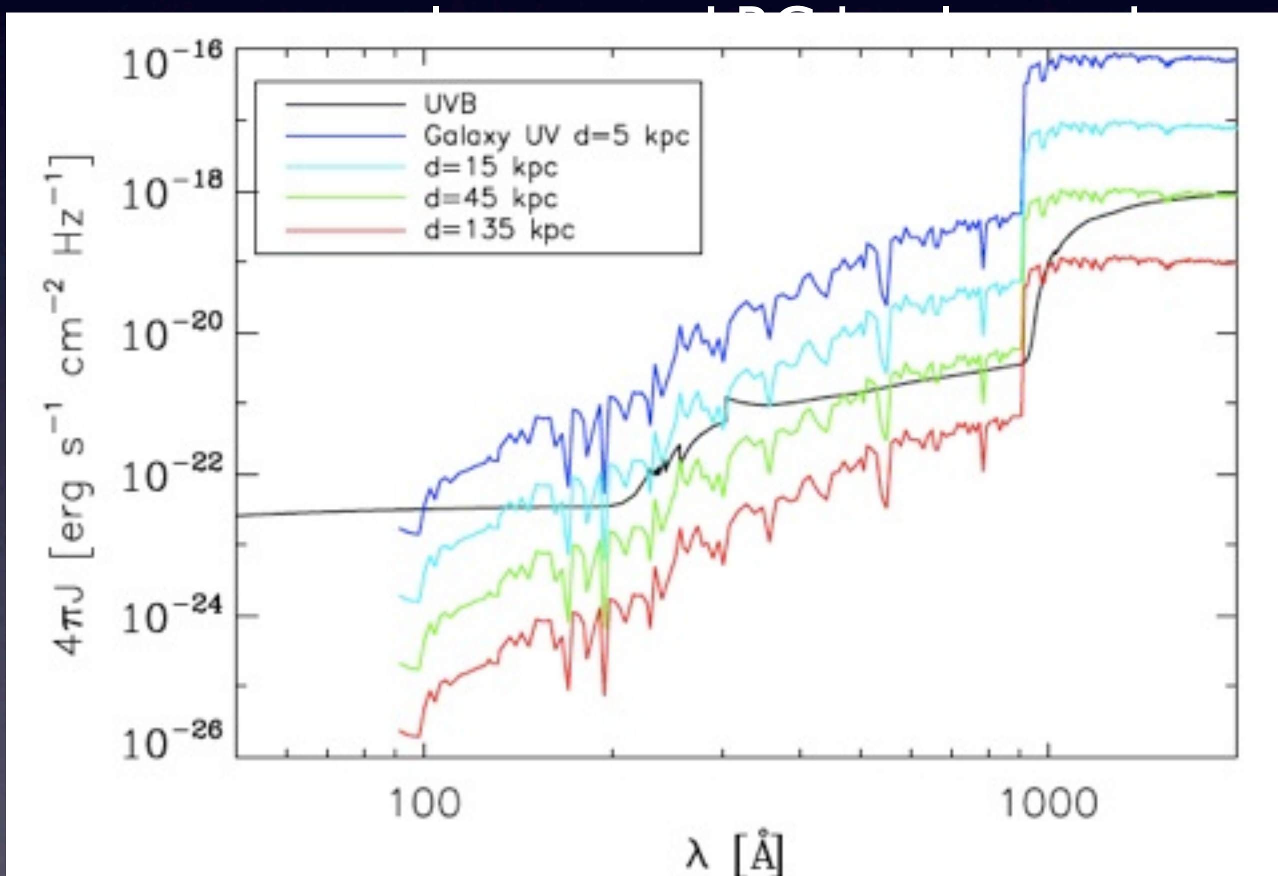

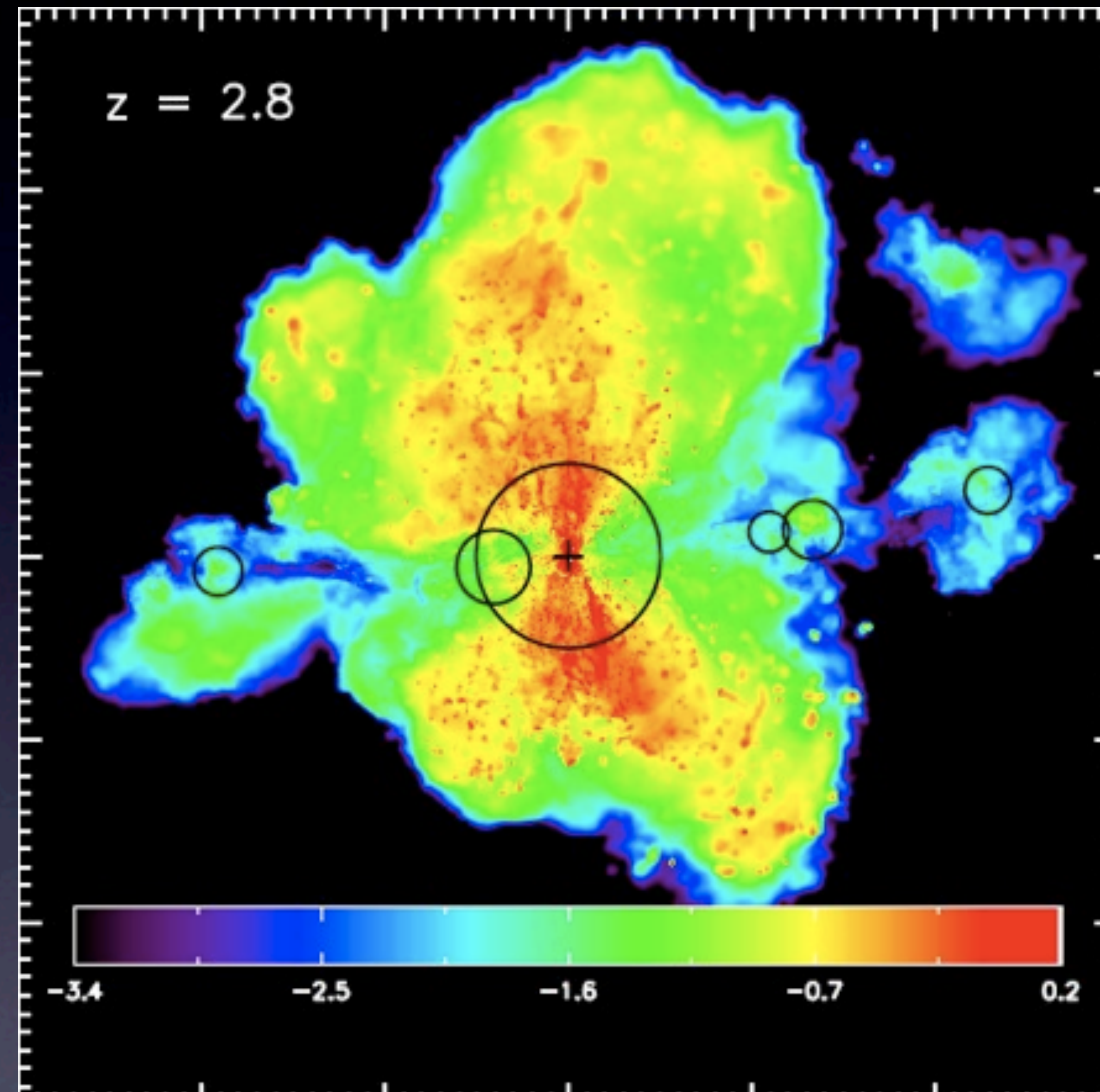

Calculating ion fractions:

- UVB + non-uniform stellar UV assuming constant SFR 20 Msun/yr
- Assuming optically thin

600 x 600 x 600 kpc^3 projected map of gas metallicity. The disk is viewed nearly edge on

Kinematics of the Metal-Enriched CGM

- 600 x 600 x 10 kpc slice, projected to x-y plane, disk nearly edge-on
- Max projected averaged velocity ~300 km/s (host)
- Metallicity is high along the miner axis but non-zero along the major axis (Rubin + 2012; Kacprzak+2012)
- Average outflow velocity decrease at larger distances and join the inflow -- halo fountain (Oppenheimer+ 2010)

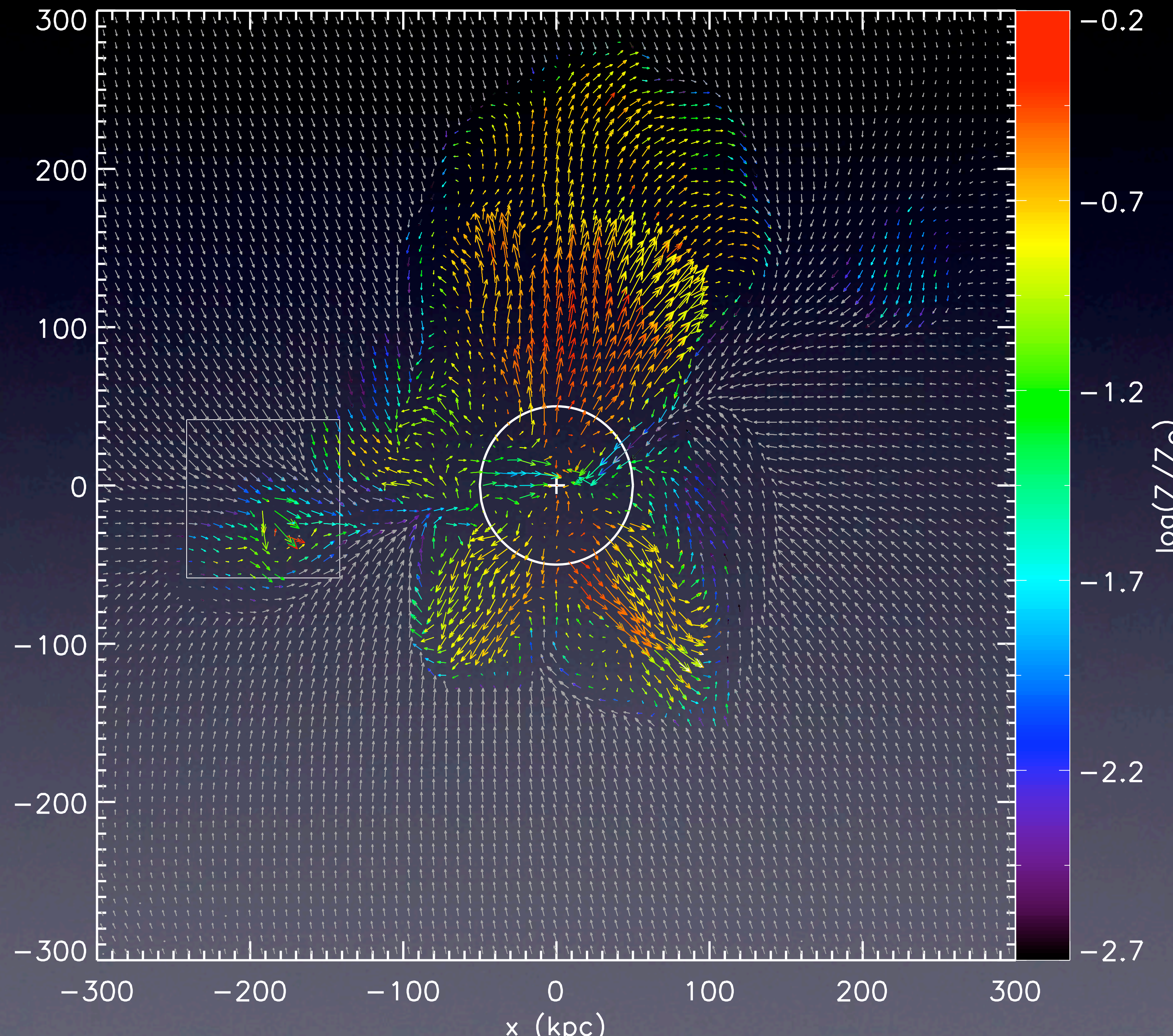

Kinematics of the Metal-Enriched CGM

- 600 x 600 x 10 kpc slice, projected to x-y plane, disk nearly edge-on
- Max projected averaged velocity ~300 km/s (host)
- Metallicity is high along the miner axis but non-zero along the major axis (Rubin + 2012; Kacprzak+2012)
- Average outflow velocity decrease at larger distances and join the inflow -- halo fountain (Oppenheimer+ 2010)

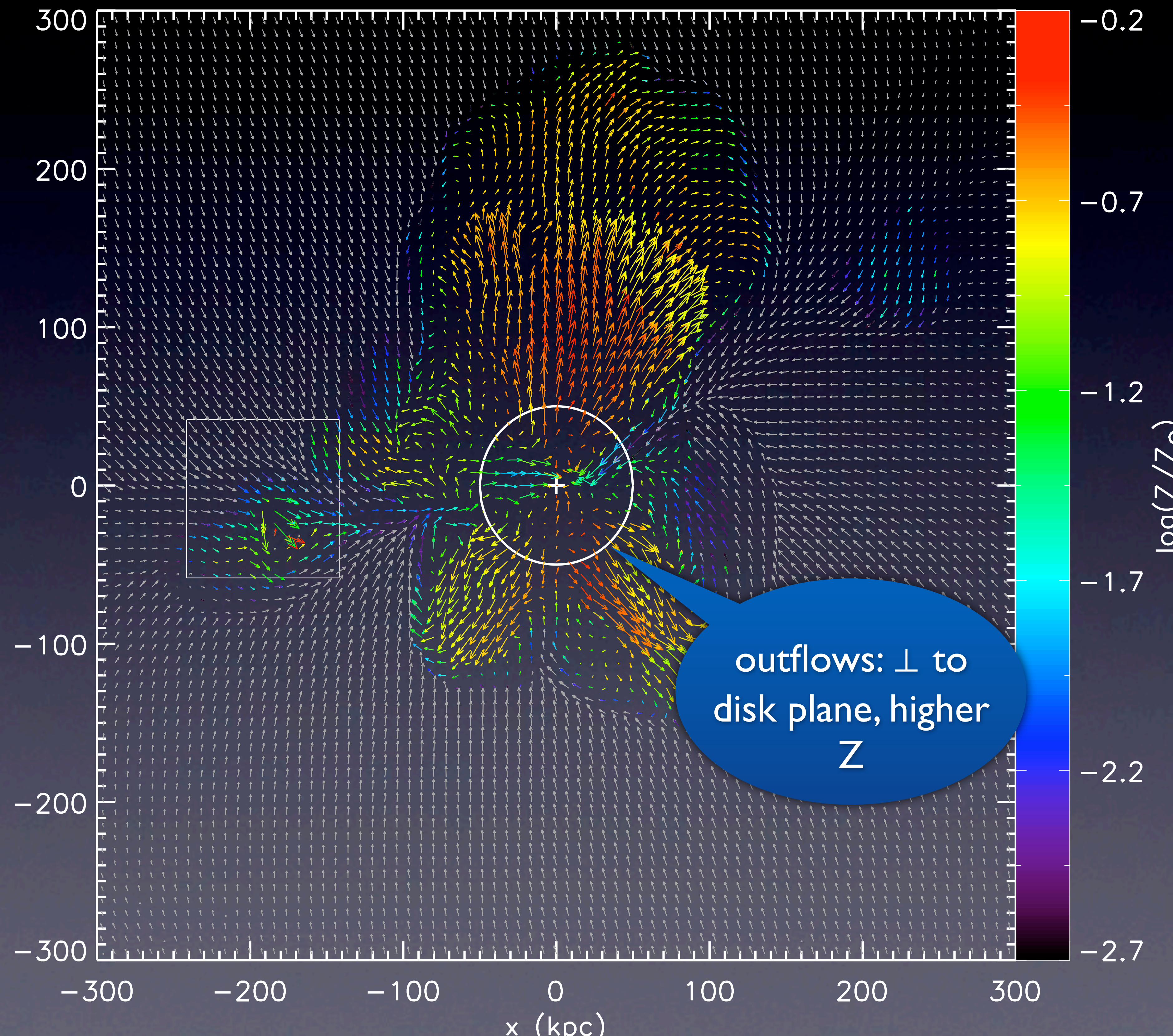

Kinematics of the Metal-Enriched CGM

- 600 x 600 x 10 kpc slice, projected to x-y plane, disk nearly edge-on
- Max projected averaged velocity ~300 km/s (host)
- Metallicity is high along the miner axis but non-zero along the major axis (Rubin + 2012; Kacprzak+2012)
- Average outflow velocity decrease at larger distances and join the inflow -- halo fountain (Oppenheimer+ 2010)

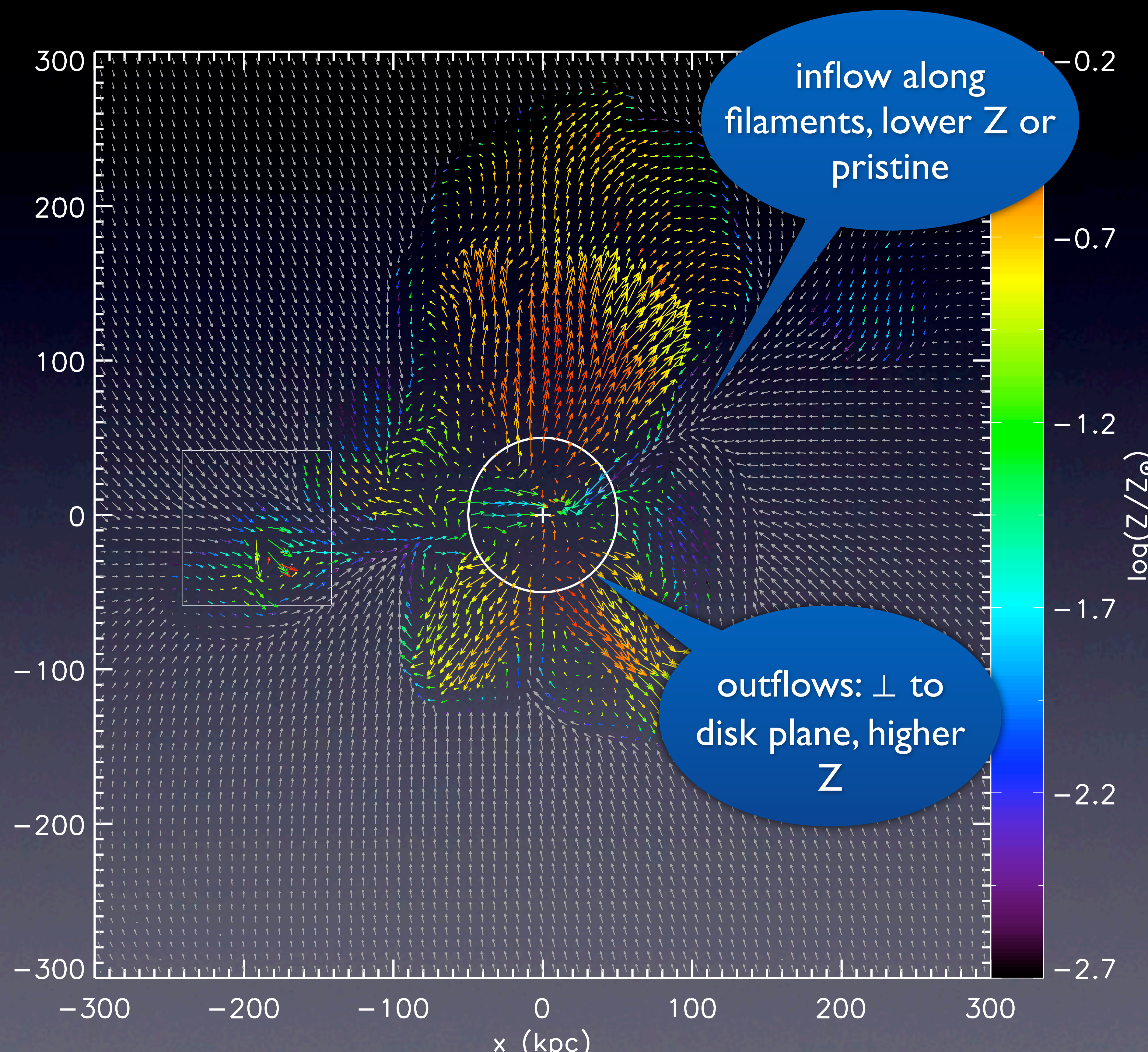

Kinematics of the Metal-Enriched CGM

- 600 x 600 x 10 kpc slice, projected to x-y plane, disk nearly edge-on
- Max projected averaged velocity ~300 km/s (host)
- Metallicity is high along the miner axis but non-zero along the major axis (Rubin + 2012; Kacprzak+2012)
- Average outflow velocity decrease at larger distances and join the inflow -- halo fountain (Oppenheimer+ 2010)

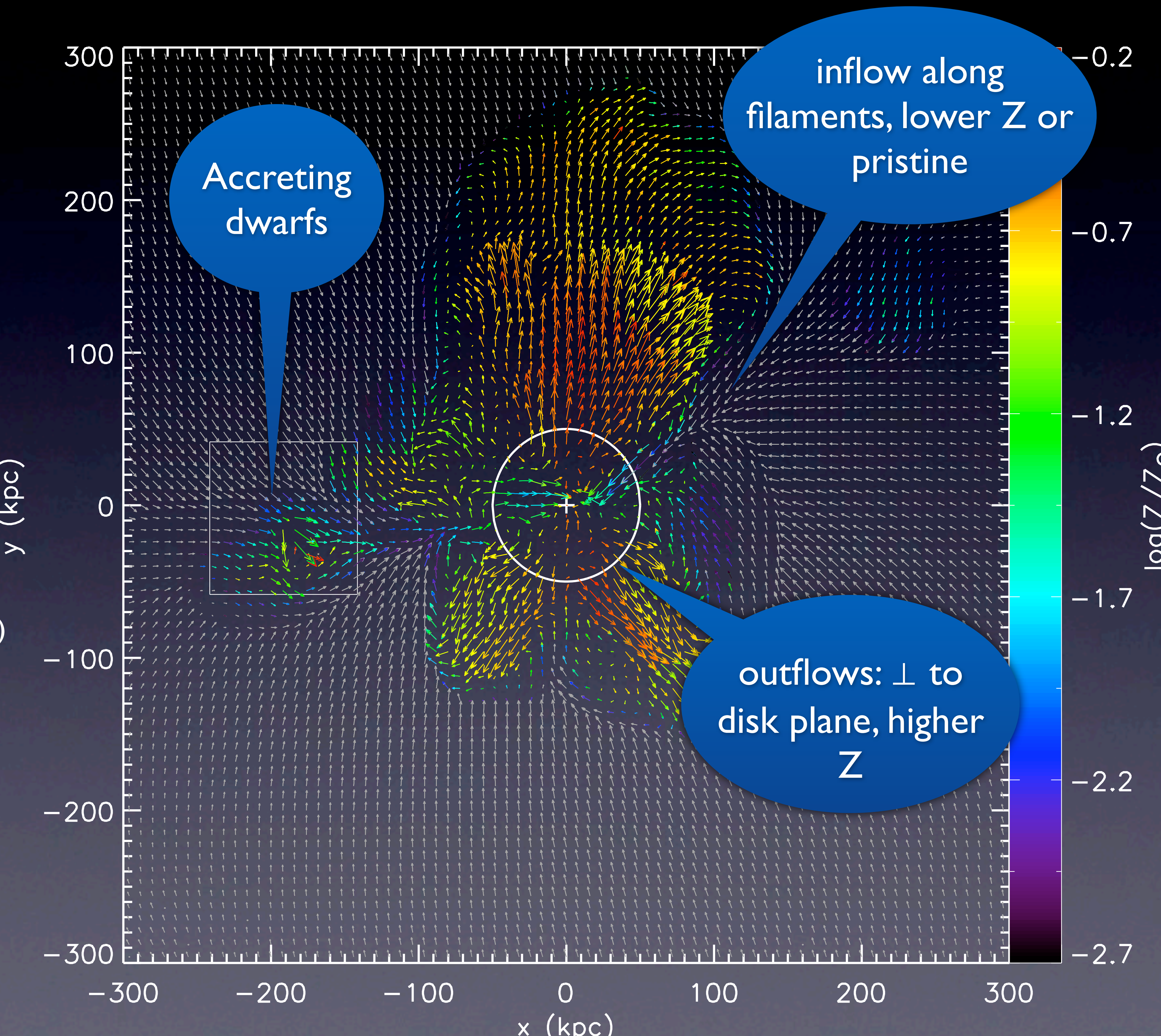

CGM Metals Traced by Different Ions

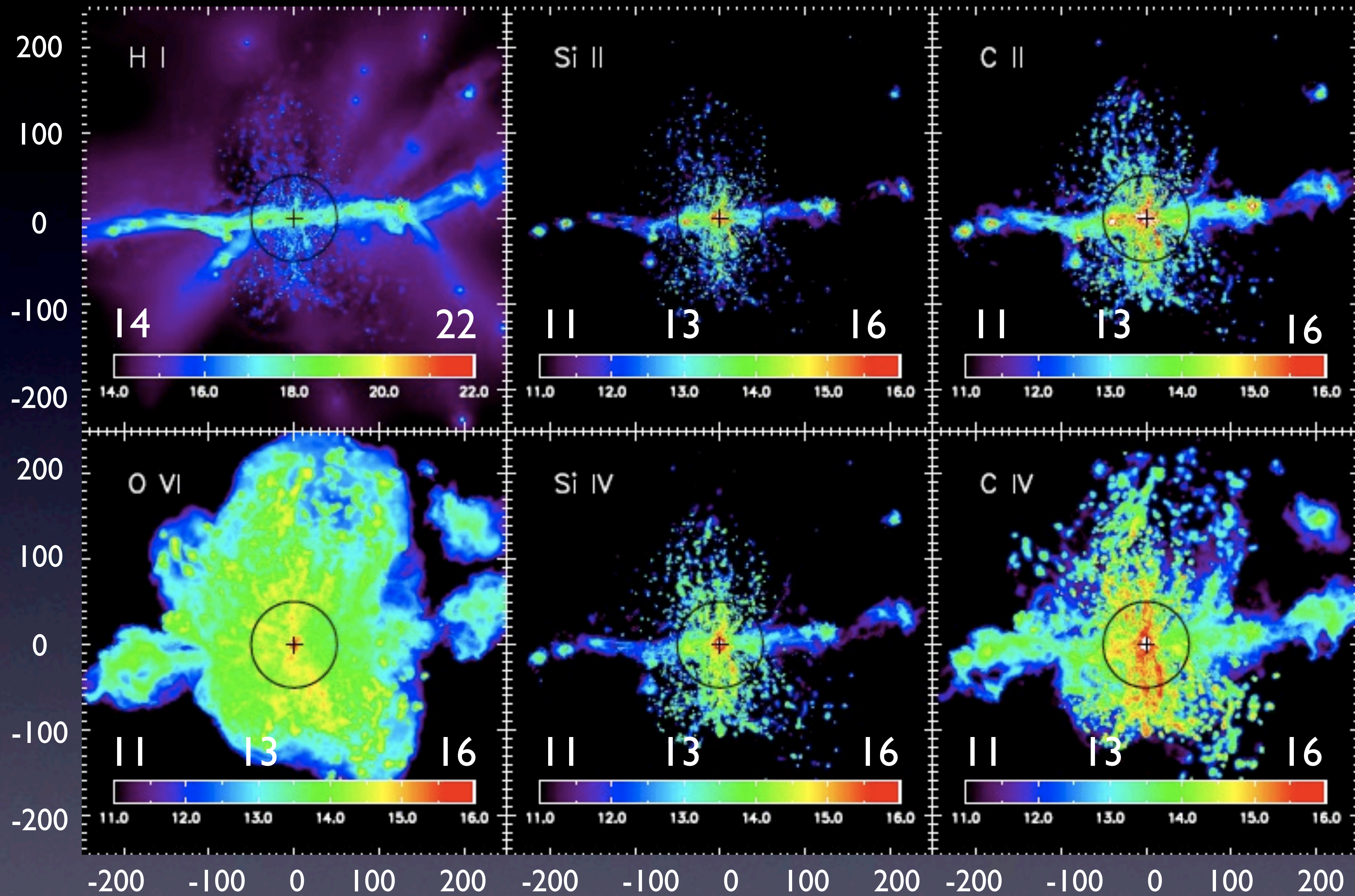

- Low and high ions co-exist in the same absorbers
- Covering factors of low ions (C II, Si II) decrease more rapidly than high ions
- O VI has large covering factor up to 3 $R_{vir,}$ M_O(CGM) ~5x 10^7 M_{sun}> M_O(ISM)

Inflowing and Outflowing CGM

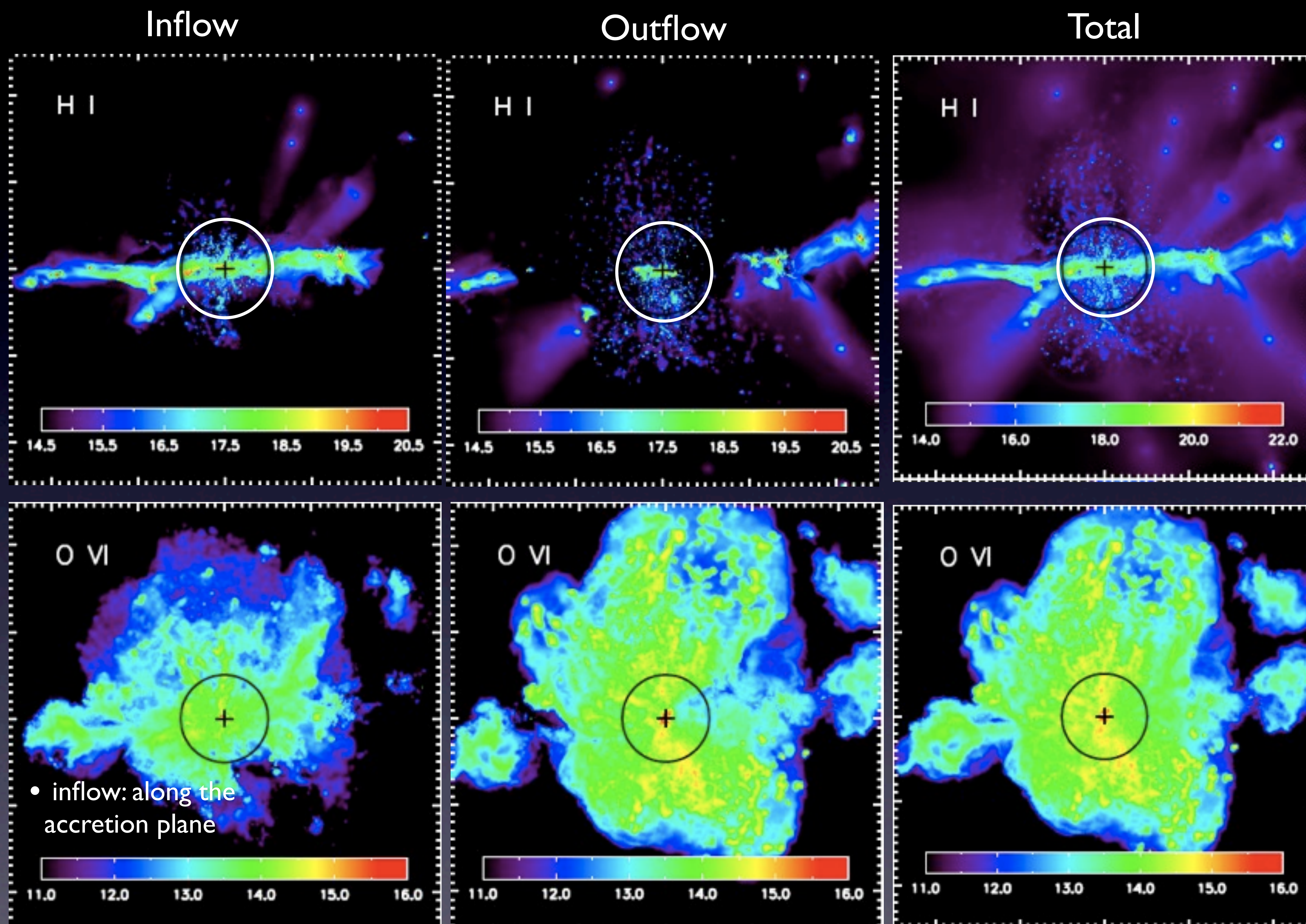

	H I	Si II	C II	Si IV	C IV	O VI
Inflow mass (%)	77%	66%	66%	50%	44%	32%

Inflowing and Outflowing CGM

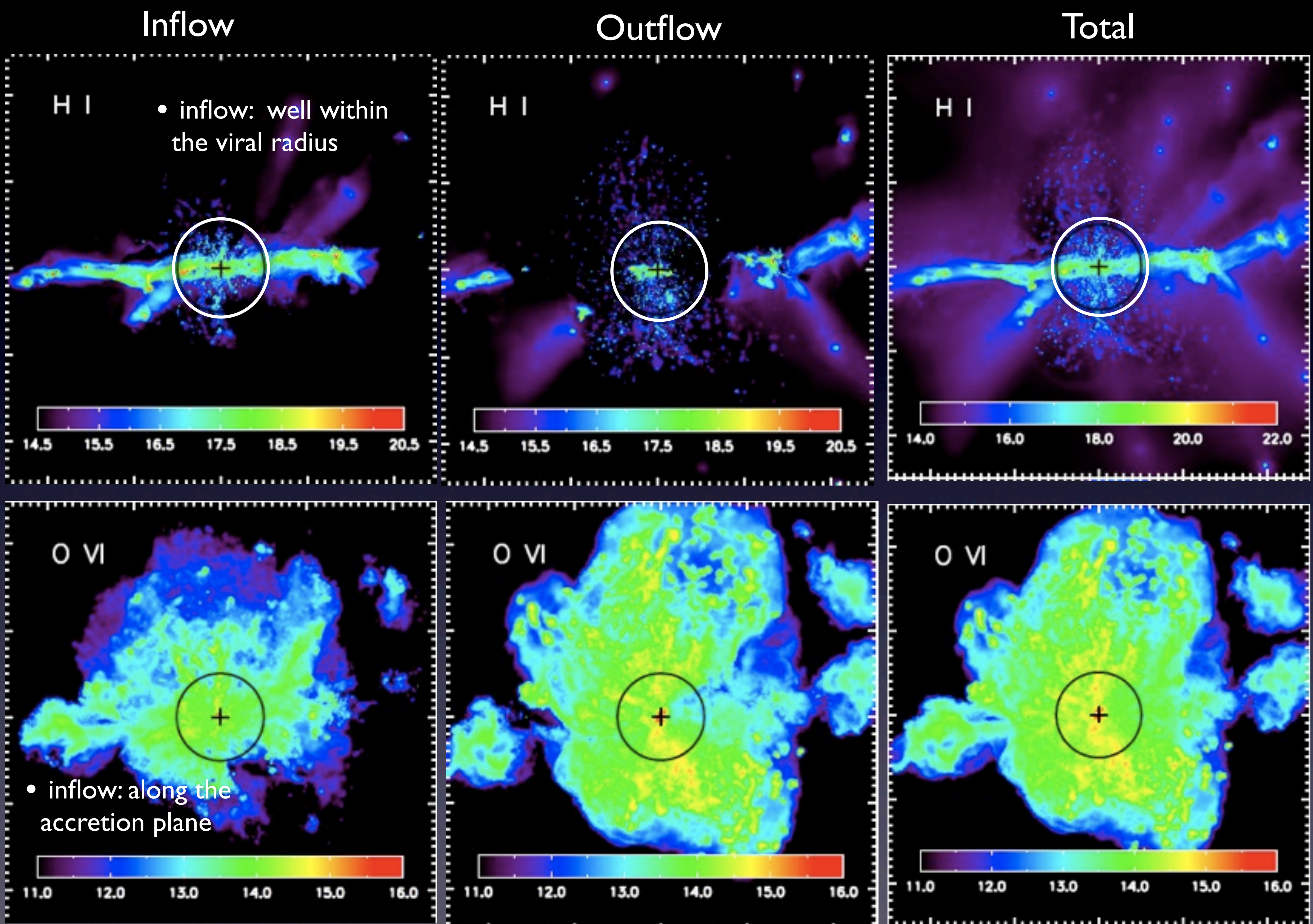

	H I	Si II	C II	Si IV	C IV	O VI
Inflow mass (%)	77%	66%	66%	50%	44%	32%

Inflowing and Outflowing CGM

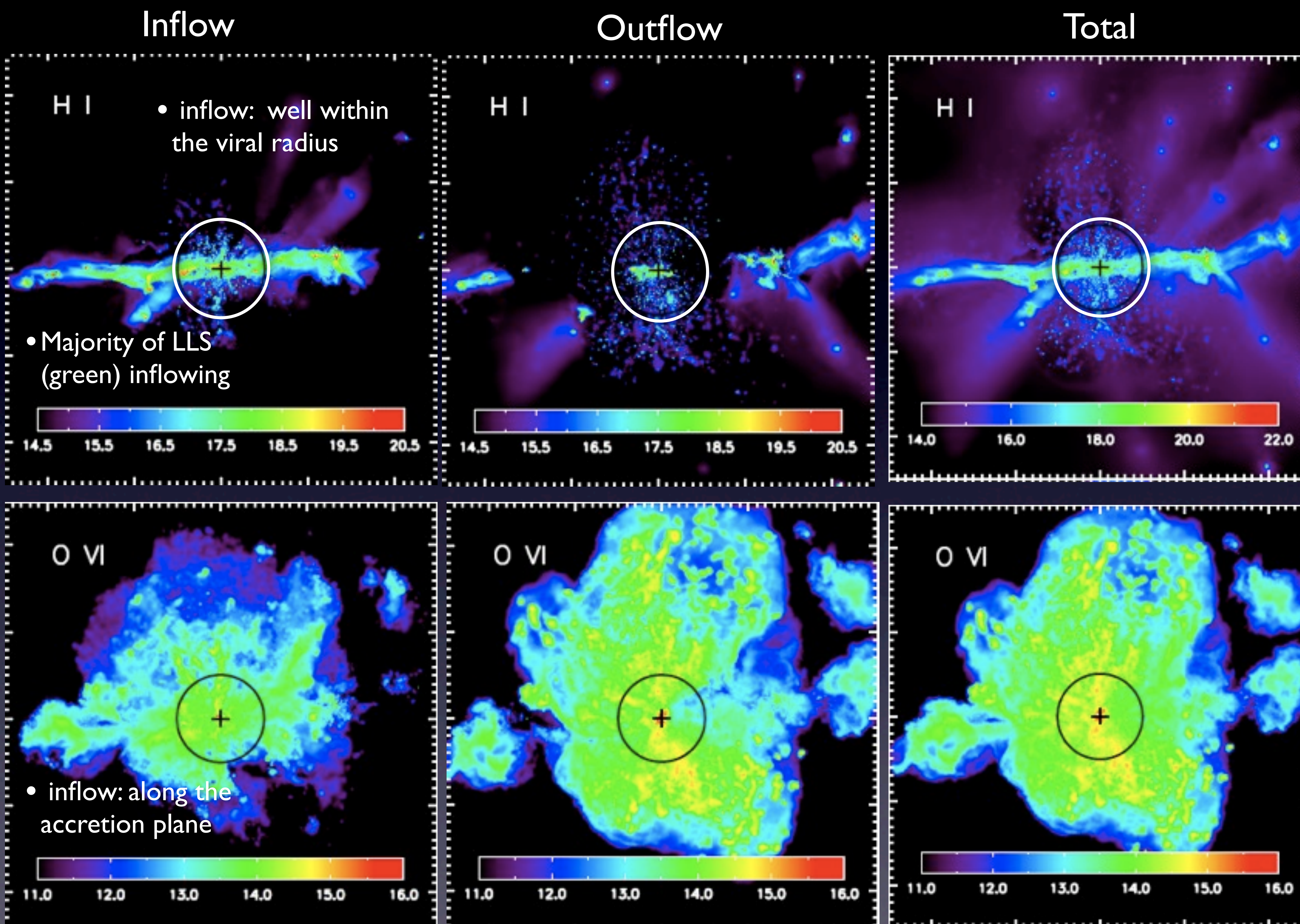

	H I	Si II	C II	Si IV	C IV	O VI
Inflow mass (%)	77%	66%	66%	50%	44%	32%

Inflowing and Outflowing CGM

Inflow | Outflow | Total

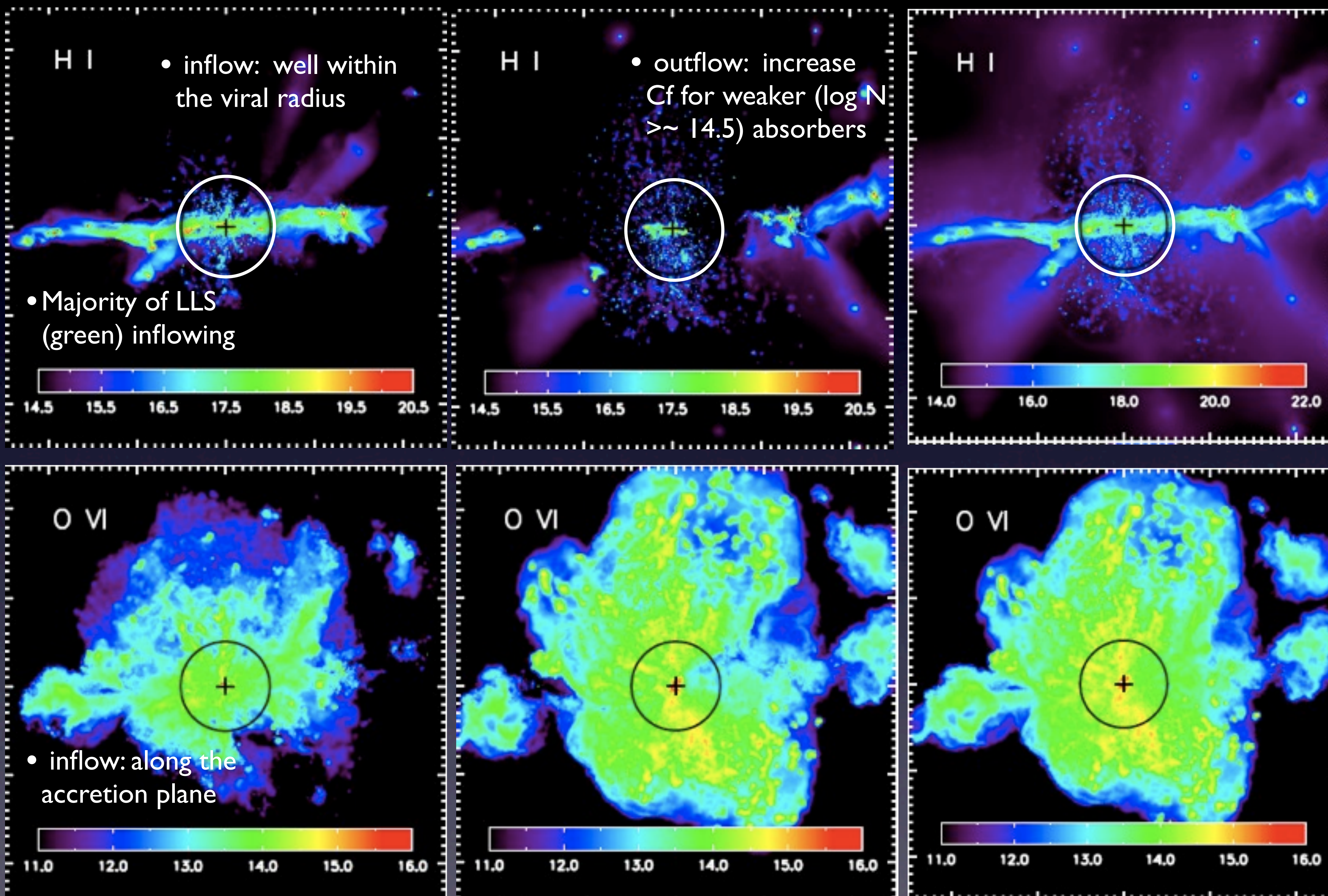

	H I	Si II	C II	Si IV	C IV	O VI
Inflow mass (%)	77%	66%	66%	50%	44%	32%

Inflowing and Outflowing CGM

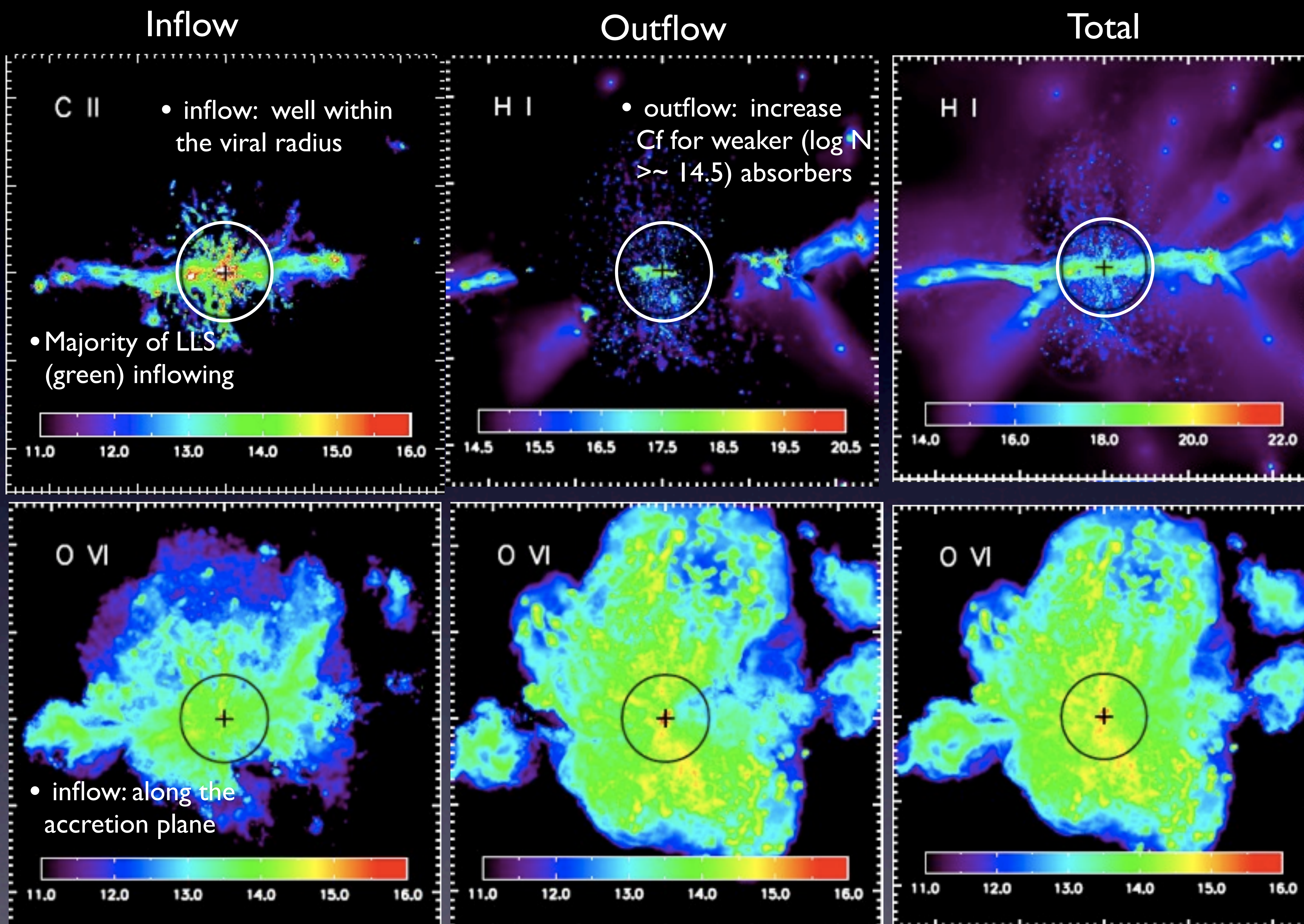

	H I	Si II	C II	Si IV	C IV	O VI
Inflow mass (%)	77%	66%	66%	50%	44%	32%

Inflowing and Outflowing CGM

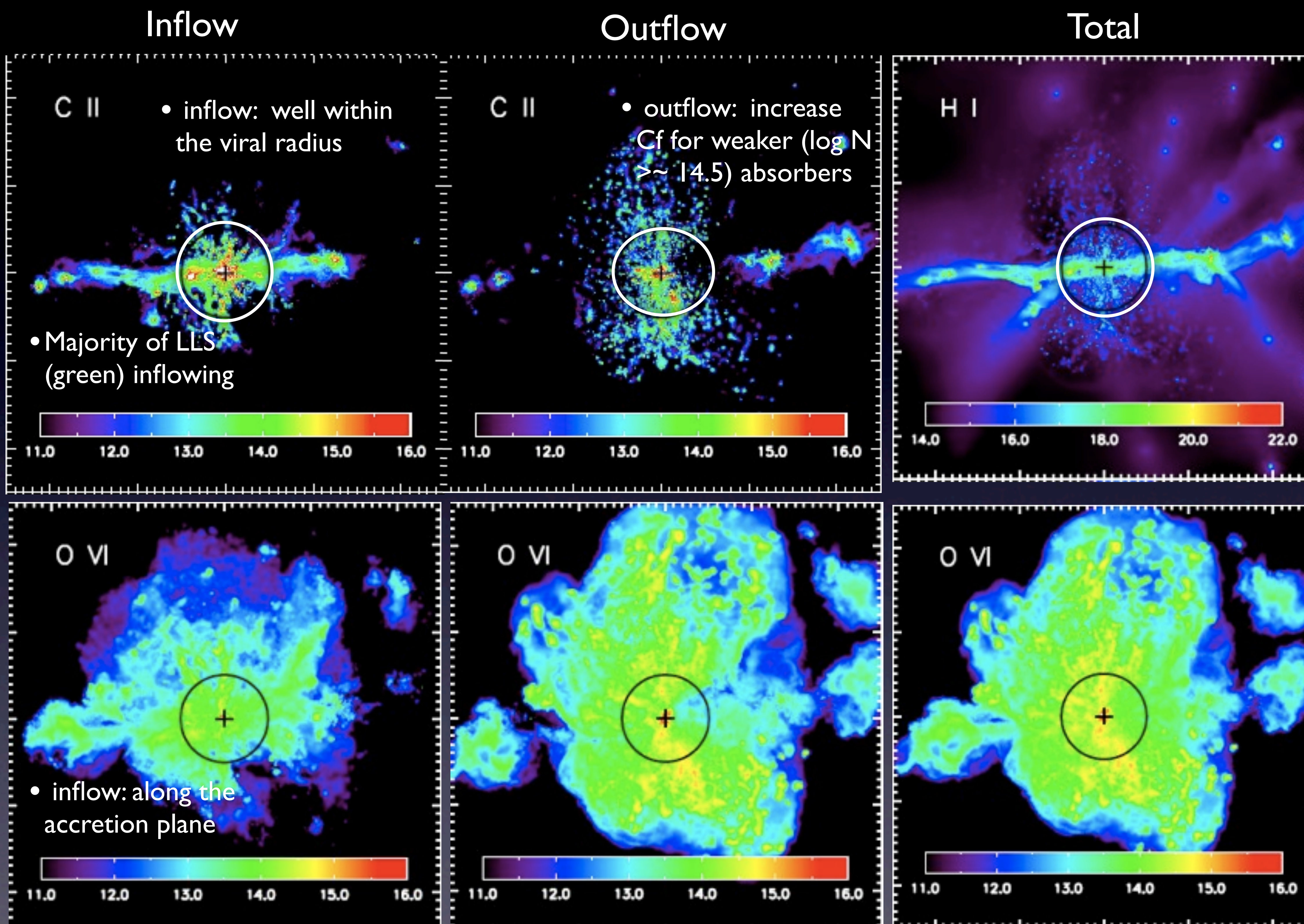

	H I	Si II	C II	Si IV	C IV	O VI
Inflow mass (%)	77%	66%	66%	50%	44%	32%

High ions: Collisional Ionization or Photoionization?

Cooler ($T \sim 3\text{-}5 \times 10^4$ K), clumpier, photoionized OVI

Hotter ($T > 10^5$K), more diffuse, collisionally ionized OVI

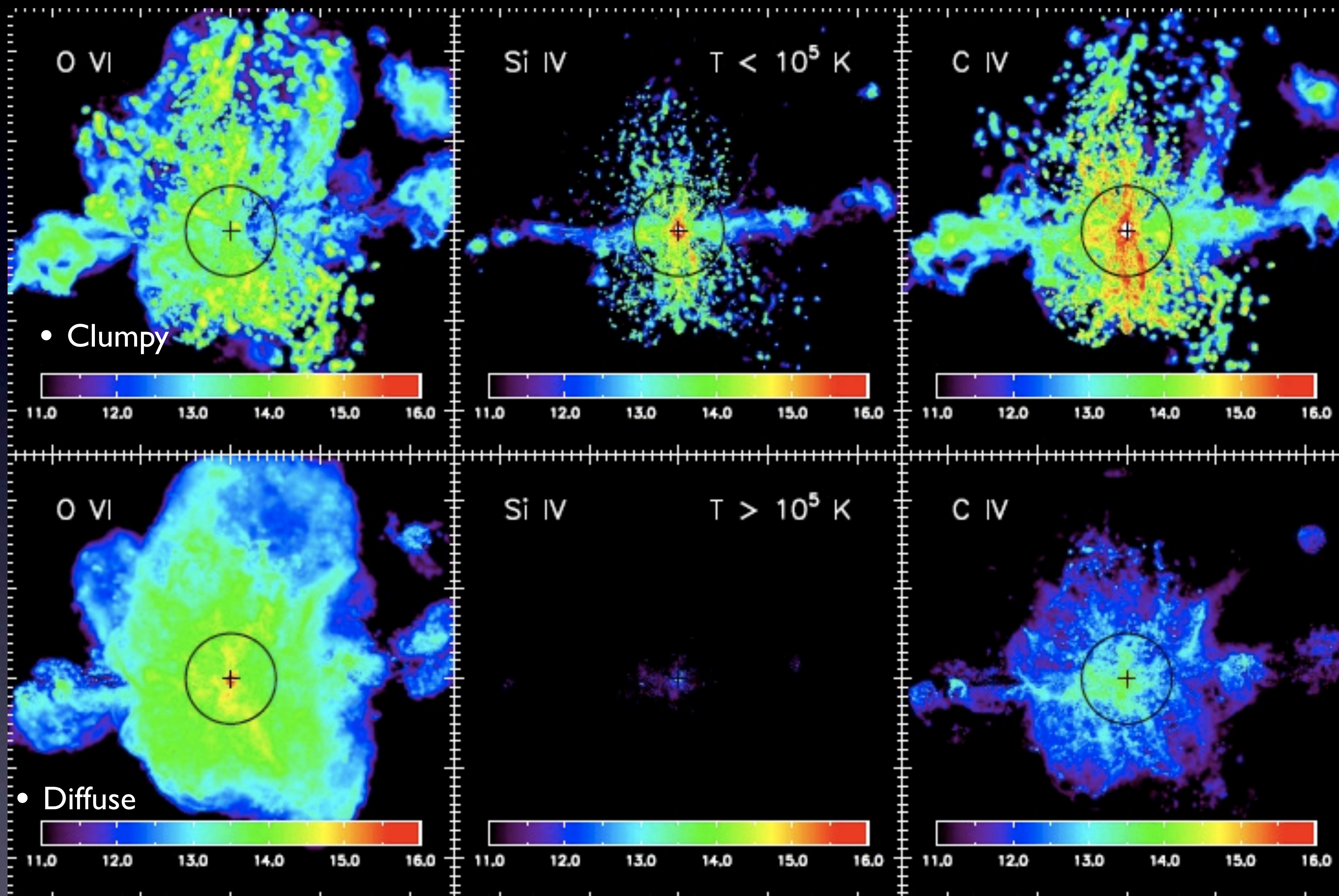

Si IV and C IV: Mostly photo-ionized

- O VI: mostly collisional ionized within 2 Rvir, but photo-ionized at larger distance

Synthetic Absorption Spectra

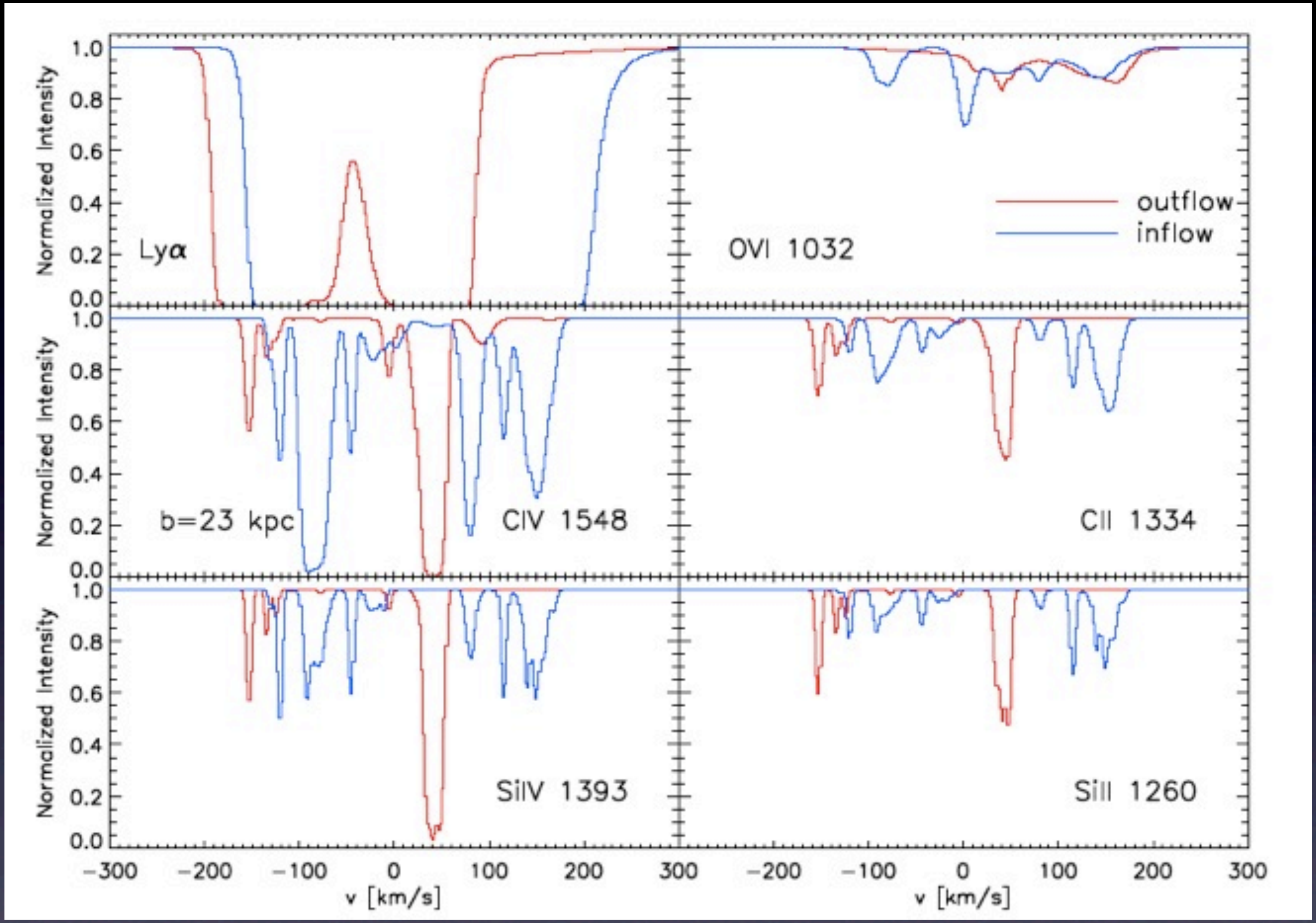

- Optical depth $\tau(\nu) = \sum_j (m_j Z_j/m) W_{2D}(r_{jl}, h_j)\sigma_j(\nu)$; $\sigma_j(\nu)$ - cross section (Voigt function), $W_{2D}(r_{jl}, h_j)$ - 2D SPH kernel

- Rest frame equivalent width: $W_0 = c/\nu_0^2 \int [1-e^{-\tau(\nu)}]d\nu$

Synthetic Absorption Spectra

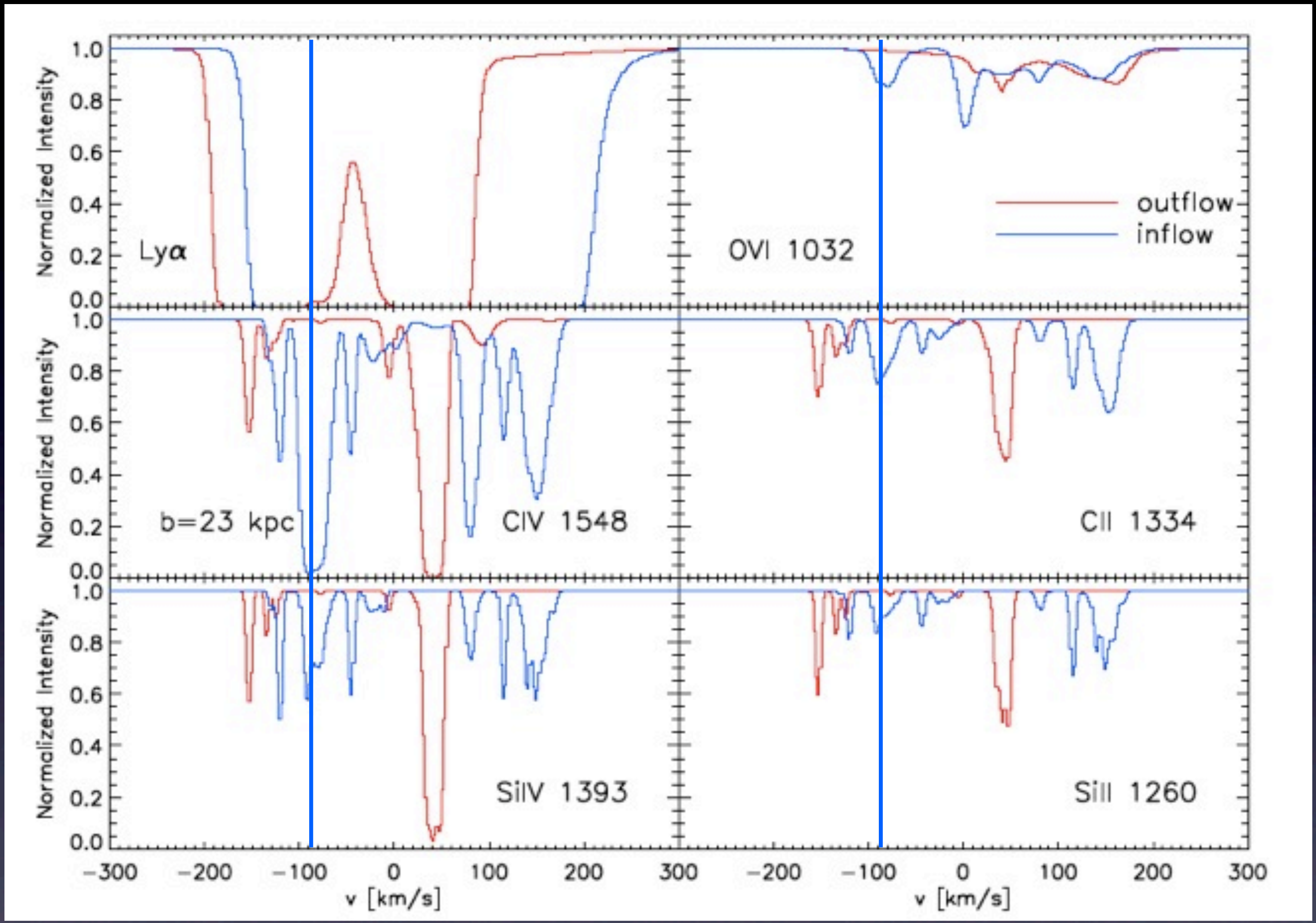

- Optical depth $\tau(\nu) = \sum_j (m_j Z_j/m) W_{2D}(r_{jl}, h_j)\sigma_j(\nu)$; $\sigma_j(\nu)$ - cross section (Voigt function), $W_{2D}(r_{jl}, h_j)$ - 2D SPH kernel

- Rest frame equivalent width: $W_0 = c/\nu_0^2 \int [1-e^{-\tau(\nu)}]d\nu$

Synthetic Absorption Spectra

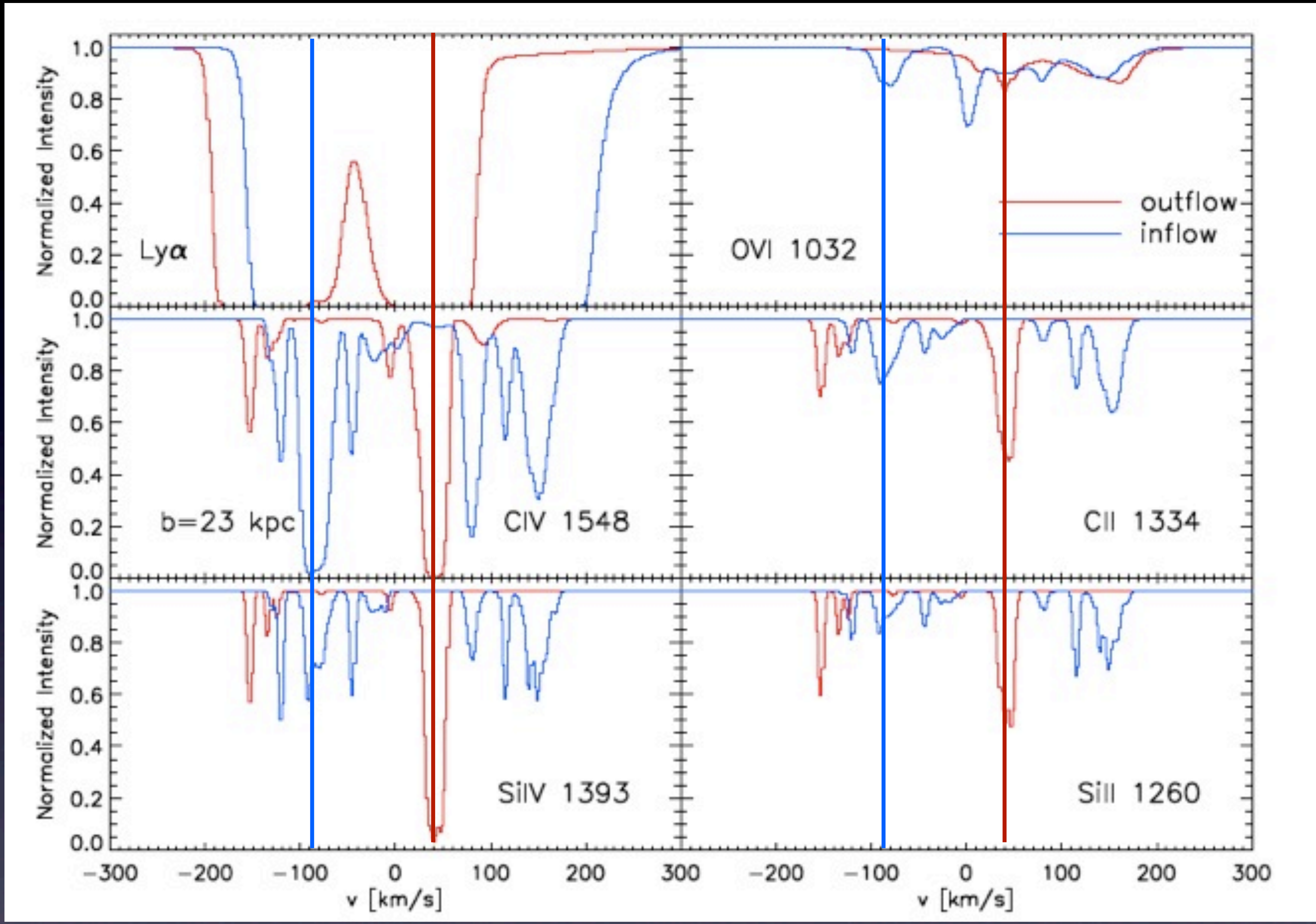

- Optical depth $\tau(\nu) = \sum_j (m_j Z_j/m) W_{2D}(r_{jl}, h_j)\sigma_j(\nu)$; $\sigma_j(\nu)$ - cross section (Voigt function), $W_{2D}(r_{jl}, h_j)$ - 2D SPH kernel
- Rest frame equivalent width: $W_0 = c/\nu_0^2 \int [1-e^{-\tau(\nu)}]d\nu$

Synthetic Absorption Spectra

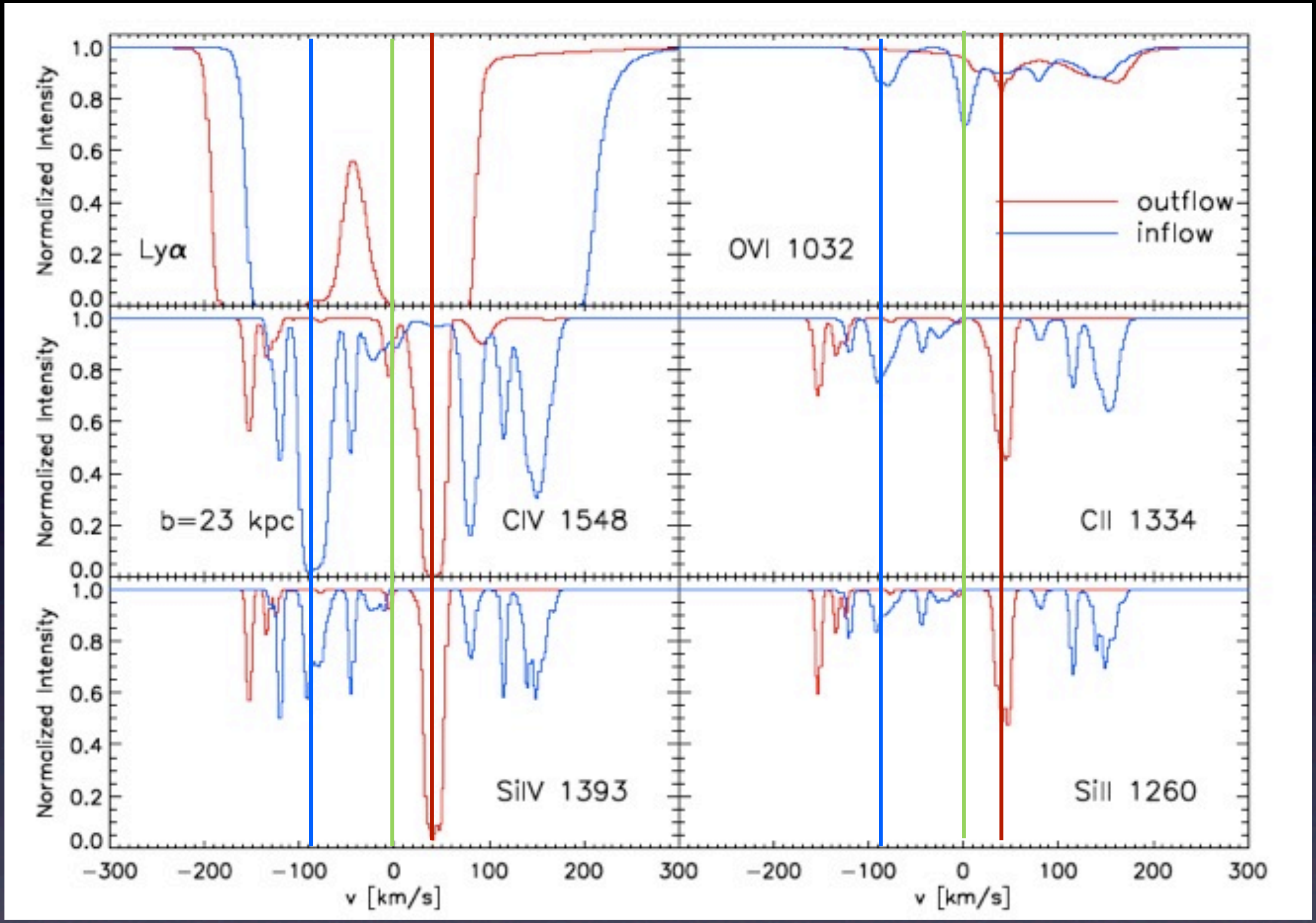

- Most, but not all, components exist in both high and low ions -- Multi-phase nature of absorbers

- Optical depth $\tau(\nu) = \sum_j (m_j Z_j/m) W_{2D}(r_{jl}, h_j)\sigma_j(\nu)$; $\sigma_j(\nu)$ - cross section (Voigt function), $W_{2D}(r_{jl}, h_j)$ - 2D SPH kernel

- Rest frame equivalent width: $W_0 = c/\nu_0^2 \int [1-e^{-\tau(\nu)}]d\nu$

Synthetic Absorption Spectra

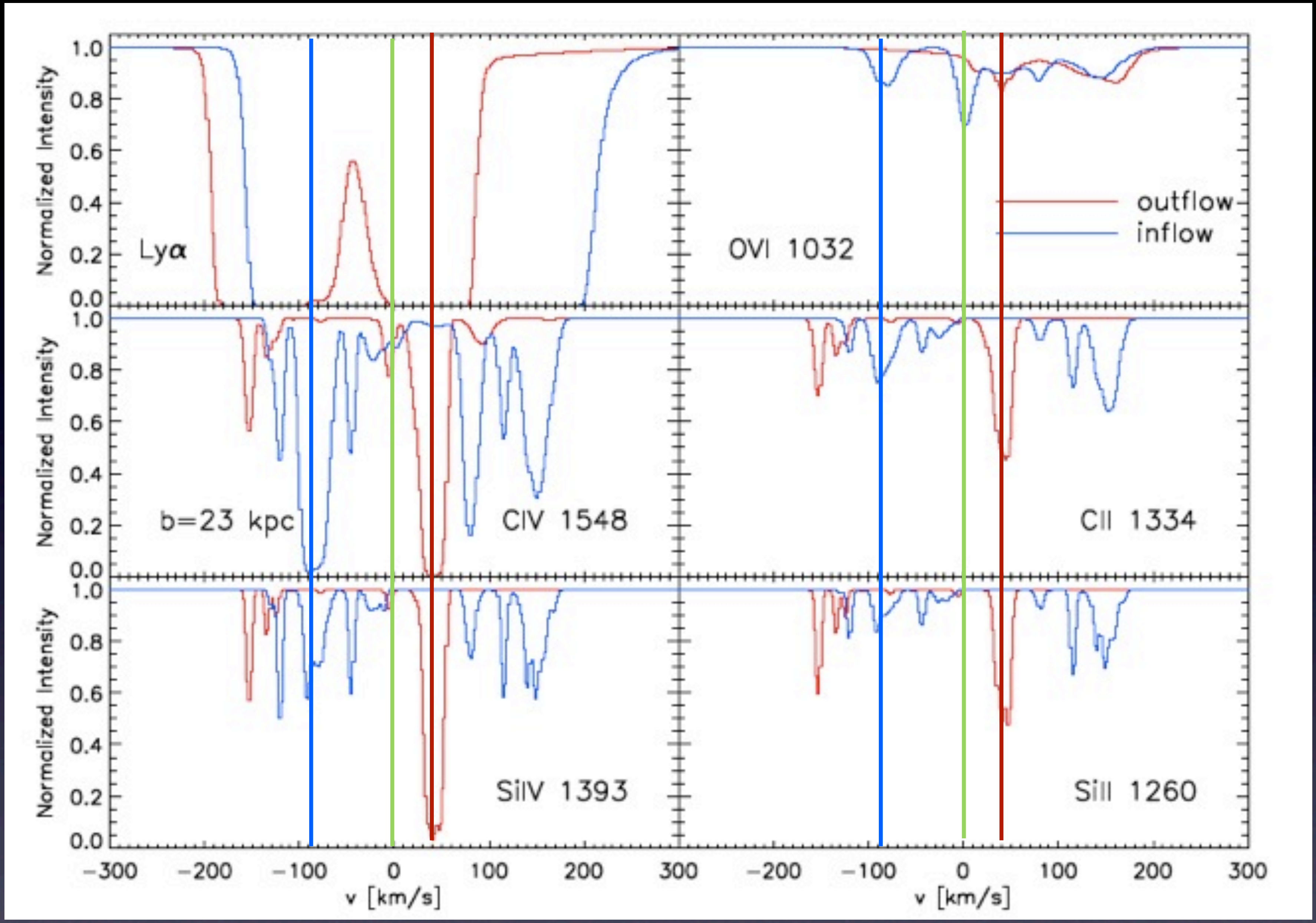

- Most, but not all, components exist in both high and low ions -- Multi-phase nature of absorbers
- Velocity range ~ ± 300 km/s

- Optical depth $\tau(\nu) = \sum_j (m_j Z_j/m) W_{2D}(r_{jl}, h_j)\sigma_j(\nu)$; $\sigma_j(\nu)$ - cross section (Voigt function), $W_{2D}(r_{jl}, h_j)$ - 2D SPH kernel
- Rest frame equivalent width: $W_0 = c/\nu_0^2 \int [1-e^{-\tau(\nu)}]d\nu$

Synthetic Absorption Spectra

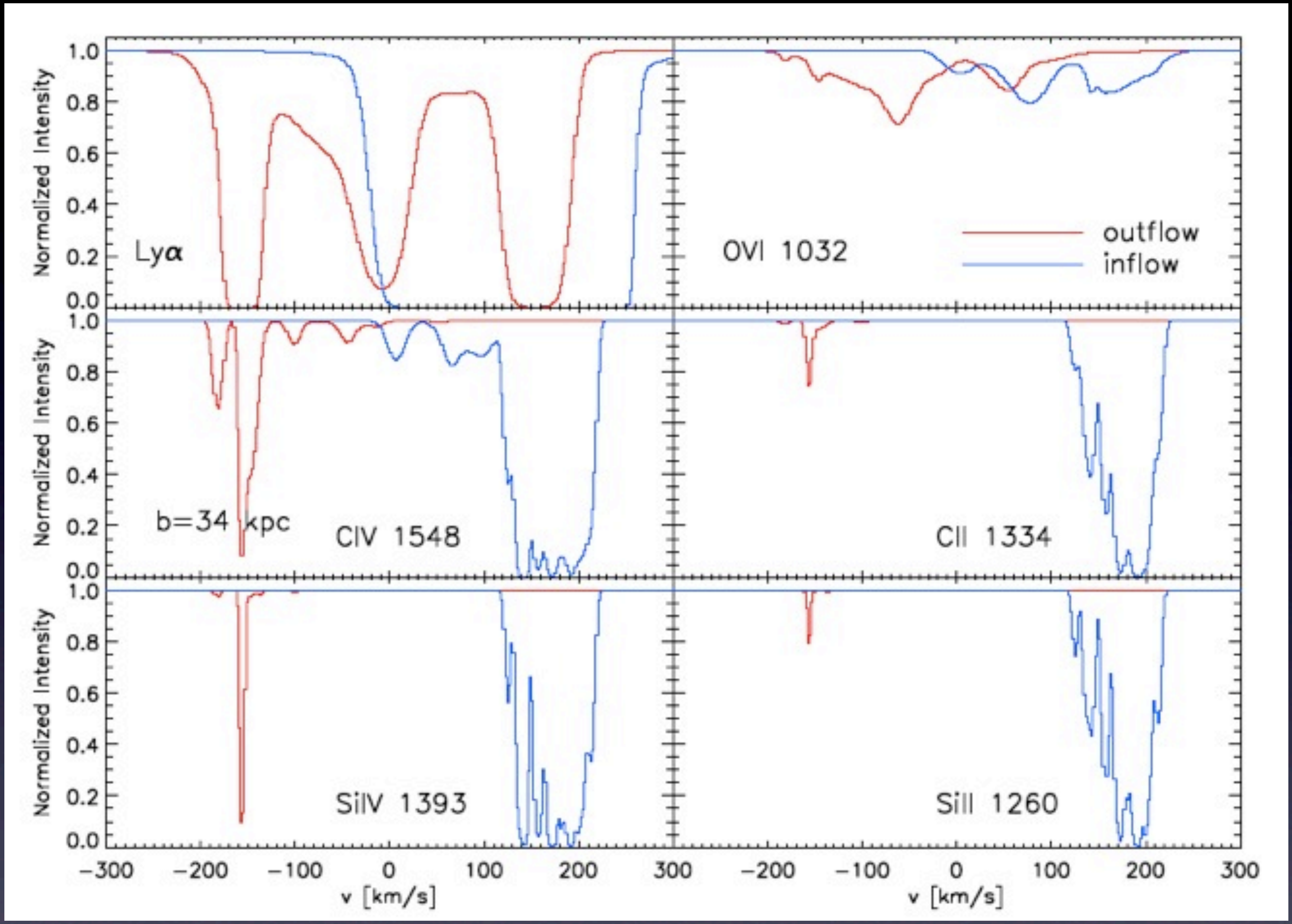

- Most, but not all, components exist in both high and low ions -- Multi-phase nature of absorbers
- Velocity range ~ ± 300 km/s

- Optical depth $\tau(\nu) = \sum_j (m_j Z_j/m) W_{2D}(r_{jl}, h_j)\sigma_j(\nu)$; $\sigma_j(\nu)$ - cross section (Voigt function), $W_{2D}(r_{jl}, h_j)$ - 2D SPH kernel
- Rest frame equivalent width: $W_0 = c/\nu_0^2 \int [1-e^{-\tau(\nu)}]d\nu$

Synthetic Absorption Spectra

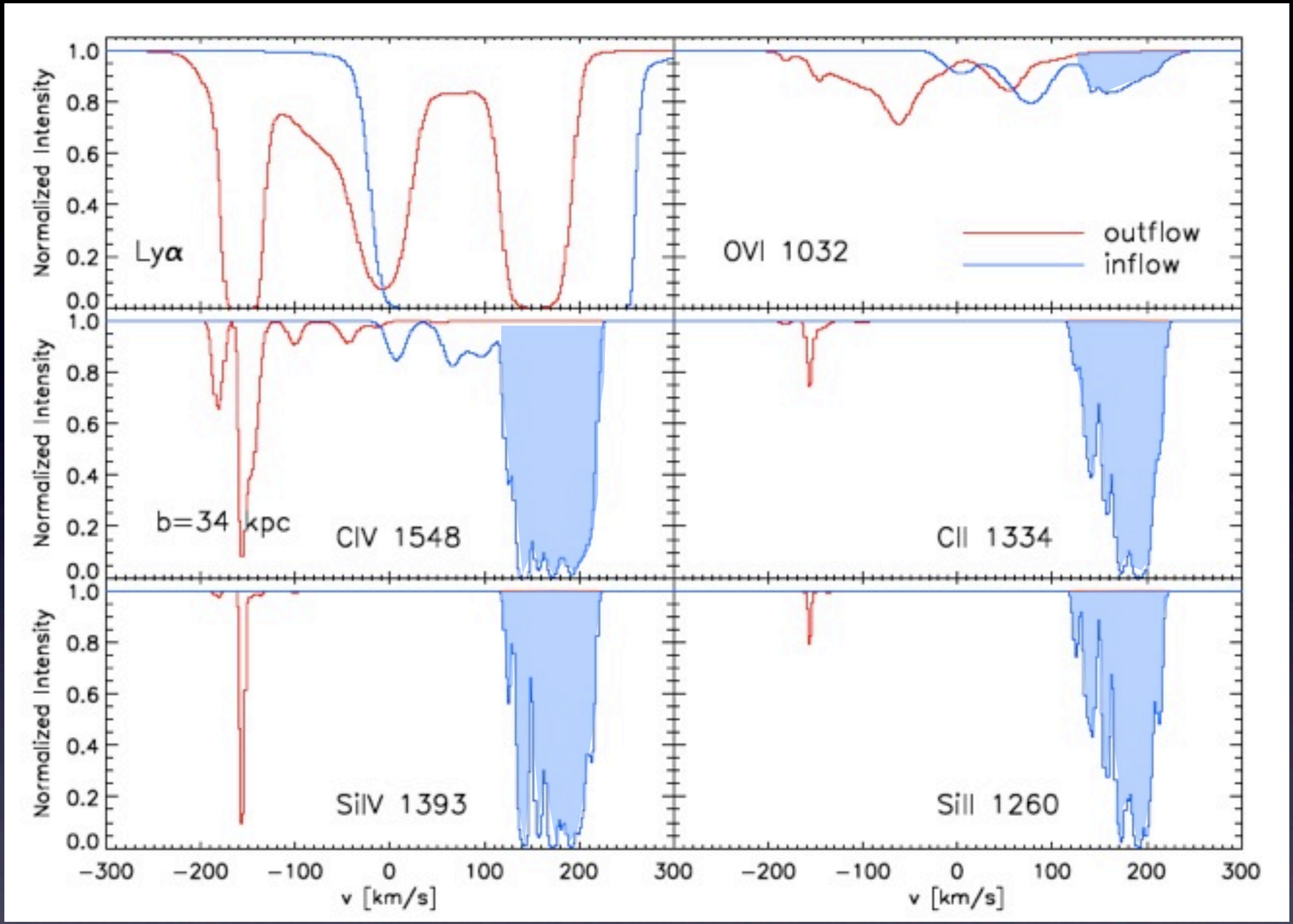

- Most, but not all, components exist in both high and low ions -- Multi-phase nature of absorbers
- Velocity range ~ ± 300 km/s

- Metal enriched infalling gas:
- $R_{vir} < r < 2R_{vir}$
- $\delta \sim 100$
- $Z > 0.03\ Z_{sun}$
- Enriched gas around nearby dwarf galaxy

- Optical depth $\tau(\nu) = \sum_j (m_j Z_j/m) W_{2D}(r_{jl}, h_j)\sigma_j(\nu)$; $\sigma_j(\nu)$ - cross section (Voigt function), $W_{2D}(r_{jl}, h_j)$ - 2D SPH kernel
- Rest frame equivalent width: $W_0 = c/\nu_0^2 \int [1-e^{-\tau(\nu)}]d\nu$

W_0-b Relation and Comparison with Observations

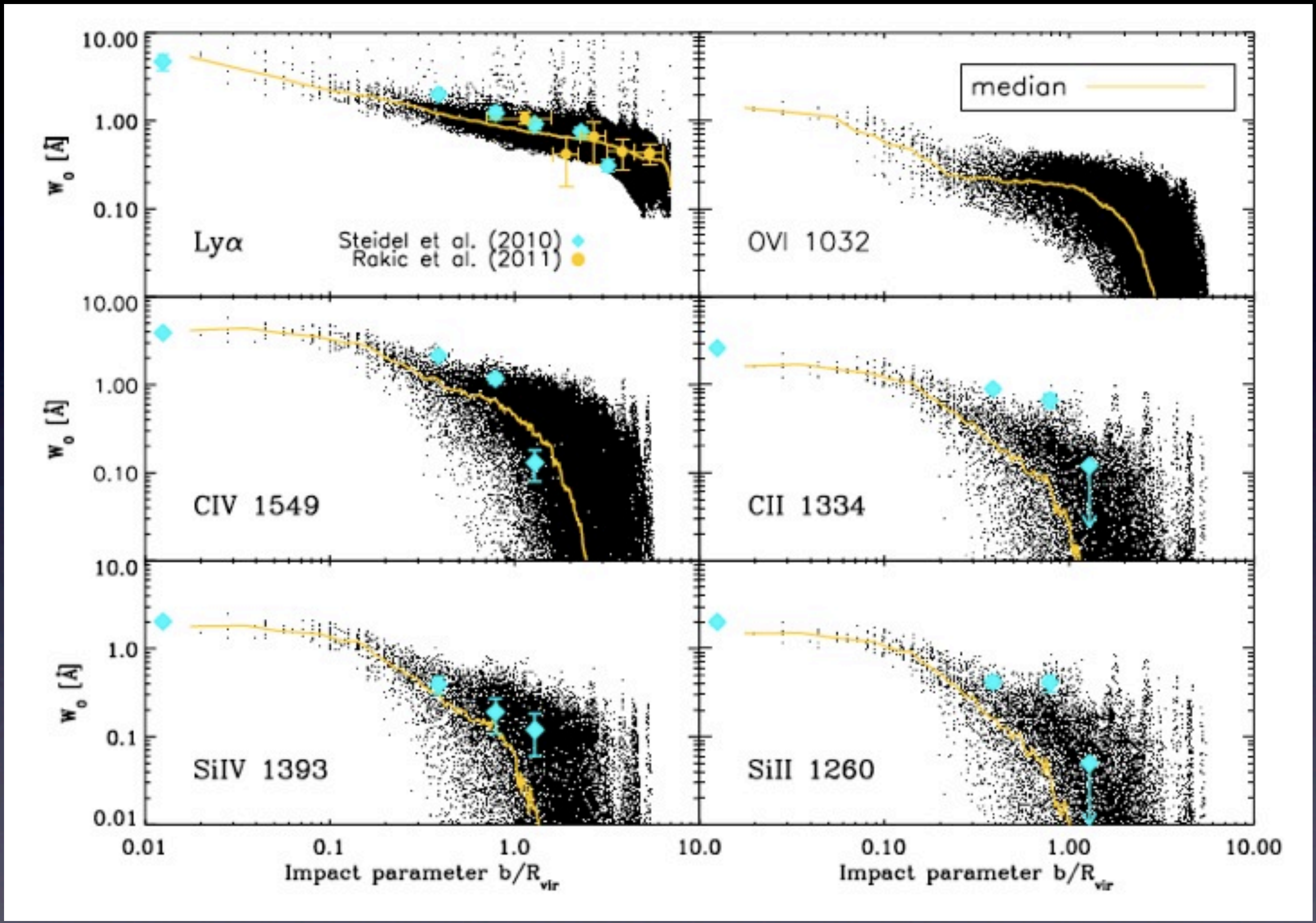

- Metal Line strength decline rapidly at 1-2 R_{vir}
- Line strength decline less fast for C IV, OVI and H I
- Ly α: remains strong to >~ 5 R_{vir}
- Broadly consistent with observations from Steidel+ (2010) and Rakic+ (2011)
- W_0 for metal ions: Higher than simulations without strong outflows (e.g., Fumagalli+ 2011; Goerdt + 2012)
- At small b, lines are mostly saturated -- W_0 determined by velocity

- 3 orthogonal projections, each has 500 x 500 evenly-spaced slightlines within b = 250 kpc region centered at the main host

Covering Factor of H I and Metal Ions

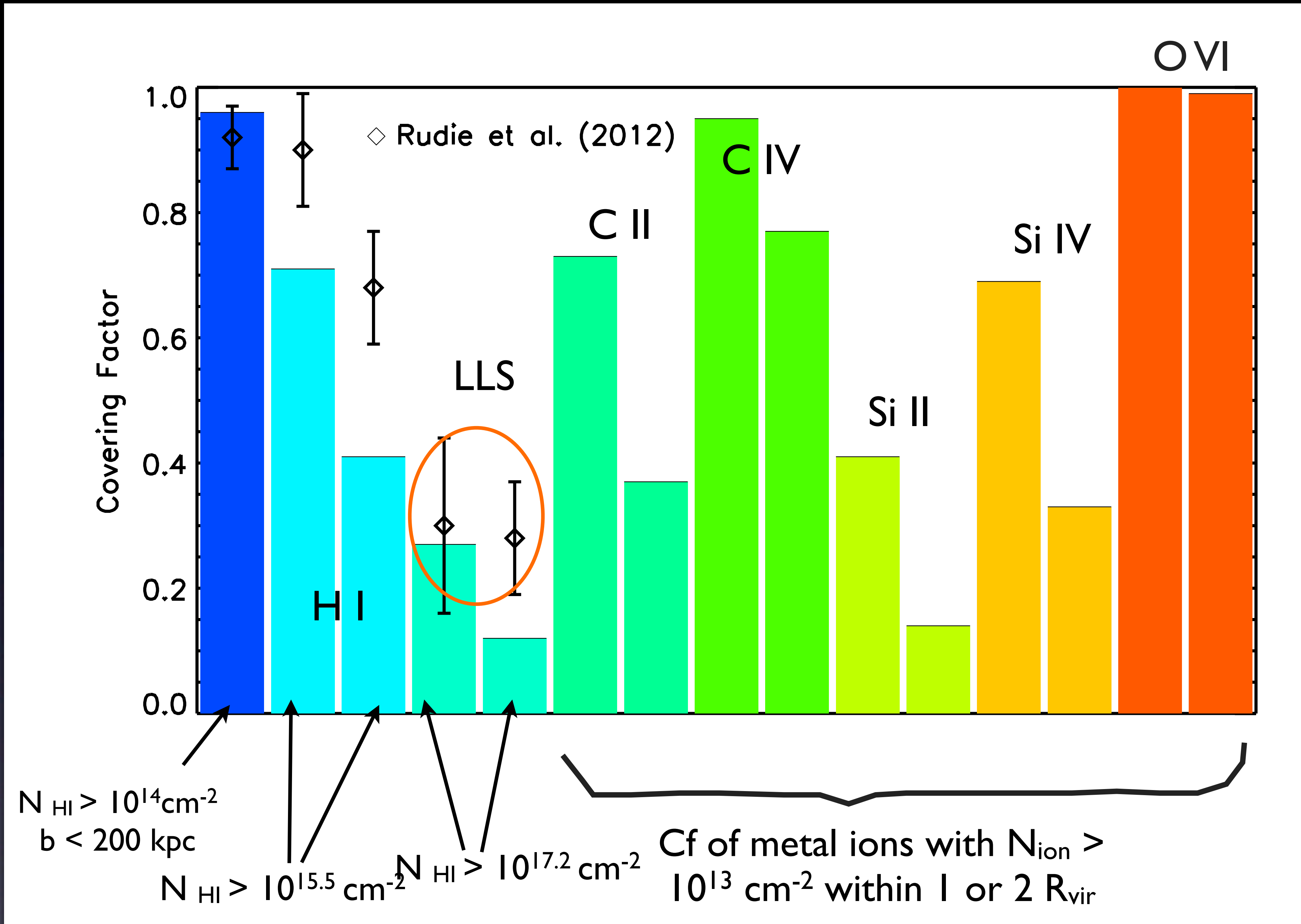

- O VI has covering factor (Cf) of unity in 2 R_{vir}. C IV also have large Cf
- C II, Si II, Si IV: smaller Cf, decline fast when $b > R_{vir}$

- In reasonable agreement with Rudie+ (2012) for H I, but in the low side for $N_{HI} > 10^{15.5}$ cm^{-2}
- H I covering factor: slightly higher but consistent with simulations without strong outflows (e.g. Fumagalli+2011, Faucher-Giguère & Kereš 2011)

Detecting the Cold Streams: H I and Low Ions

- Cold ($T < 10^5$ K) inflow rates at R_{vir} $dM_{in, cold}/dt = 18\ M_{sun}/yr$, comparable to the SFR; $M_{in, hot}/dt \sim 5M_{sun}/yr$
- 35% inflow gas from nearby dwarfs
- Within 2 Rvir: 90% of LLS are inflowing gas, v_{in} <~ 150 -200 km/s

Detecting the Cold Streams: H I and Low Ions

Inflow only, optically thick gas

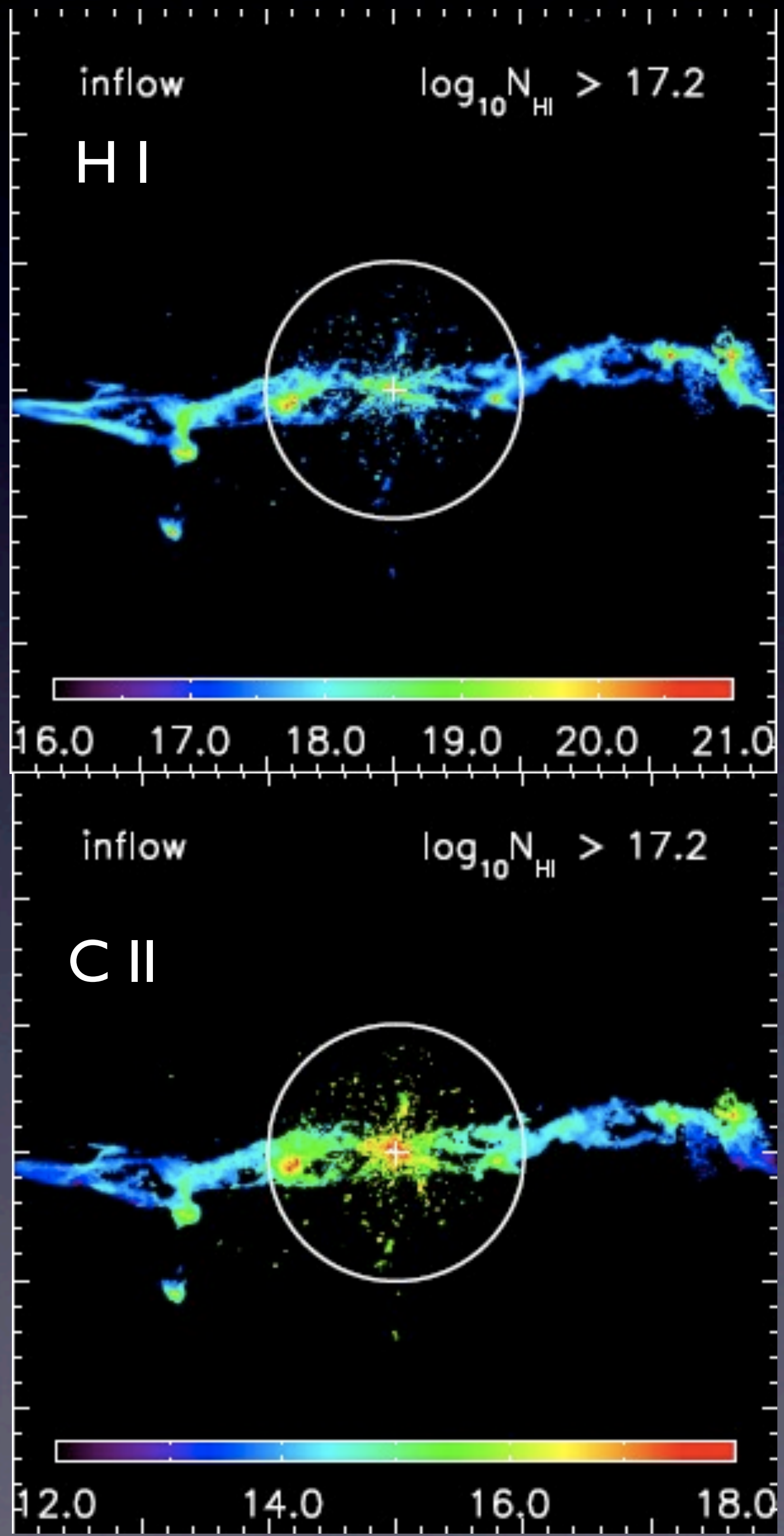

- Cold ($T < 10^5$ K) inflow rates at R_{vir} $dM_{in,\,cold}/dt = 18\ M_{sun}/yr$, comparable to the SFR; $M_{in,\,hot}/dt \sim 5M_{sun}/yr$
- 35% inflow gas from nearby dwarfs
- Within 2 Rvir: 90% of LLS are inflowing gas, v_{in} <~ 150 -200 km/s

Detecting the Cold Streams: H I and Low Ions

Inflow only, optically thick gas

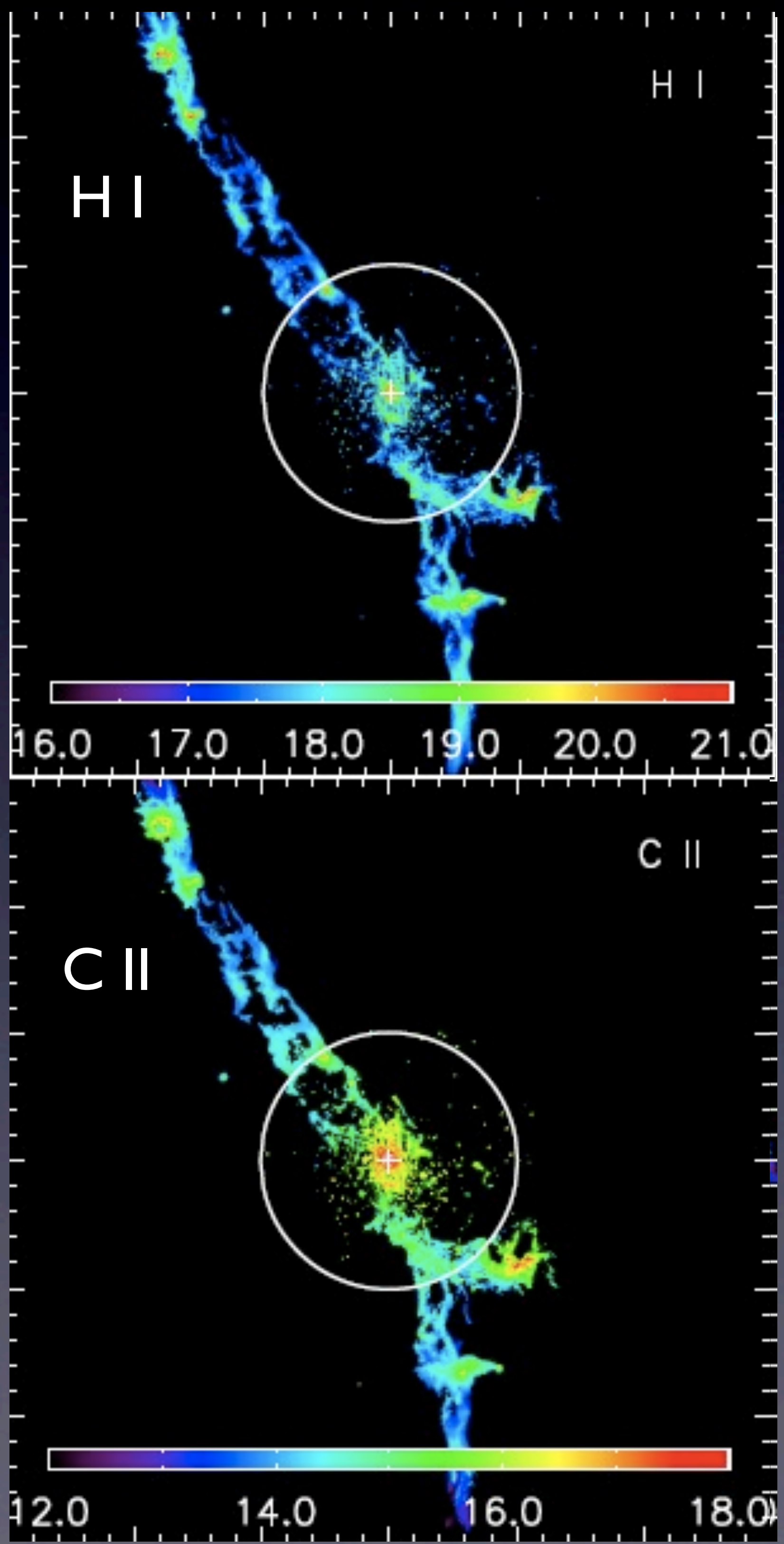

- Cold ($T < 10^5$ K) inflow rates at R_{vir} $dM_{in,\,cold}/dt$ = 18 M_{sun}/yr, comparable to the SFR; $M_{in,\,hot}/dt \sim 5 M_{sun}$/yr
- 35% inflow gas from nearby dwarfs
- Within 2 Rvir: 90% of LLS are inflowing gas, v_{in} <~ 150 -200 km/s

Detecting the Cold Streams: H I and Low Ions

Inflow only, optically thick gas

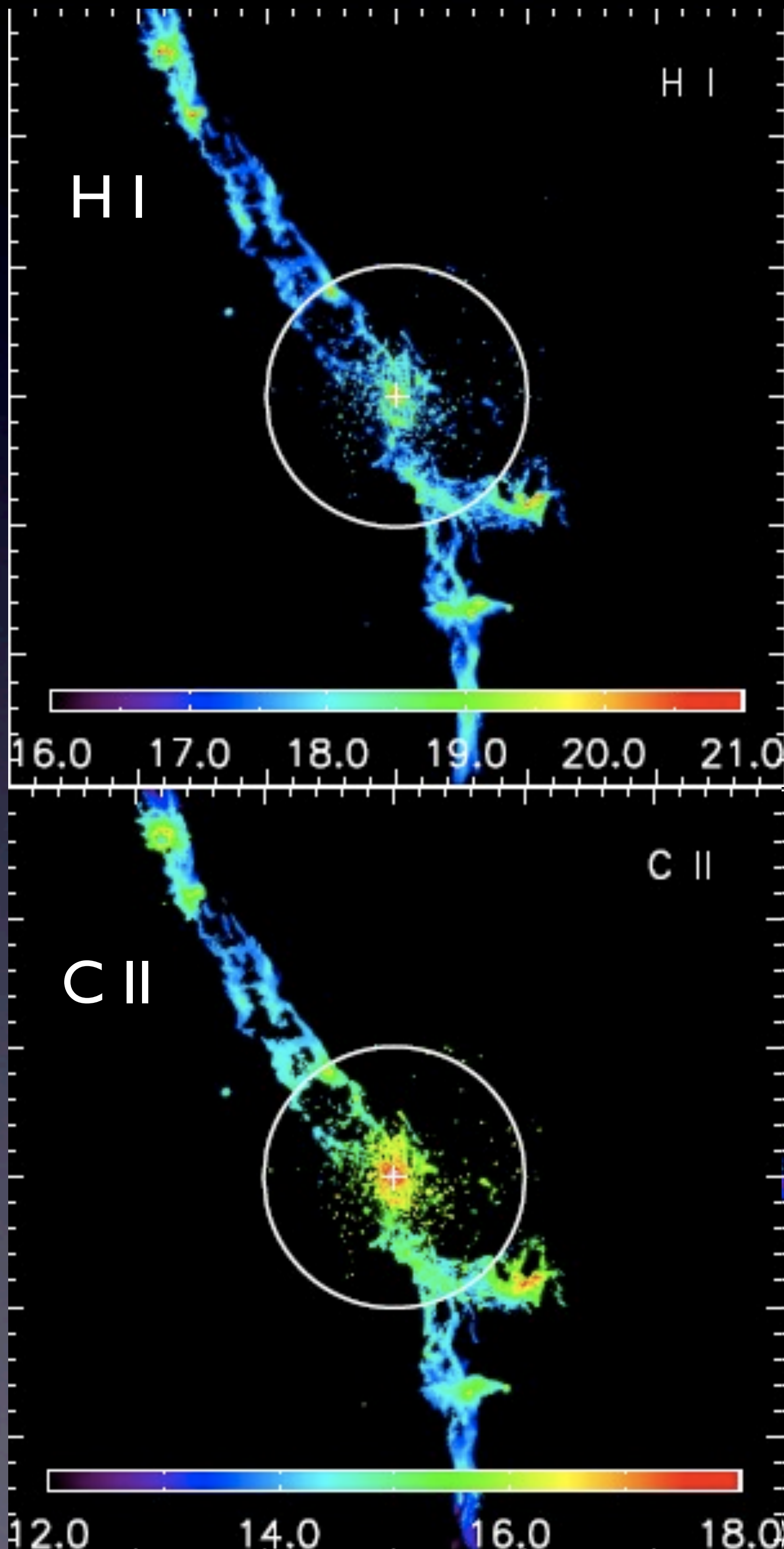

- Cold ($T < 10^5$ K) inflow rates at R_{vir} $dM_{in,\,cold}/dt = 18\ M_{sun}/yr$, comparable to the SFR; $M_{in,\,hot}/dt \sim 5 M_{sun}/yr$
- 35% inflow gas from nearby dwarfs
- Within 2 Rvir: 90% of LLS are inflowing gas, v_{in} <~ 150 -200 km/s
- Cold inflows are enriched: $Z_{LLS} > 0.03\ Z_{sun}$ for $r < R_{vir}$, and $Z_{LLS} > 0.01\ Z_{sun}$ within $2R_{vir}$
- Still lower than outflow metallicities Z_{out} = 0.1-0.5 Z_{sun}

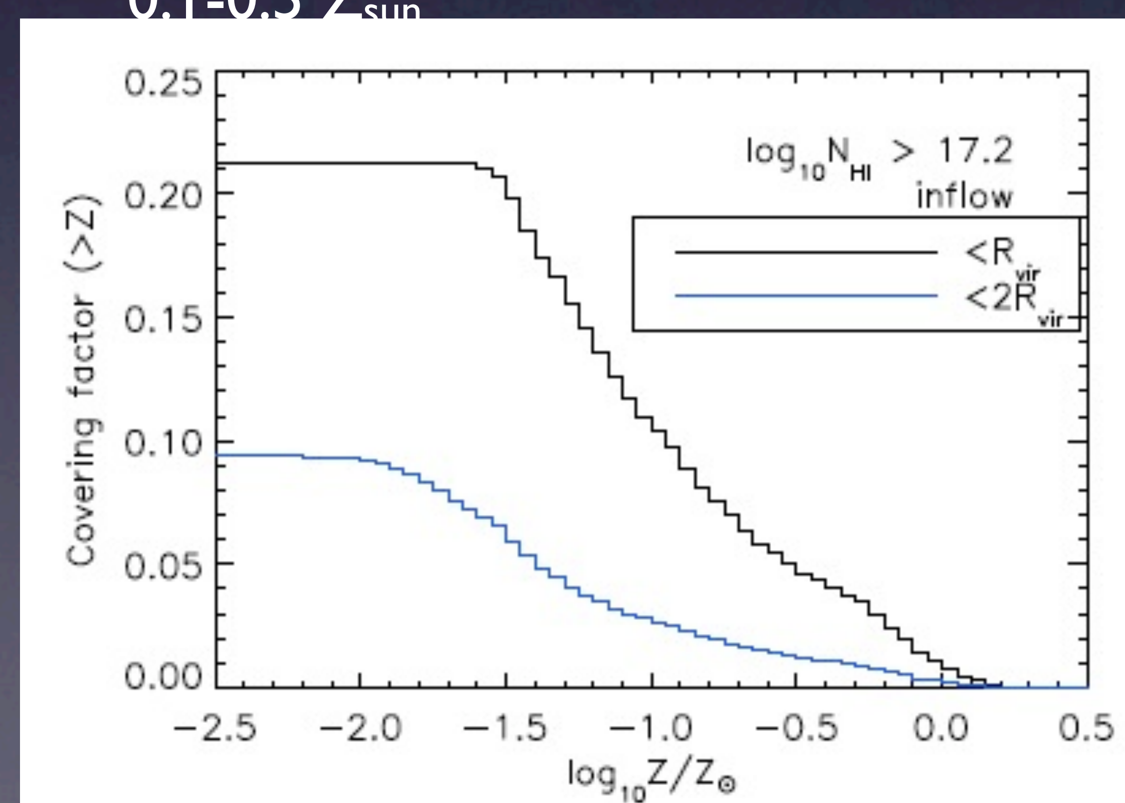

Bimodal Metallicity Distribution of Cold CGM

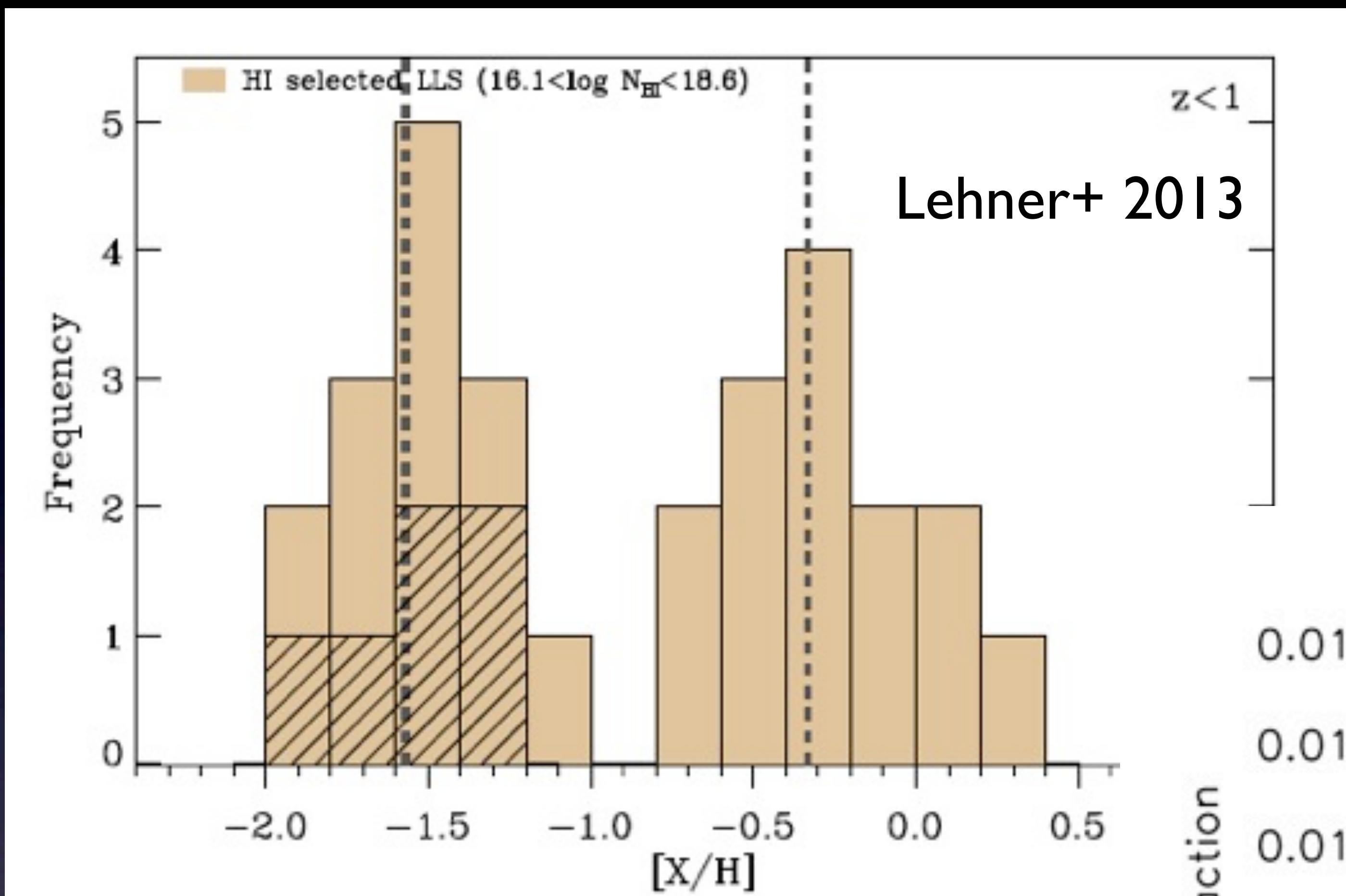

At z = 2.8, metallicity comparable to z ~ 1:

1. Halo assembly history: M* ~ 1/3 of $M*_{Mw}$ at z =2.8
2. Winds recycle too much?
3. Mixing?

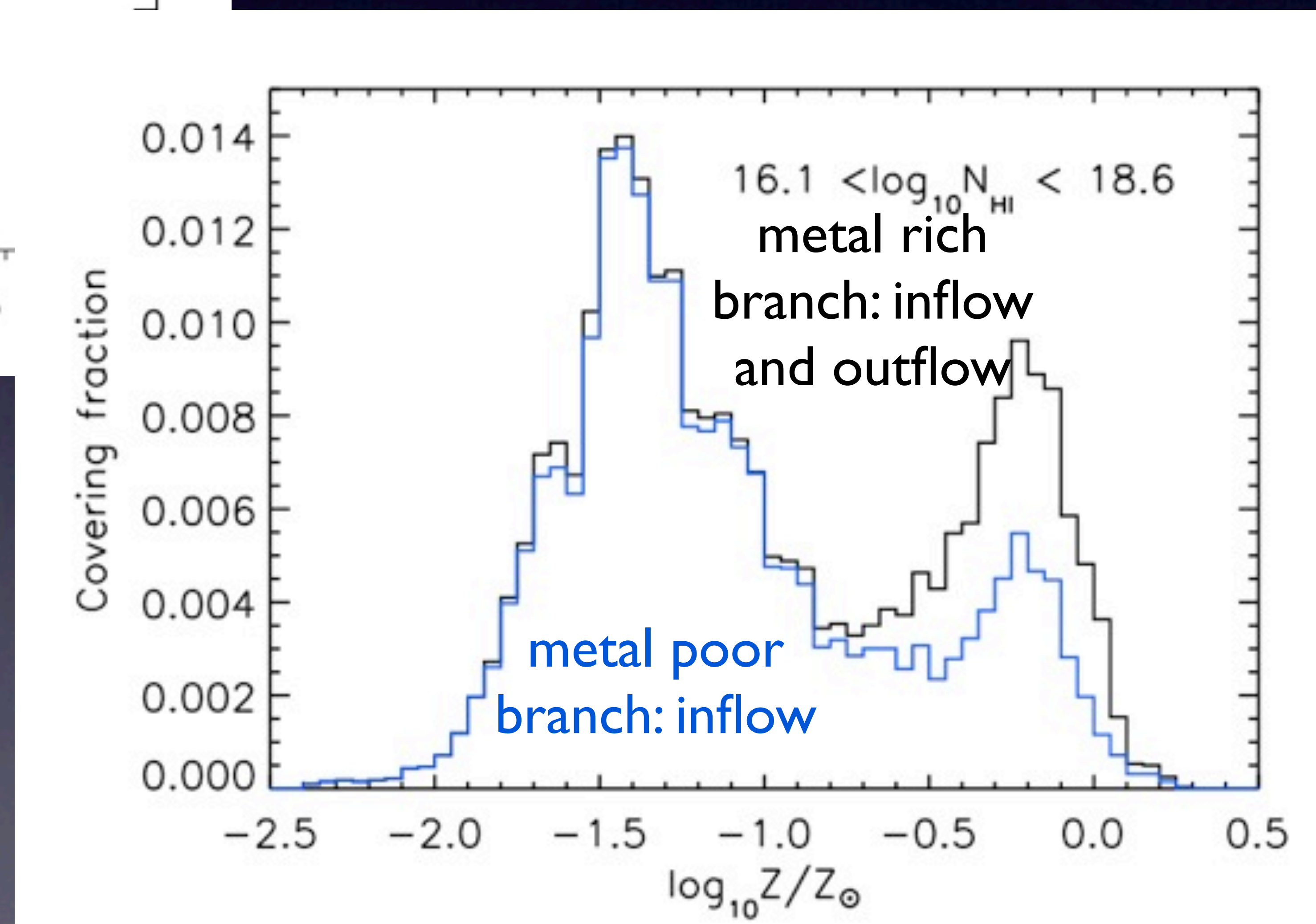

- LLS systems at z < *1*, 16.1 < log N_{HI} < 18.6
  - Bimodal distribution:
  - metal-poor: accretion flows
  - metal-rich: outflows, recycled wind?

Evolution of the CGM around Massive Galaxies
(Preliminary)

Evolution of the CGM: H I

Preliminary!

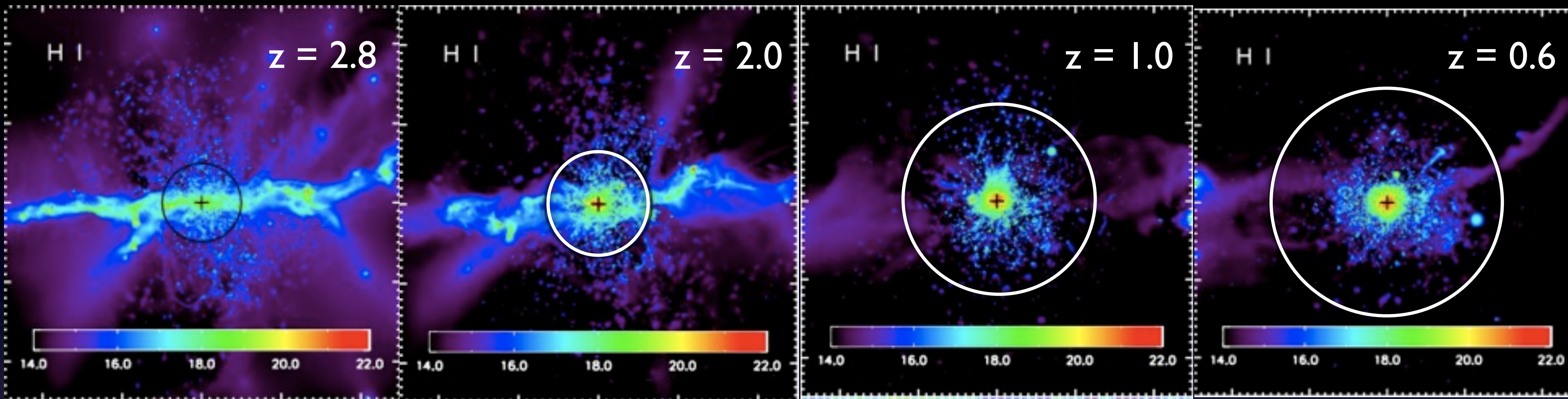

- "Cold stream" mode decays;
- Covering fraction (Cf) of optically thick H I (LLS) decrease rapidly at larger distances due to the fading of code streams (increases in the center due to growth of disk)
- Cf above 20% at z = 2-3, larger than simulations without outflows (e.g., Faucher-Giguere+2011; Fumagalli+2011)

Redshift	Cf (< R_{vir})	Cf (<2 R_{vir})
z = 2.8	27%	12%
z = 2.0	24%	7.5%
z = 1.0	7.9%	2%
z = 0.6	4.4%	1.1%

Evolution of the CGM: H I

Preliminary!

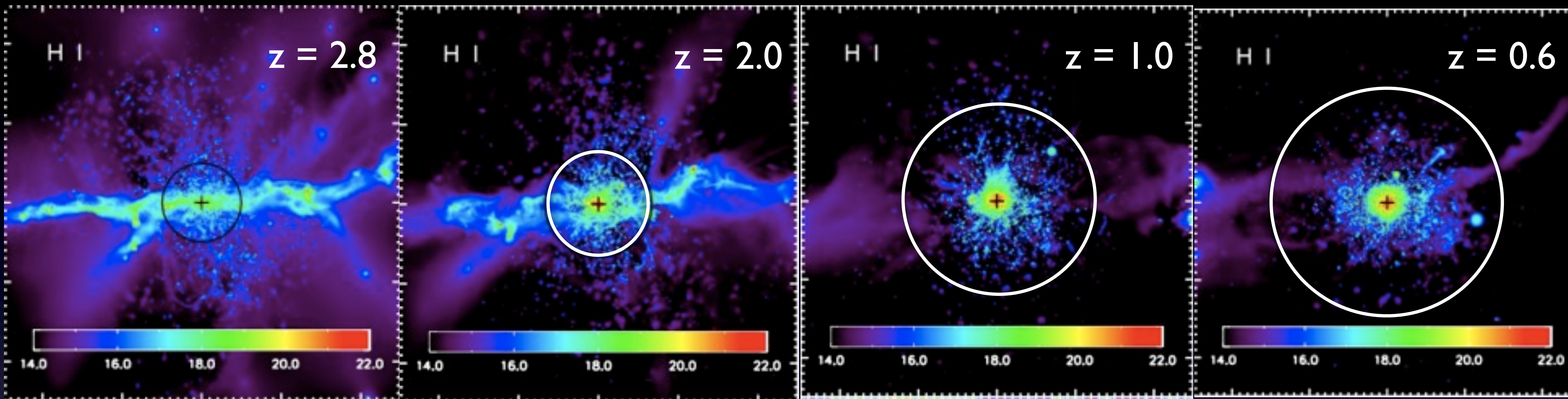

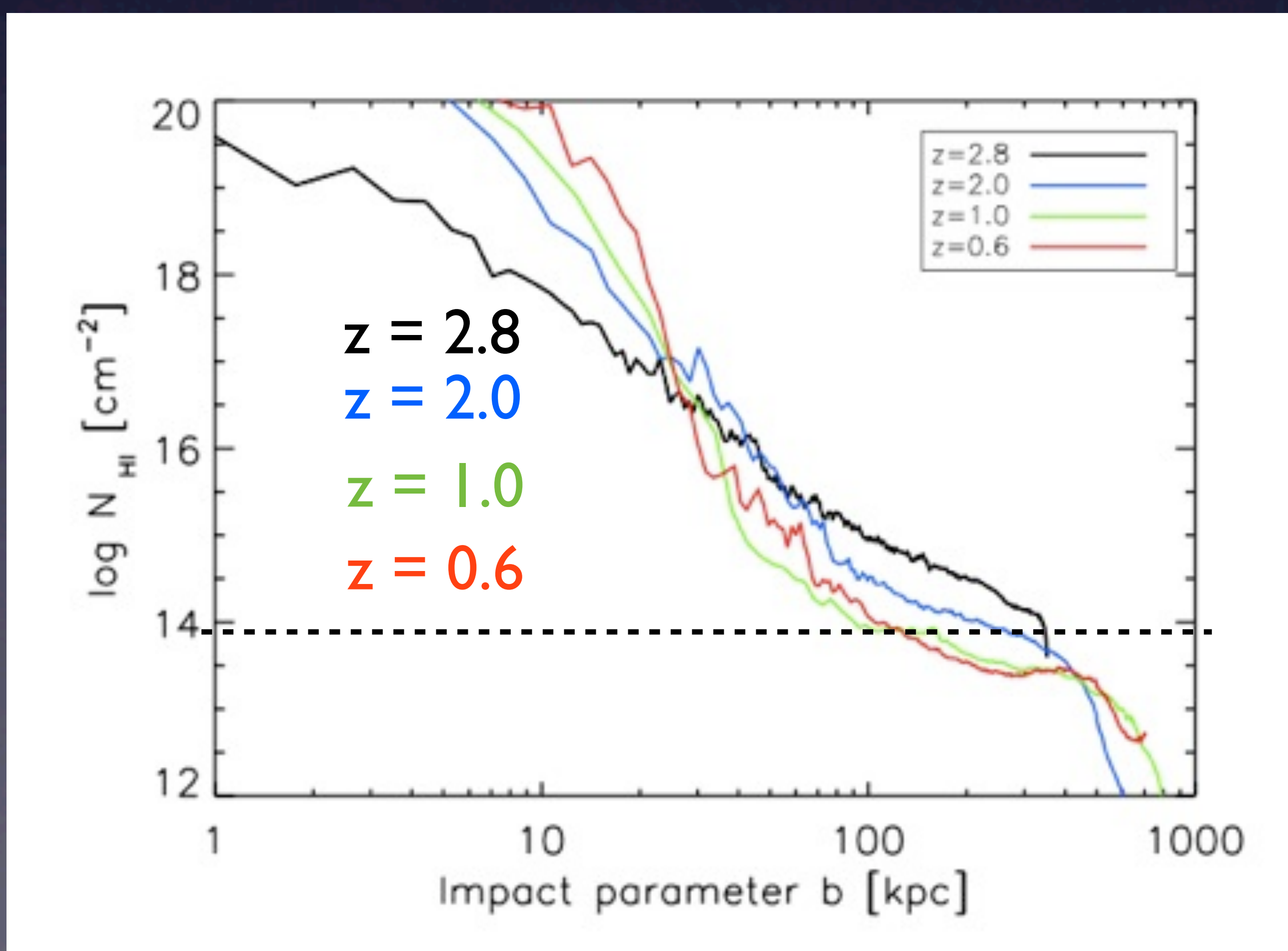

Redshift	Cf (< R_{vir})	Cf (<2 R_{vir})
z = 2.8	27%	12%
z = 2.0	24%	7.5%
z = 1.0	7.9%	2%
z = 0.6	4.4%	1.1%

Although the Cf of LLS declines, the Cf of the systems >~ 10^{14} cm^{-2} remain high up to 100 kpc at z = 0.6, consistent with Werk et al. 2013

Evolution of the CGM: Total Metal Column Density

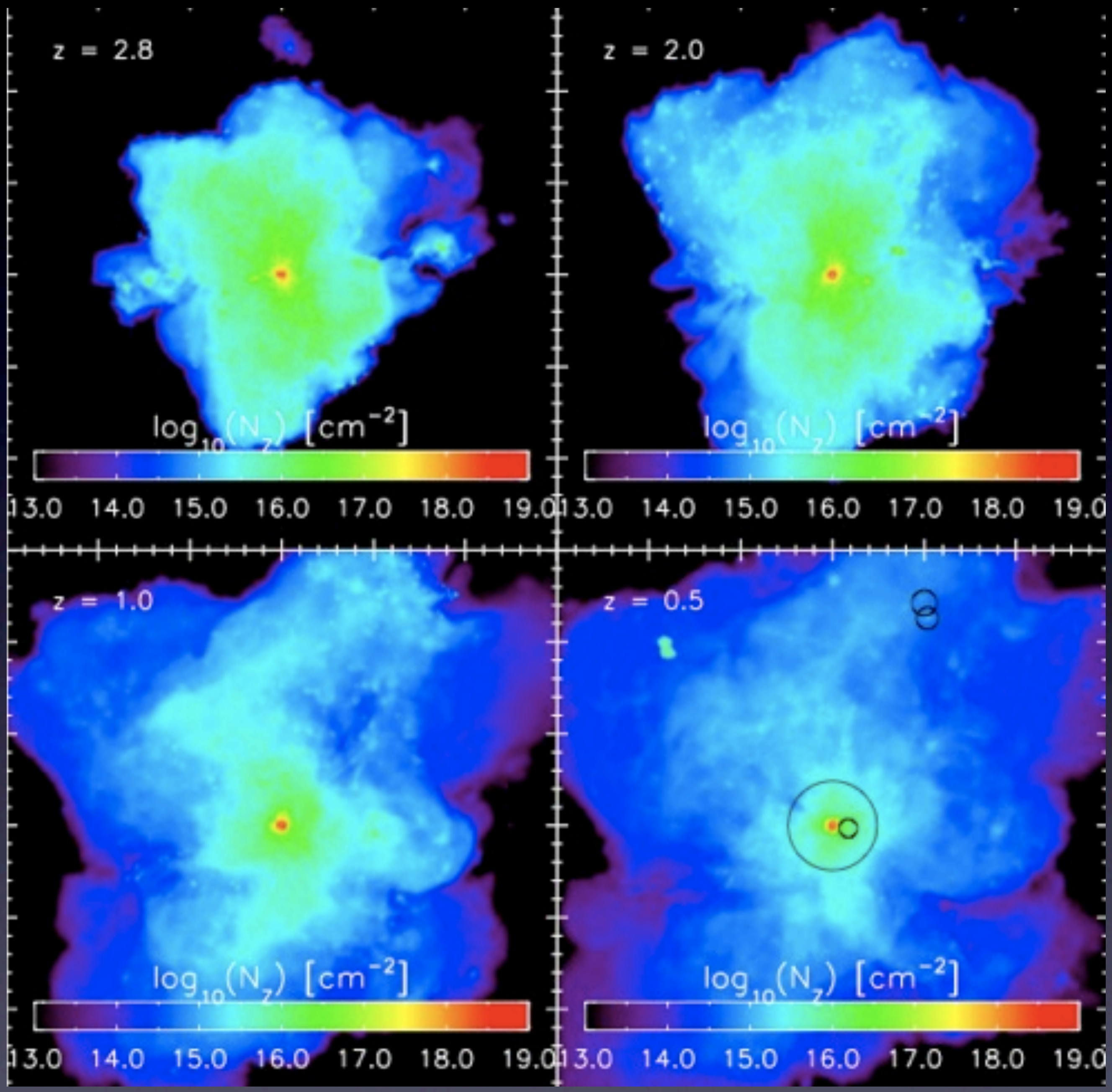

The growth of metal-enriched region in comoving coordinates, box size 3 Mpc on a side. The column density is physical, NOT comoving.

- The SFR decreases from 20 M_{sun}/yr to 4 M_{sun}/yr; Halo mass increase from 2e11 to 6e11 M_{sun}
- Enriched region grows in comoving space, and does not grow significantly below z = 1.0. Metals passively dispersed from the expansion of the Universe

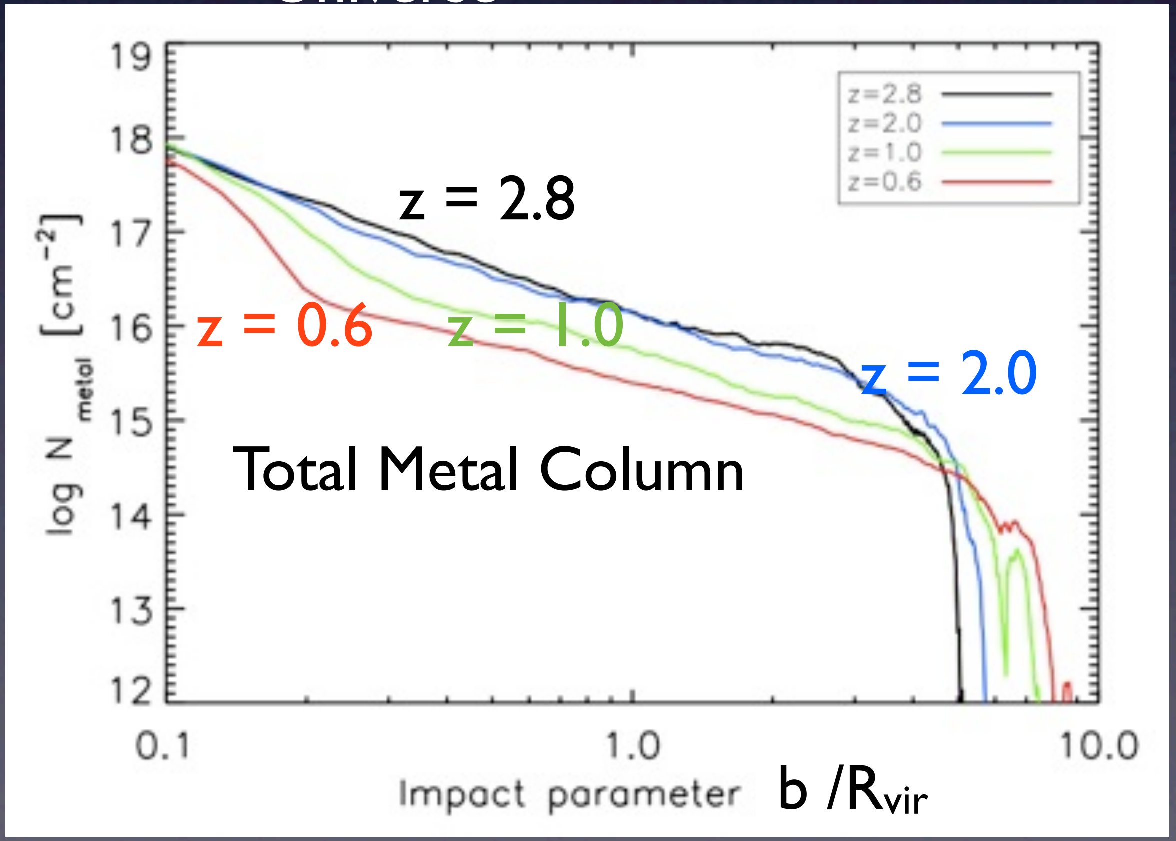

Evolution of the CGM: O VI

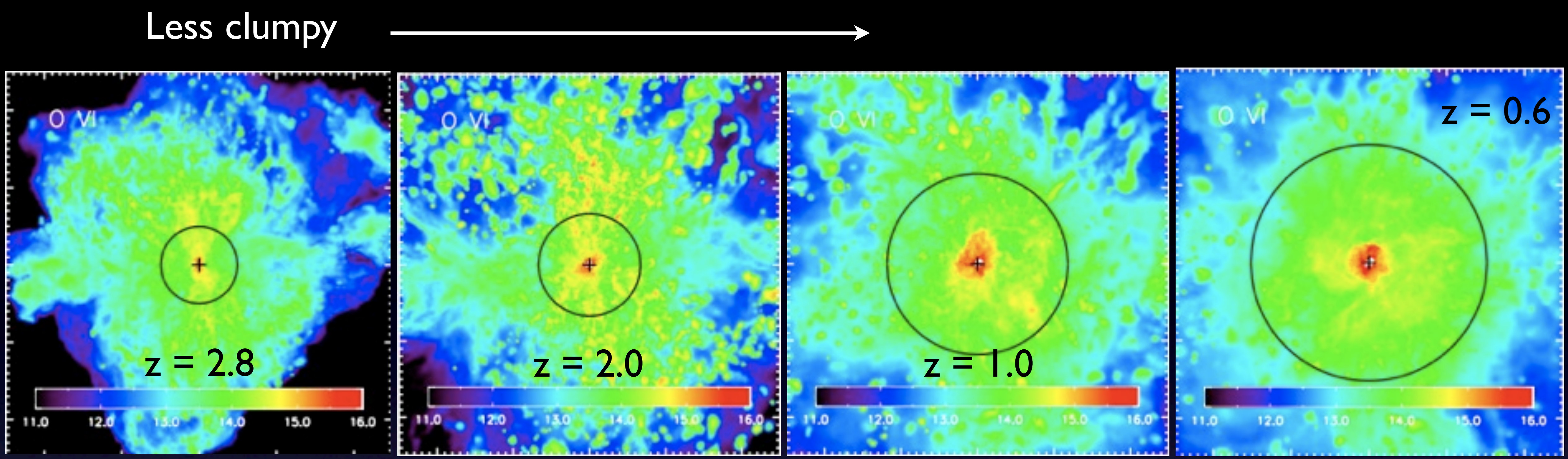

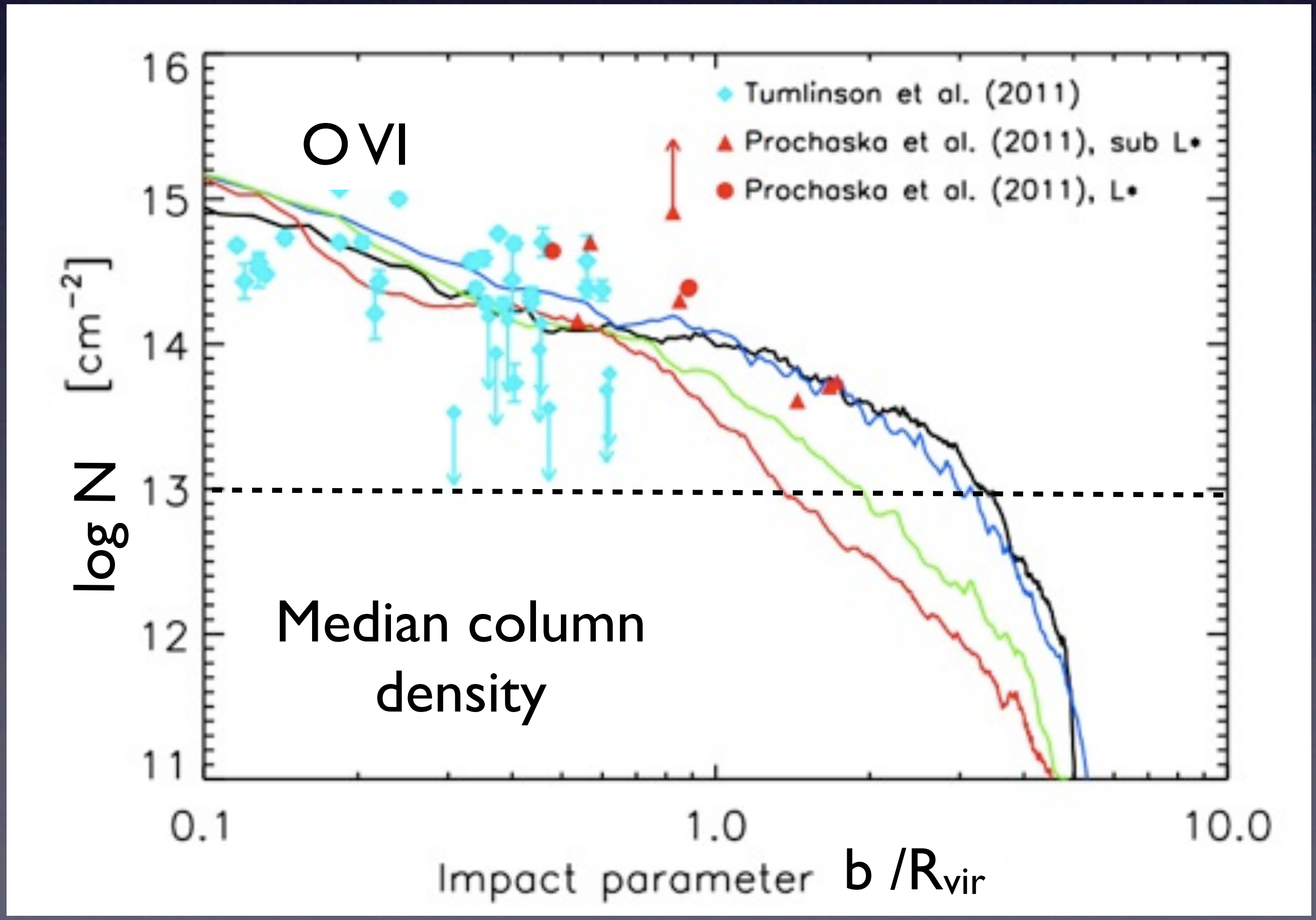

- From z =2.8 to 0.6, the O VI halo grows with R_{vir}, strong absorption within R_{vir}
- All redshift consistent with the Tumlinson+ (2011) data;
- Cf of $N_{OVI} > 10^{13}$ cm^{-2} remains unity for all redshift within R_{vir}

Evolution of the CGM: Low and Intermediate Ions

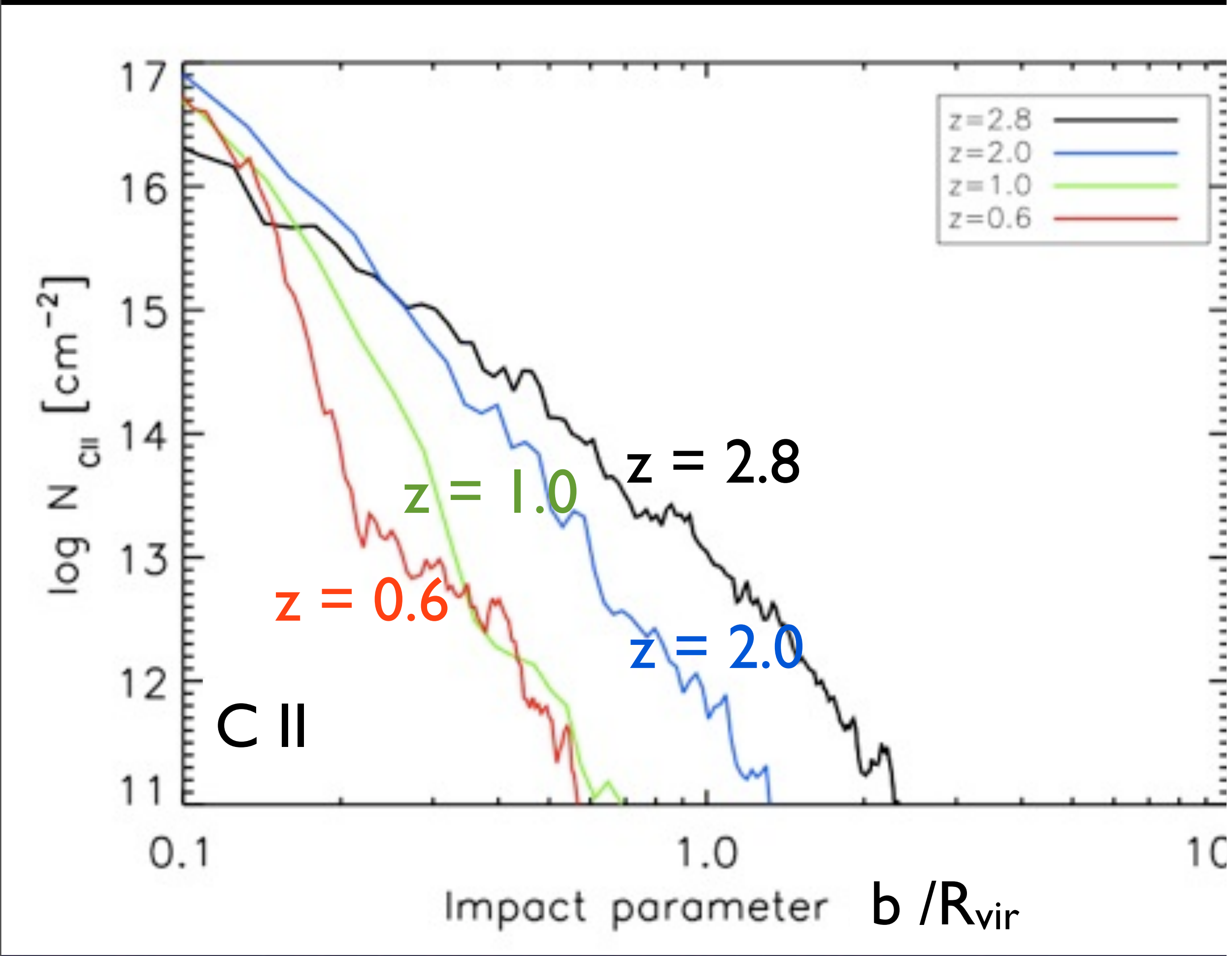

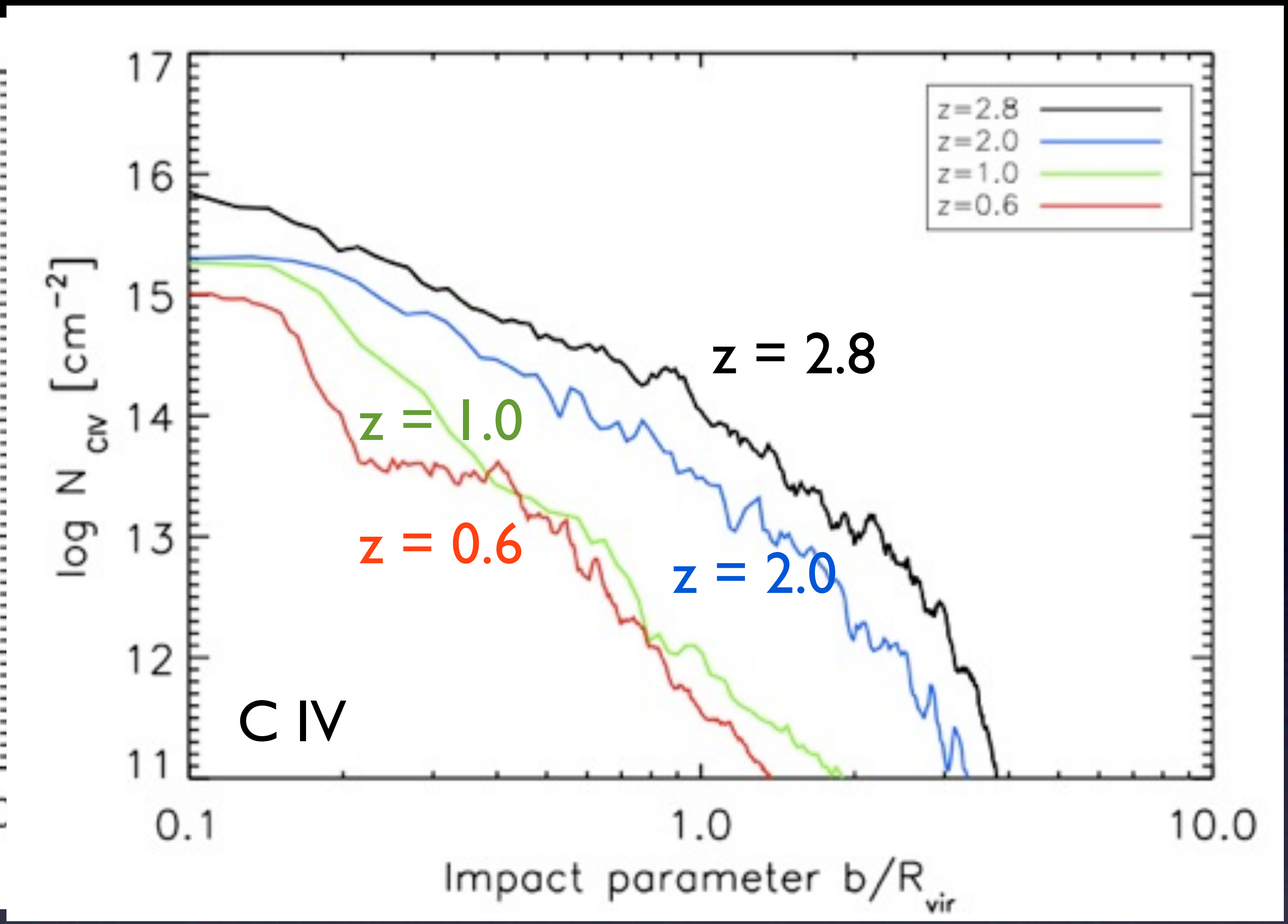

- From z =2.8 to z=0.6, C II and C IV enriched region increases slower than R_{vir}
- Covering fraction within R_{vir} of N > 10^{13} also decreases
- The absolute size of C IV and C II region remains similar from z = 2.8 - 0.6 (Chen et al. 2012), although the total metal enriched region increases with R_{vir}

Within R_{vir}, covering fraction of N > 10^{13} cm^{-2}

Redshift	C IV Cf	C II Cf
z = 2.8	97%	77%
z = 2.0	81%	52%
z = 1.0	46%	23%
z = 0.6	36%	14%

Evolution of the CGM: Low and Intermediate Ions

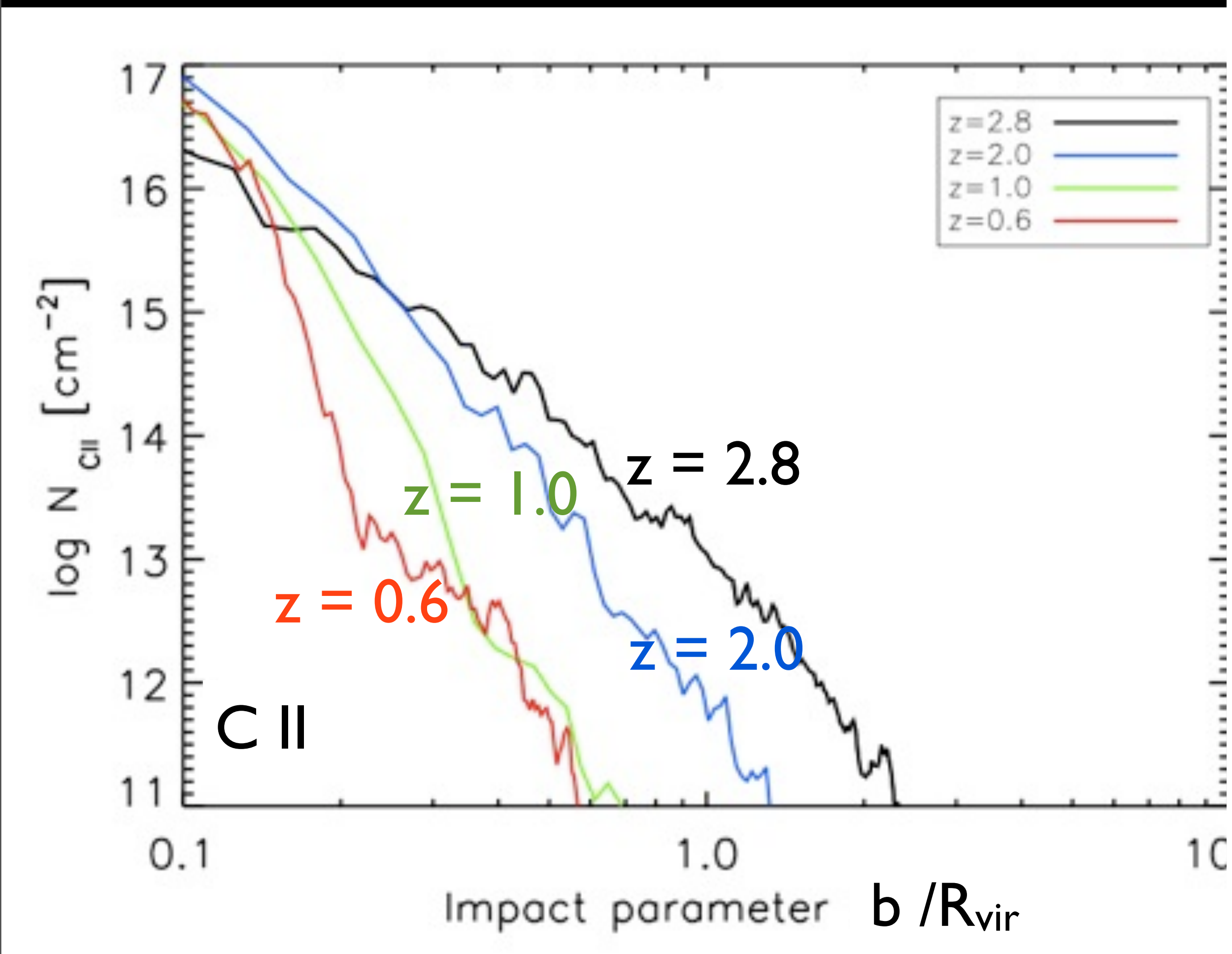

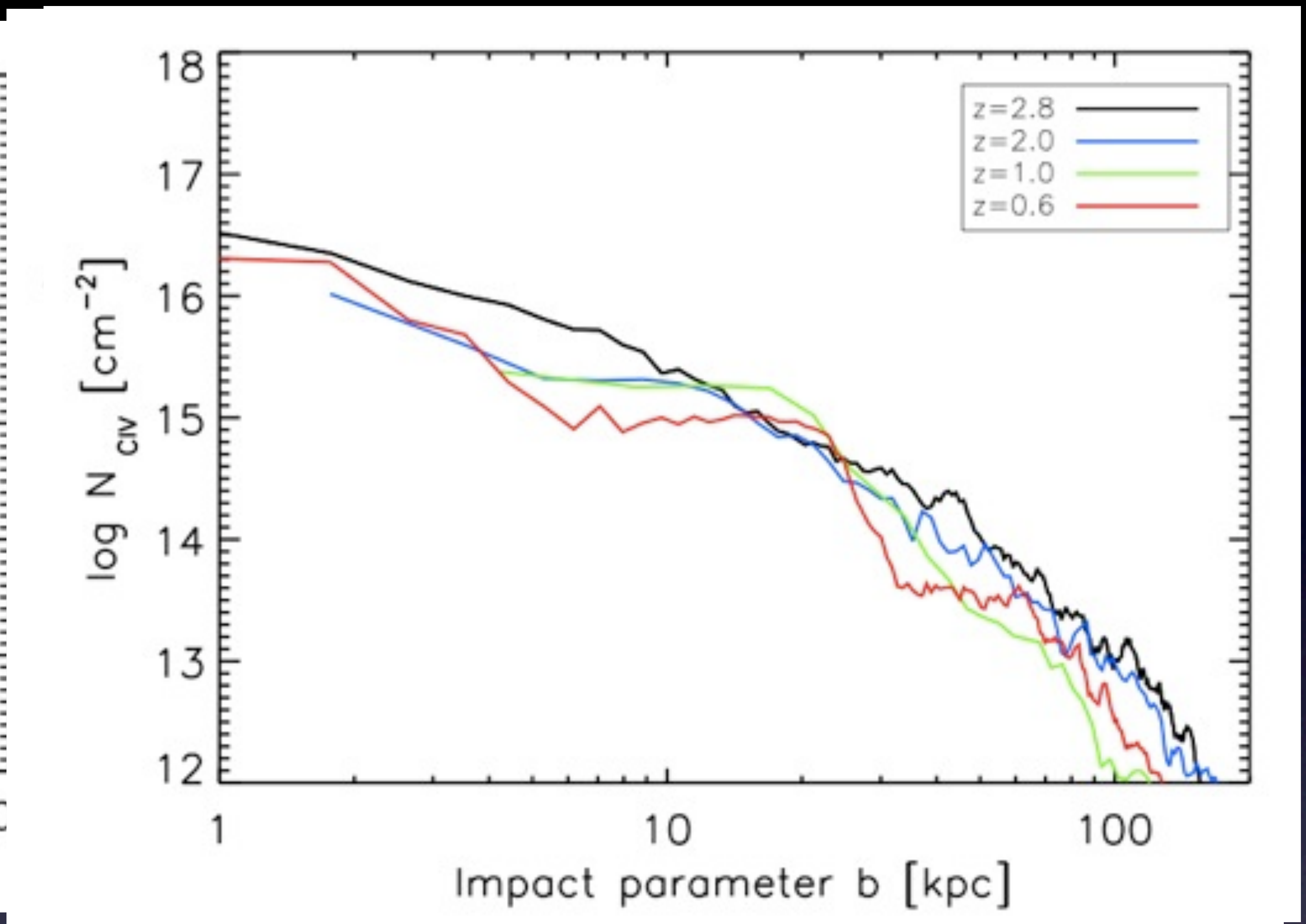

- From z =2.8 to z=0.6, C II and C IV enriched region increases slower than R_{vir}
- Covering fraction within R_{vir} of N > 10^{13} also decreases
- The absolute size of C IV and C II region remains similar from z = 2.8 - 0.6 (Chen et al. 2012), although the total metal enriched region increases with R_{vir}

Within R_{vir}, covering fraction of N > 10^{13} cm^{-2}

Redshift	C IV Cf	C II Cf
z = 2.8	97%	77%
z = 2.0	81%	52%
z = 1.0	46%	23%
z = 0.6	36%	14%

Evolution of the CGM: Low and Intermediate Ions

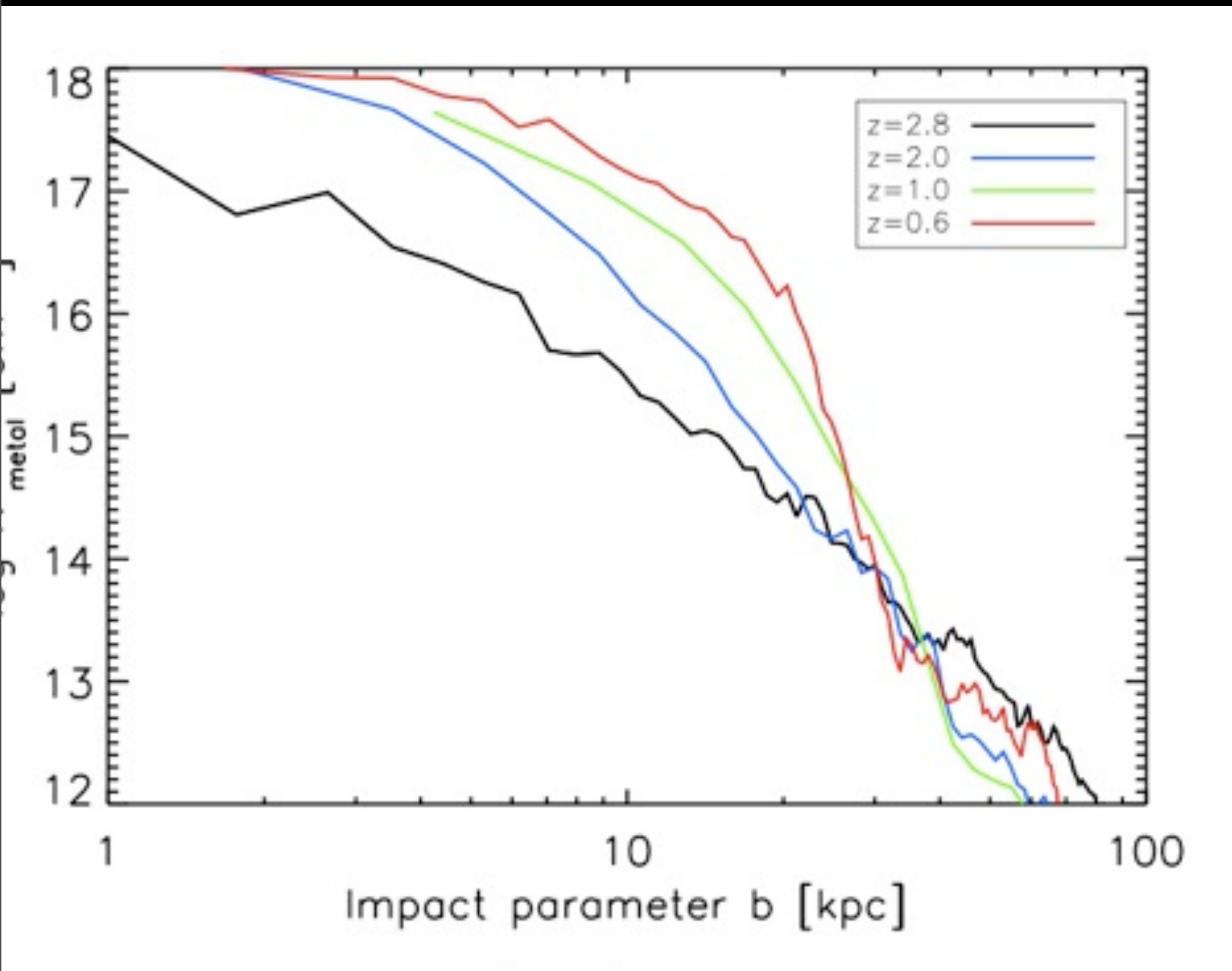

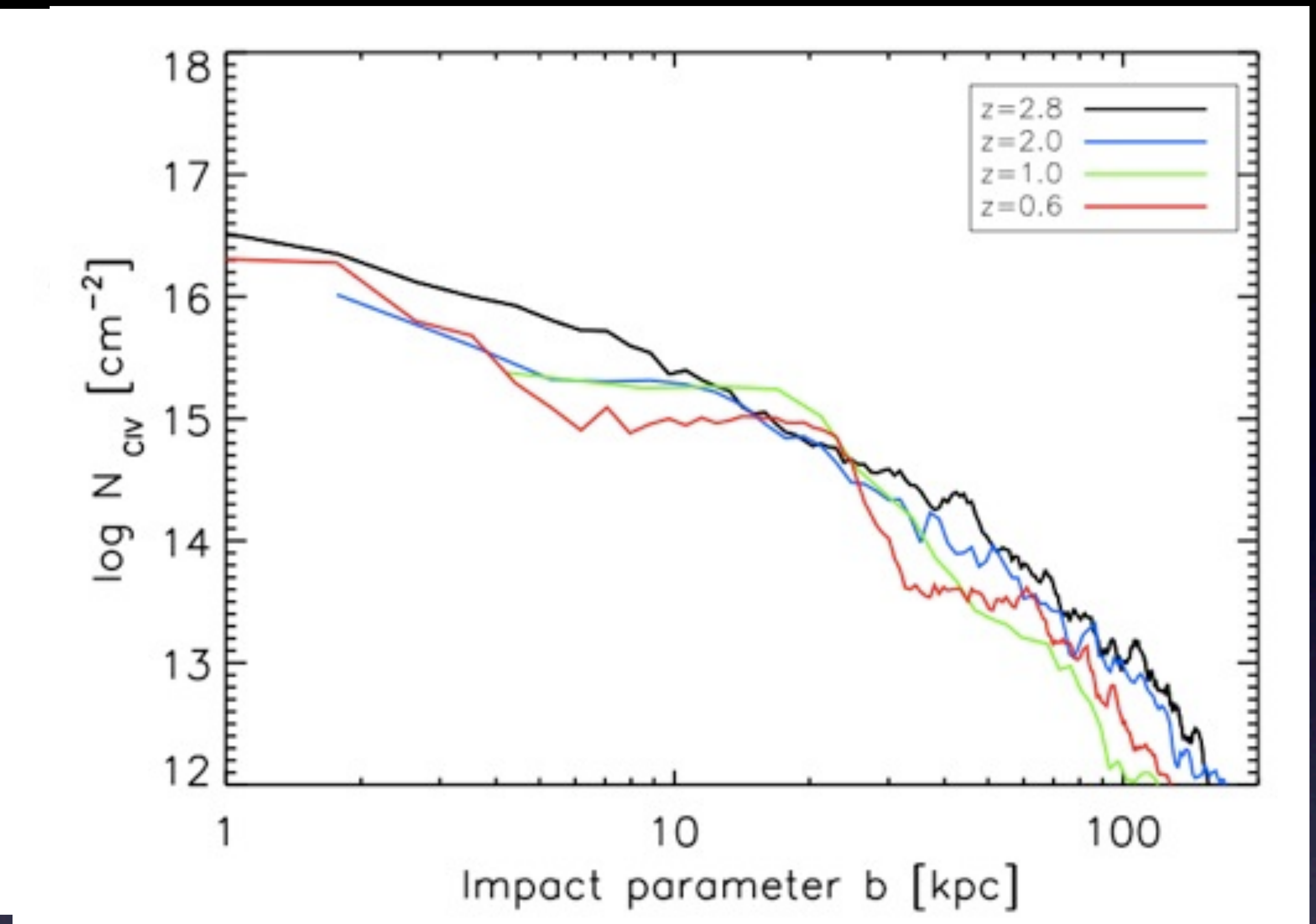

- From z =2.8 to z=0.6, C II and C IV enriched region increases slower than R_{vir}
- Covering fraction within R_{vir} of $N > 10^{13}$ also decreases
- The absolute size of C IV and C II region remains similar from z = 2.8 - 0.6 (Chen et al. 2012), although the total metal enriched region increases with R_{vir}

Within R_{vir}, covering fraction of $N > 10^{13}$ cm^{-2}

Redshift	C IV Cf	C II Cf
z = 2.8	97%	77%
z = 2.0	81%	52%
z = 1.0	46%	23%
z = 0.6	36%	14%

Summary I: CGM around MW like Galaxies in the Eris2 Simulations

- Zoom-in simulations provide rich information on the distribution, kinematics and evolution of the CGM;
- Coexistence of high and low ions for most absorbers, although *not all* the O_{VI} systems has corresponding low ion counterpart.
- W_0-b relation from Eris2 appears to be in reasonable agreement of observations of Steidel +(2010). Feedback & outflows are crucial to reproduce the W_0-b relation.
- The covering factor of LLS system is about 27% within R_{vir} at z ~ 2-3, in good agreement with Rudie+ (2012), it is slightly higher than simulations with no strong outflows (Fumagalli+ 2011; Faucher-Giguère & Kereš 2011);
- The cold streams are enriched with Cf of CII > 10^{13} cm^{-2} about 22% within R_{vir} -- possible to detect inflows with metal line absorption. The metallicities of the LLSs have a bimodal distribution (Lehner+2013)

Summary I: CGM around MW like Galaxies in the Eris2 Simulations

- As the CGM evolve to lower redshift, the cold streams gradually fade, and the covering fraction of LLS declines. However, the Cf of systems with log N_{HI} > 14 stays high at z = 0.6.
- The size of total metal enriched region increases with R_{vir}, Rz ~ 5-8 R_{vir}
- O VI halo: the column density remains high within R_{vir}, and the N-b/R_{vir} relations appear consistent with the Tumlinson+ 2011 data for star-forming galaxies
- The median $N_{C\ IV}$-b relation does not change significantly from z = 2.8 to z = 0.6, the size of C IV bubble 70 - 100 kpc

Simulation of Seven Dwarfs

Working in progress

Simulation of Dwarf Galaxies

Shen+ 13, to be sumitted

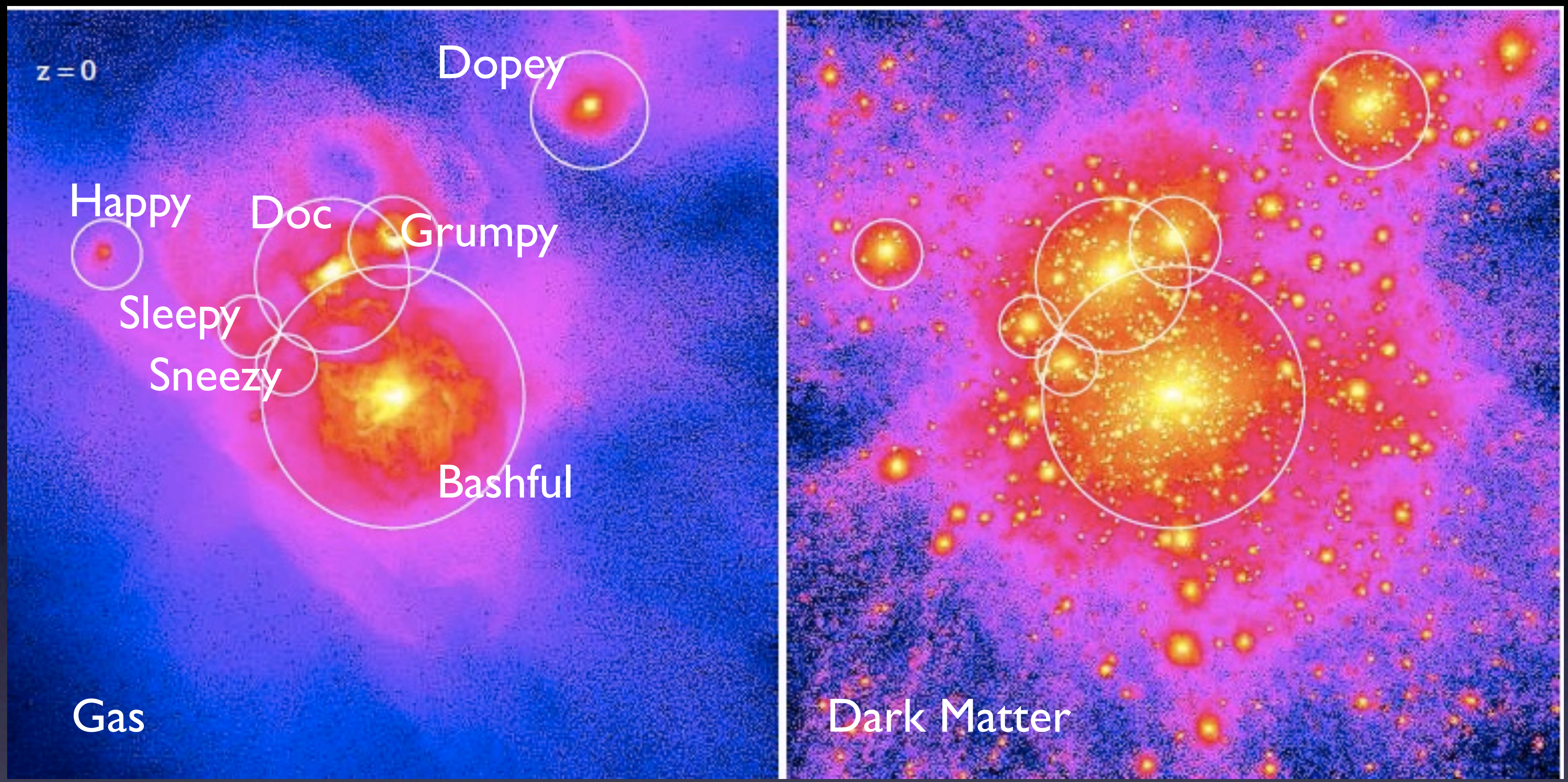

- Same initial condition as in Governato+ 2010
- Resolution: DM 1.6×10^4 M_{sun}; Gas 3300 M_{sun}; Star 1100 M_{sun}; force resolution 86 pc
- n_{th} = 100 atoms/cc -- Transition from H I to H_2 (Gnedin+2009; Christensen+2012)
- Blastwave feedback (Stinson+2006), metal dependent cooling & diffusion(Shen+2010);
- "Field" dwarfs -- with nearest massive halo > 3 Mpc away

Properties of the Most Massive Seven

Name	$M_{\rm vir}$ [$M_\odot$]	$R_{\rm vir}$ [kpc]	$V_{\rm max}$ [$\rm km\,s^{-1}$]	M_* [$M_\odot$]	$M_{\rm gas}$ [$M_\odot$]	$M_{\rm HI}$ [$M_\odot$]	f_b	$\langle$SFR$\rangle$ [$10^{-3}\ M_\odot\ \rm yr^{-1}$]	[Fe/H]	
Bashful	3.59×10^{10}	85.23	50.7	1.15×10^8	8.14×10^8	2.34×10^7	0.026	8.9	-0.96 ± 0.50	
Doc	1.16×10^{10}	50.52	38.2	3.40×10^7	1.74×10^8	1.98×10^7	0.018	5.1	-1.14 ± 0.44	
Dopey	3.30×10^9	38.45	22.9	9.60×10^4	4.47×10^7	1.96×10^6	0.014	0.07	-1.97 ± 0.33	
Grumpy	1.78×10^9	29.36	22.2	5.30×10^5	3.00×10^7	5.40×10^5	0.017	0.27	-1.52 ± 0.54	
Happy	6.60×10^8	22.49	15.6	—	2.54×10^6	270	0.004	—	—	—
Sleepy	4.45×10^8	19.71	14.8	—	—	—	—	—	—	—
Sneezy	4.38×10^8	19.62	13.2	—	1.64×10^5	—	0.0004	—	—	—

NOTE. — Column 1 lists the dwarf name. Columns 2, 3, 4, 5, 6, 7, 8, 9 and 10 give the present-day virial mass, virial radius (defined as the radius enclosing a mean density of 93 times the critical density), maximum circular velocity, stellar mass, gas mass, H I mass, baryon fraction $f_b \equiv (M_* + M_{\rm gas})/M_{\rm vir}$, average SFR calculated over the last 1 Gyr of the simulation, mean stellar metallicity and dispersion, respectively.

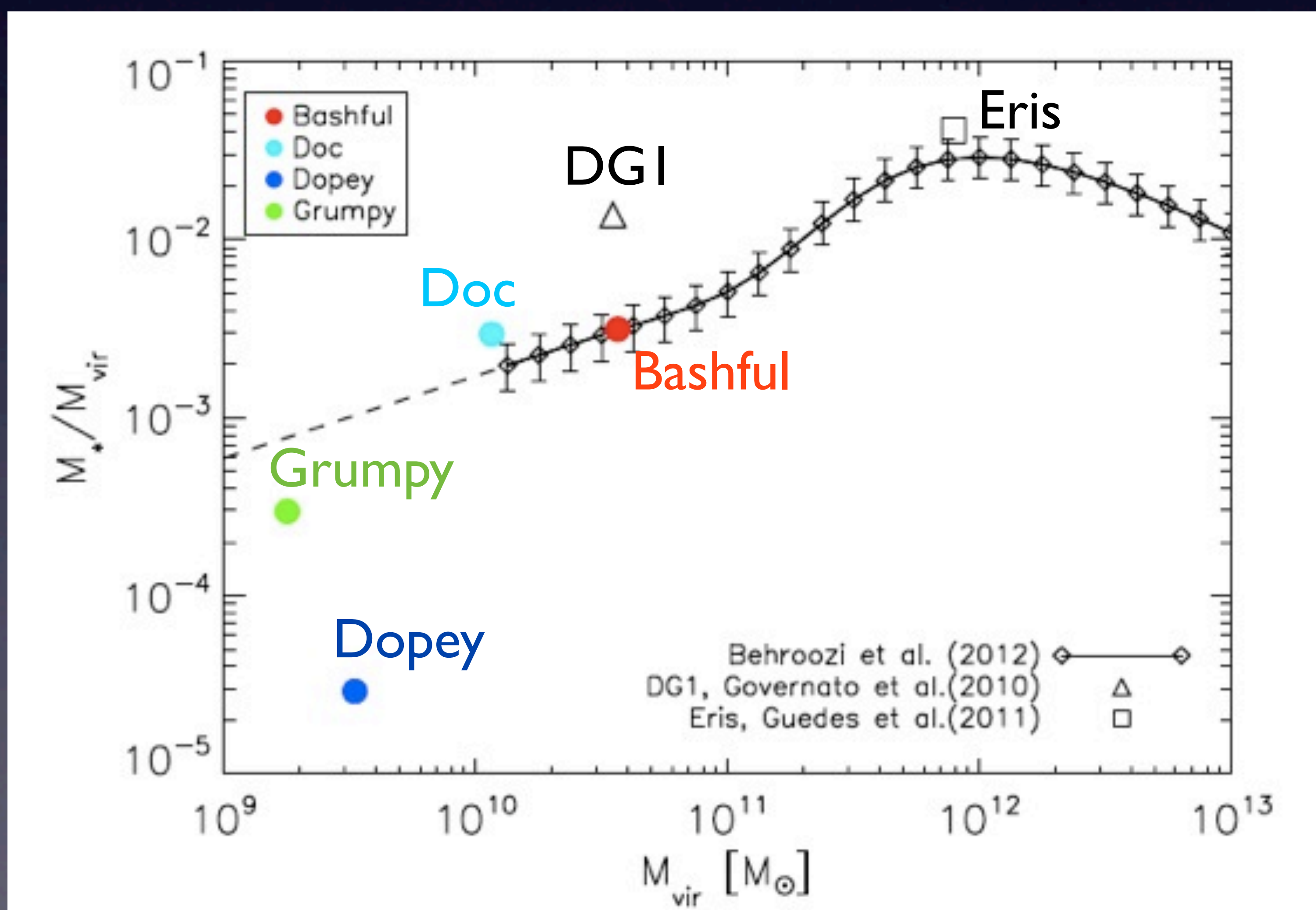

- 4 luminous dwarfs, with M* from 9.6 x 10^4 M_{sun} to 1.1 x 10^8 M_{sun}
- Bashful & Doc: M_*/M_h on the Behroozi + 2012 curve
- Dopey & Grumpy: very small stellar fraction
- Dopey is H I rich: $M_{HI} \sim 10\ M_*$

Mass-Metallicity Relationship (MZR)

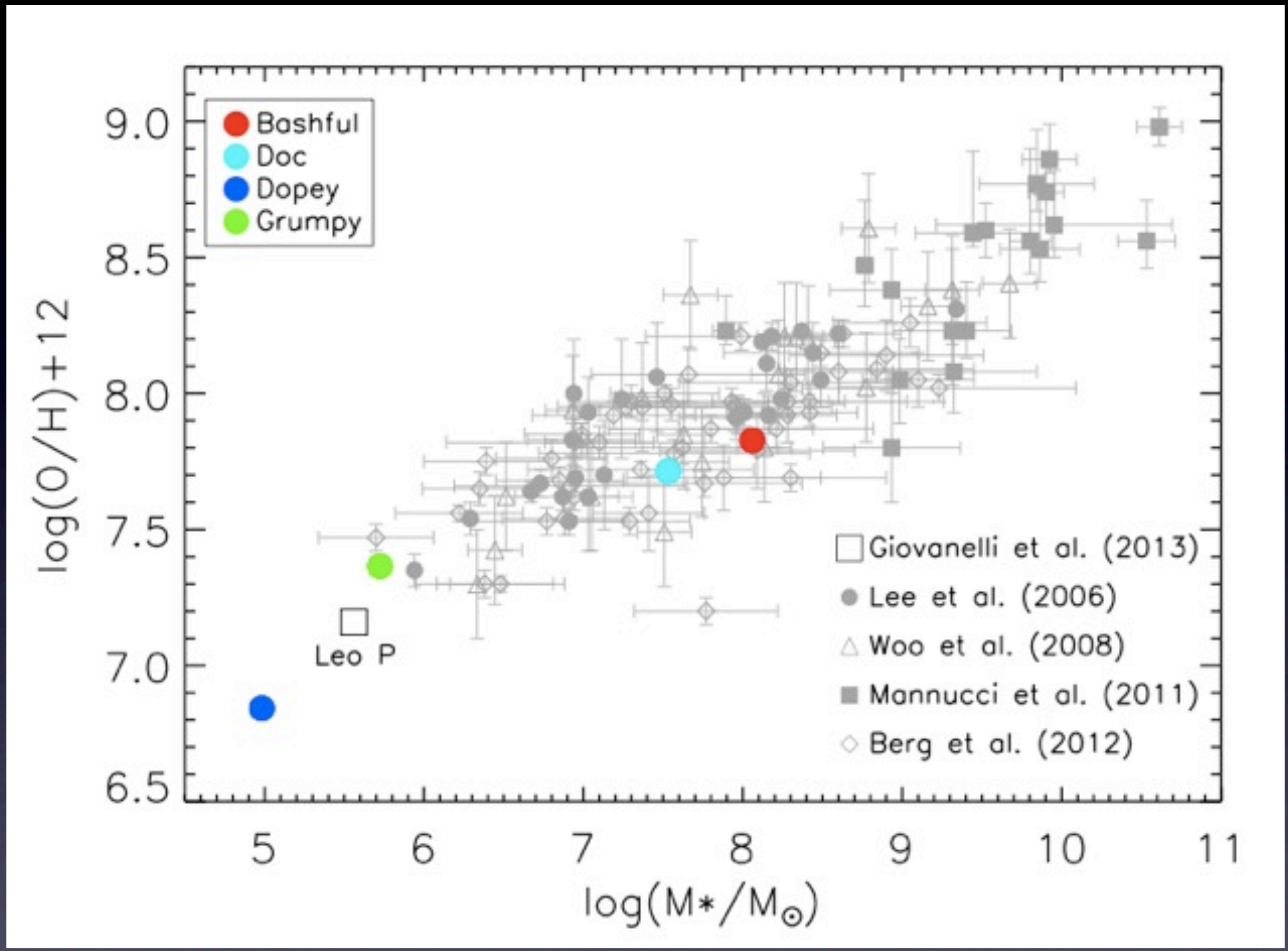

- Oxygen abundances in the ISM for the 4 dwarfs lie on the mass metallicity relationship and in good agreements with observations (Lee+2006, Woo+2008, Mannucci +2011, Berg+2012)
- Dopey and Grumpy are extremely metal poor galaxies, but still on the MZR. Similar to a very recently discovered H I-rich dwarf, Leo P (Giovanelli+2013)

The Environment: CGM and Galactic Wind from Dwarfs

- Bursty SFR & Low gas and Stellar Metallicity indicates effective winds

- Fraction of metals that is ejected out of the halo:
  - Bashful: 90%
  - Doc: 88.5%
  - Dopey: 8.3 %
  - Grumpy: 54.1%

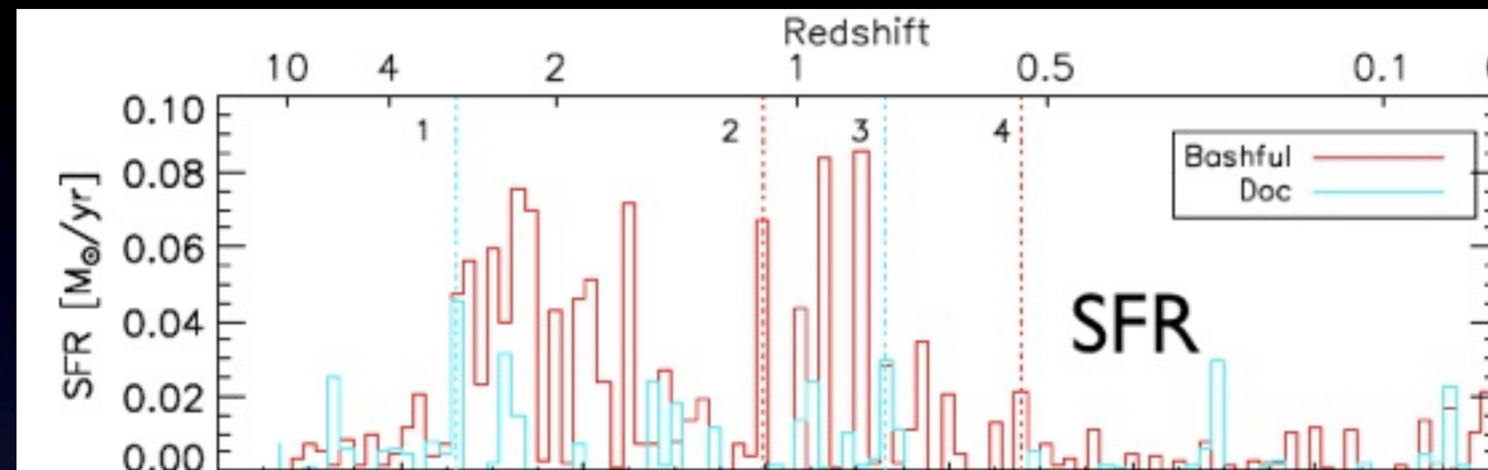

- Cumulative mass loading (M_{eject}/M_*) as function of redshift: generally > 10
- Mass loading similar to the dwarf satellites in Eris

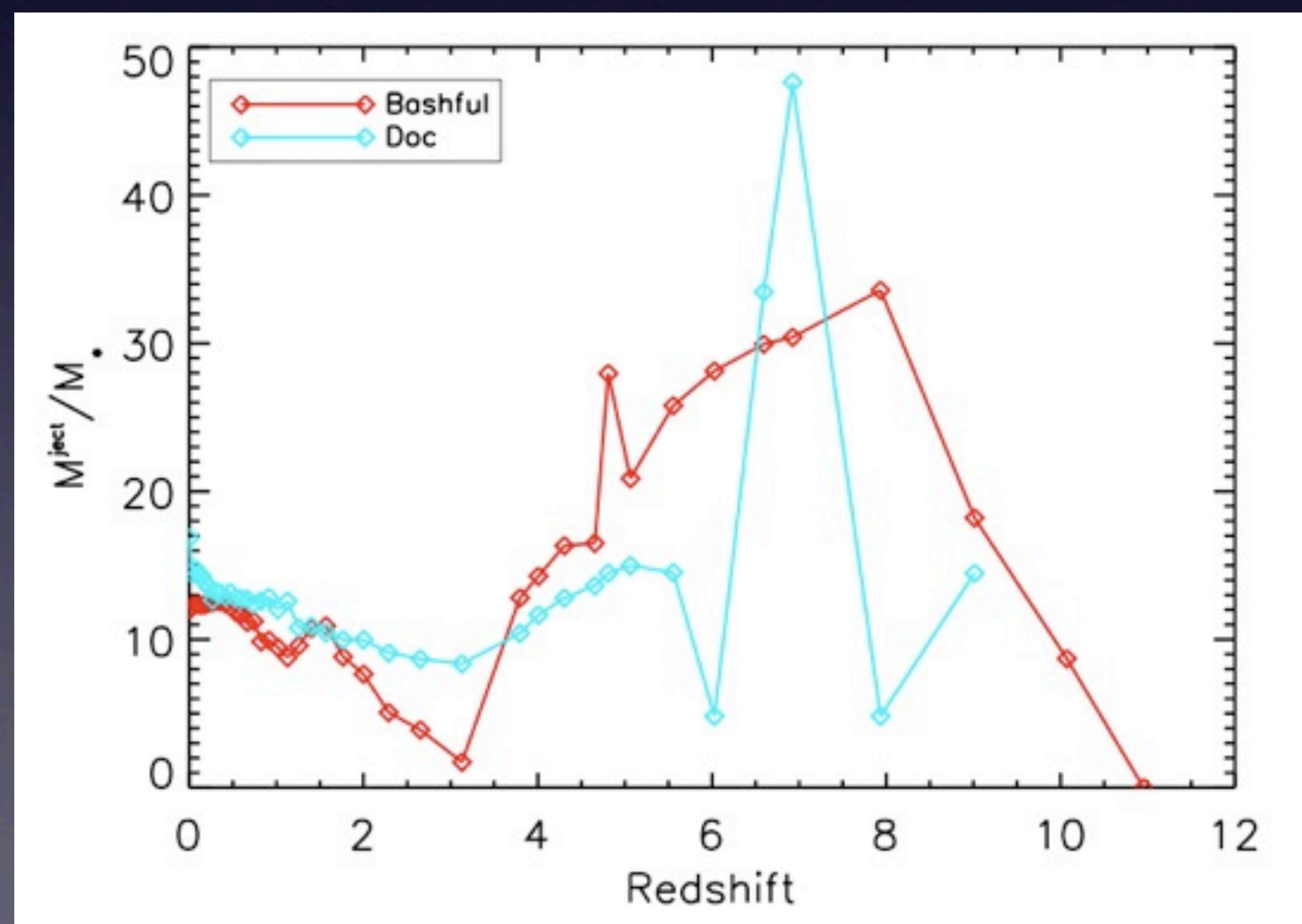

Evolution of the CGM around Field Dwarf Galaxies

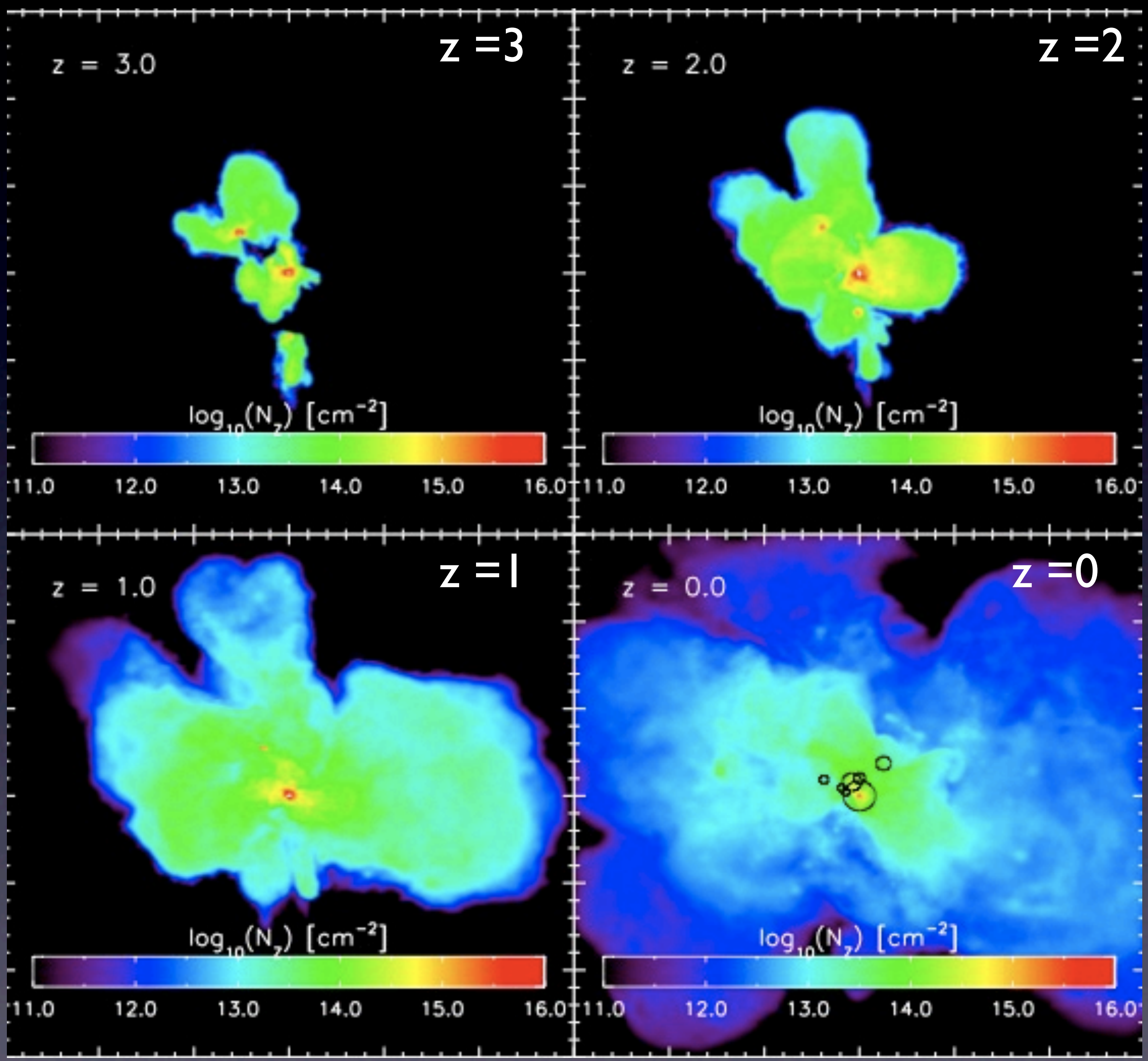

- Bashful has R_{vir} = 85 kpc ;
- The extend of enriched region R_Z >~ 15 R_{vir}

Box size: 3 comoving Mpc on a side
Centered at the most massive dwarf

Evolution of the CGM around Field Dwarf Galaxies

- Bashful has R_{vir} = 85 kpc ;
- The extend of enriched region R_Z >~ 15 R_{vir}

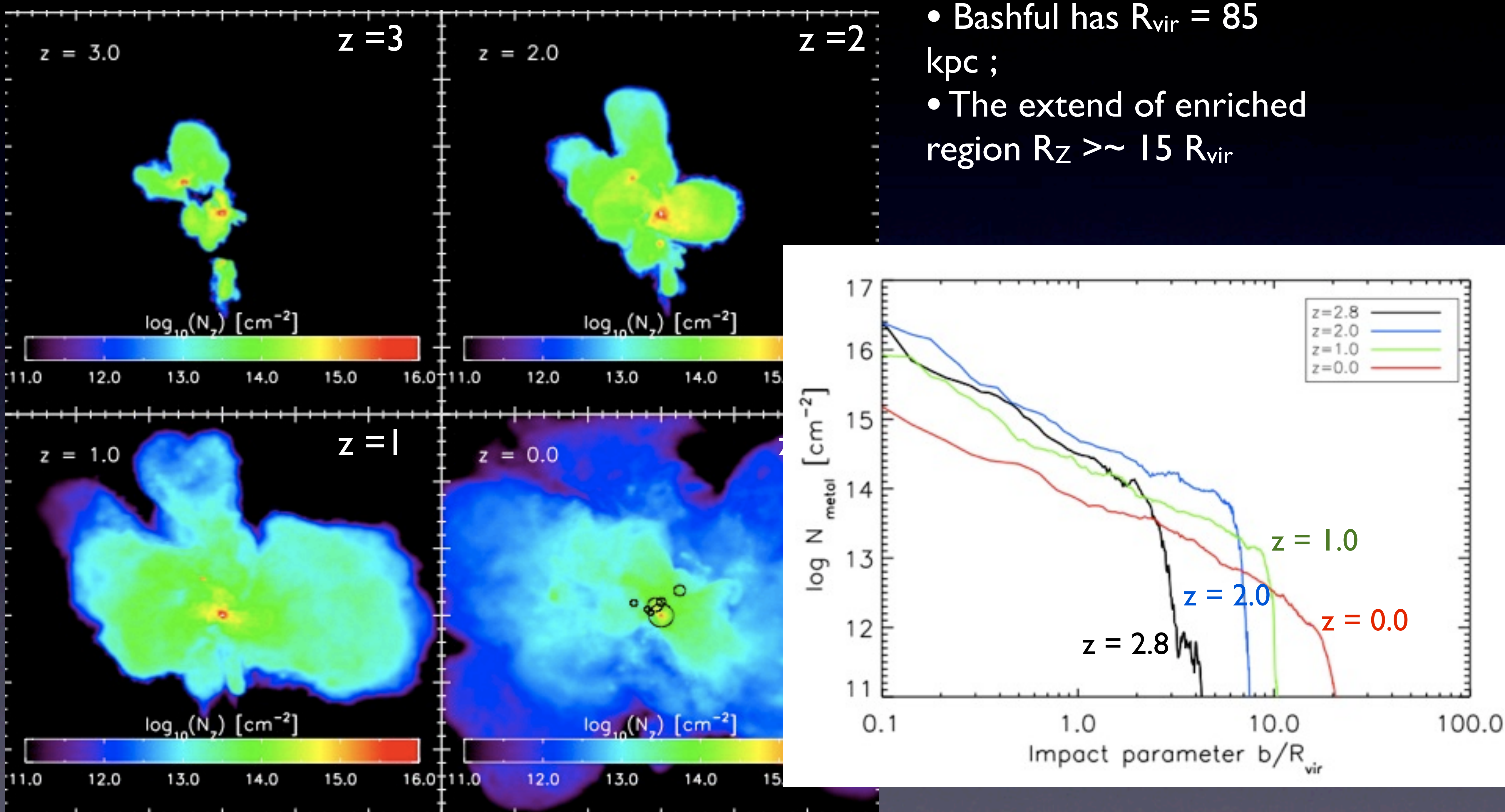

Box size: 3 comoving Mpc on a side
Centered at the most massive dwarf

Column Density Map of Various Ions at z = 0

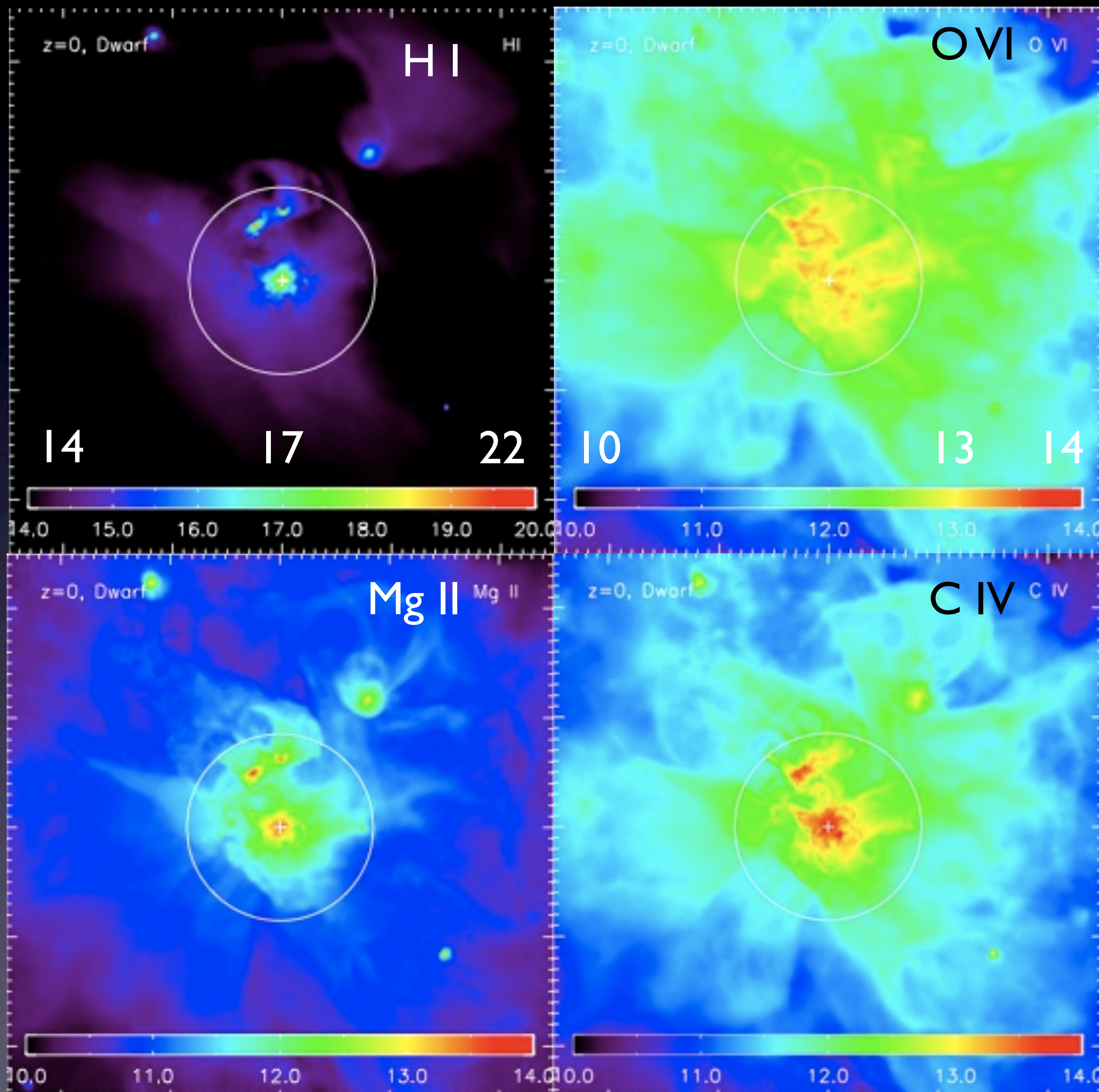

Box Size 500 kpc on a side

N HI : 10^{14} to 10^{20} cm^{-2}
Metals: 10^{10} to 10^{14} cm^{-2}
Yellow color = 10^{13} cm^{-2}

- High ionization metals extended further than low ions
- Low ions such as Mg II drop below 10^{13} rapidly as impact parameter increases, < 20 kpc or so
- Metals are highly ionized at larger distances
- The CGM is less "clumpy" as the one near massive galaxies

Comparison With COS-Dwarfs Data

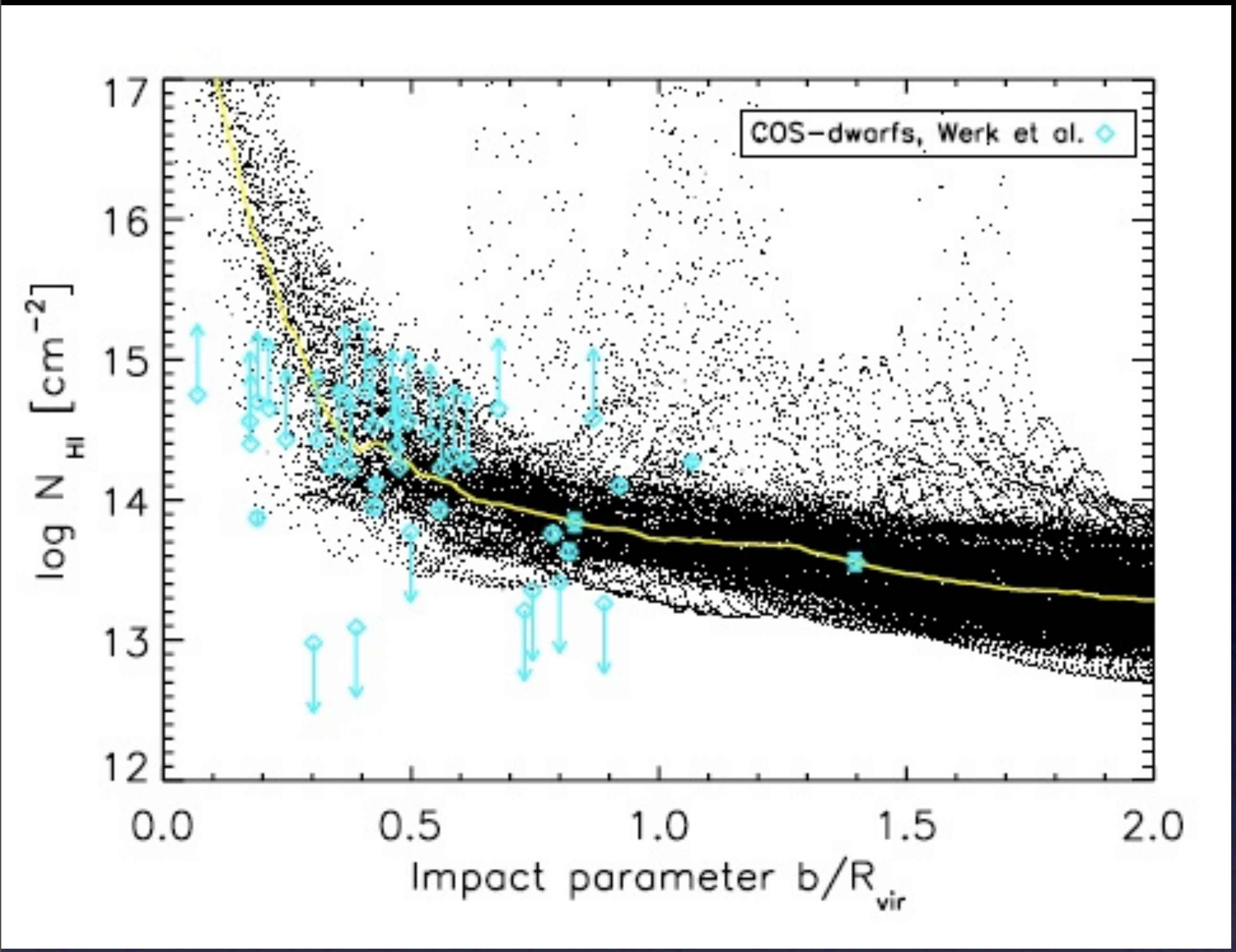

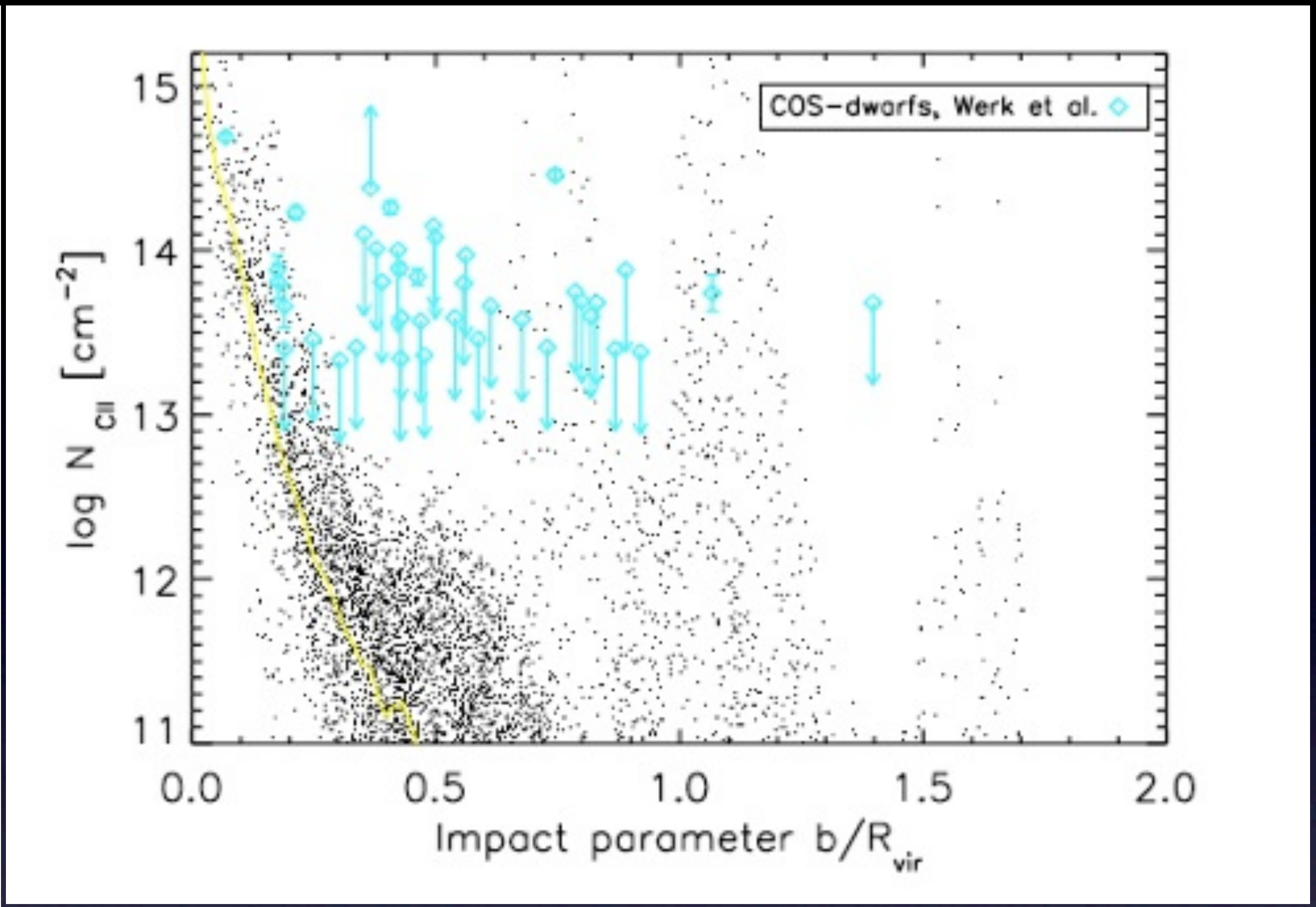

Comparison With COS-Dwarfs Data

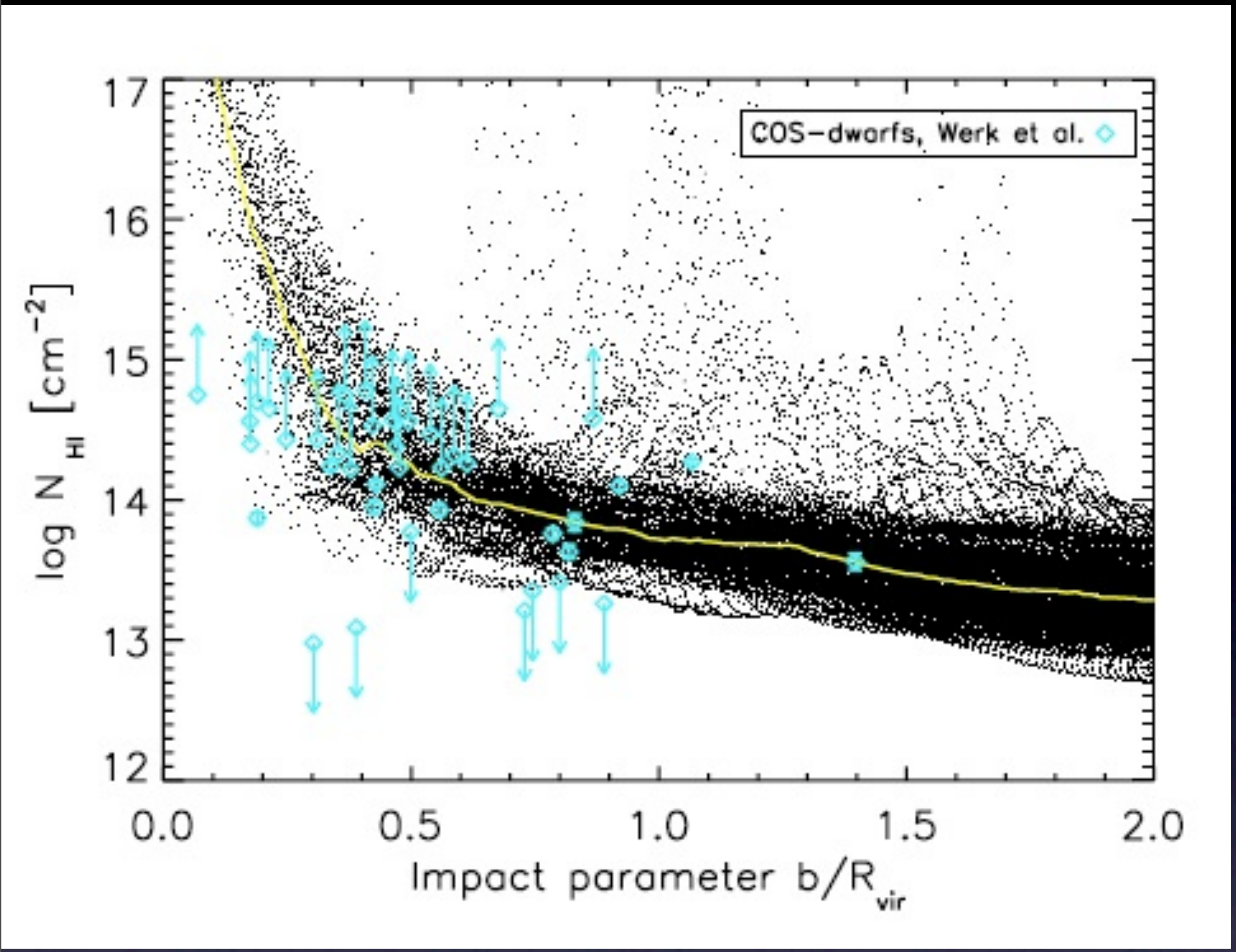

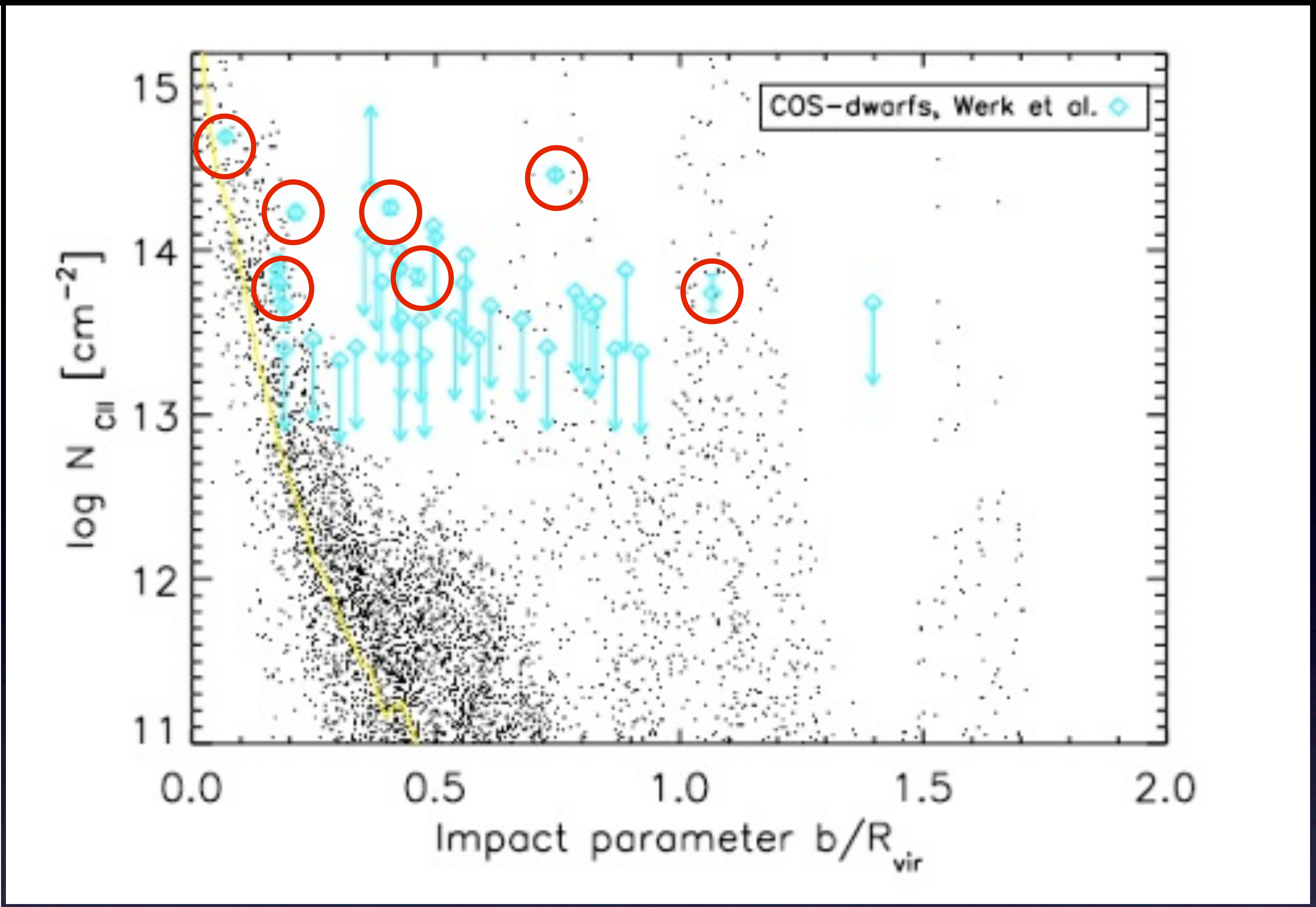

Comparison With COS-Dwarfs Data

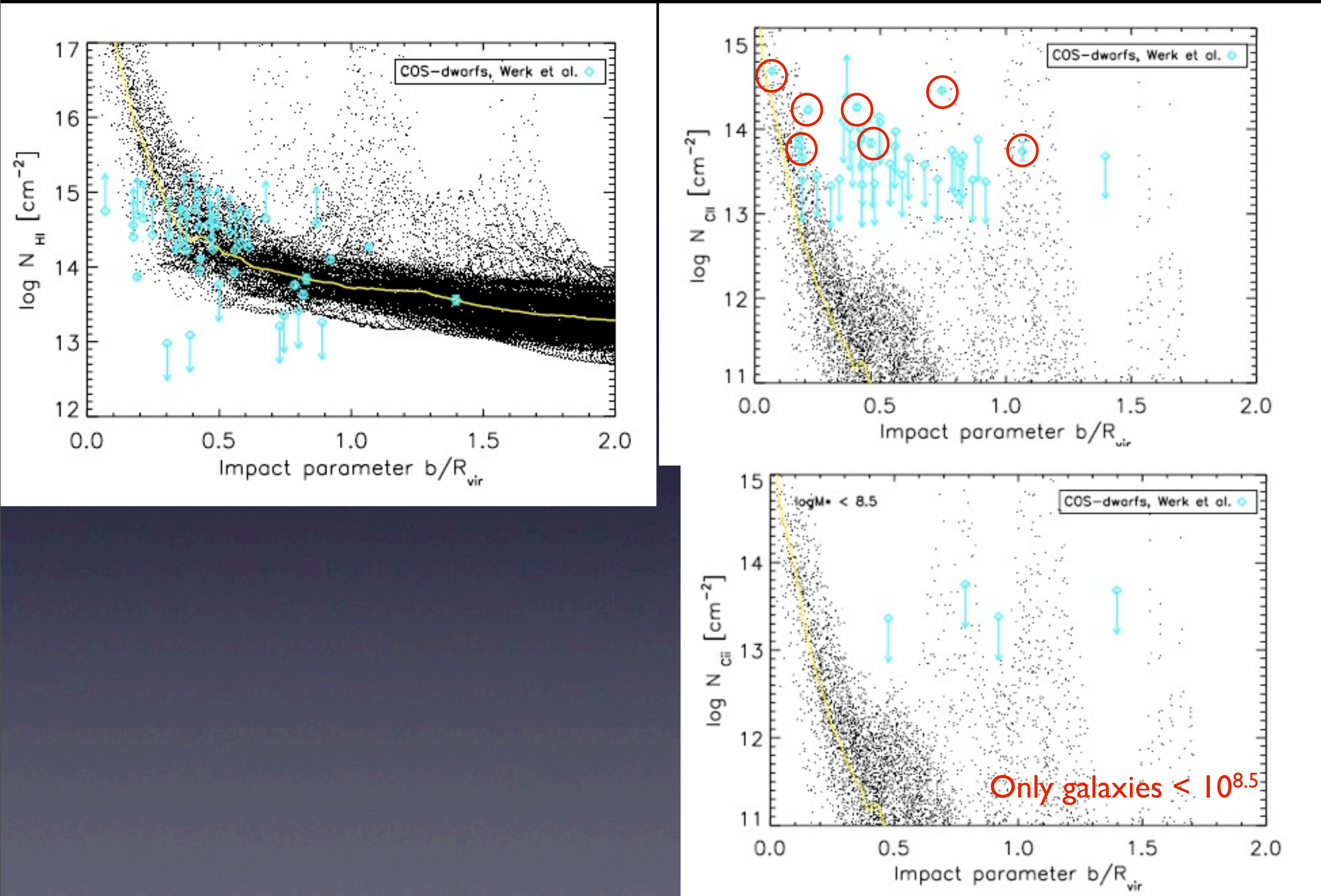

Comparison With COS-Dwarfs Data

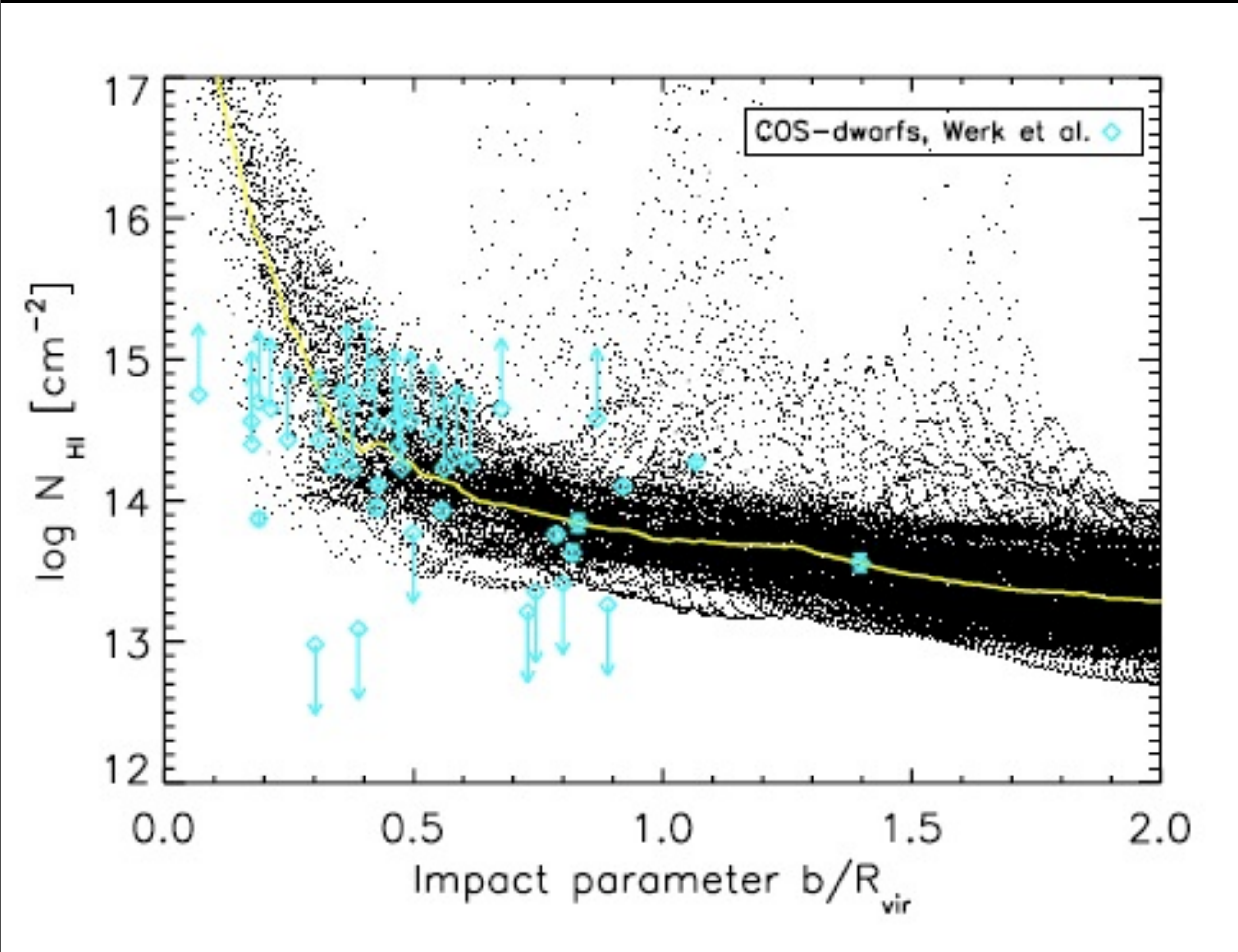

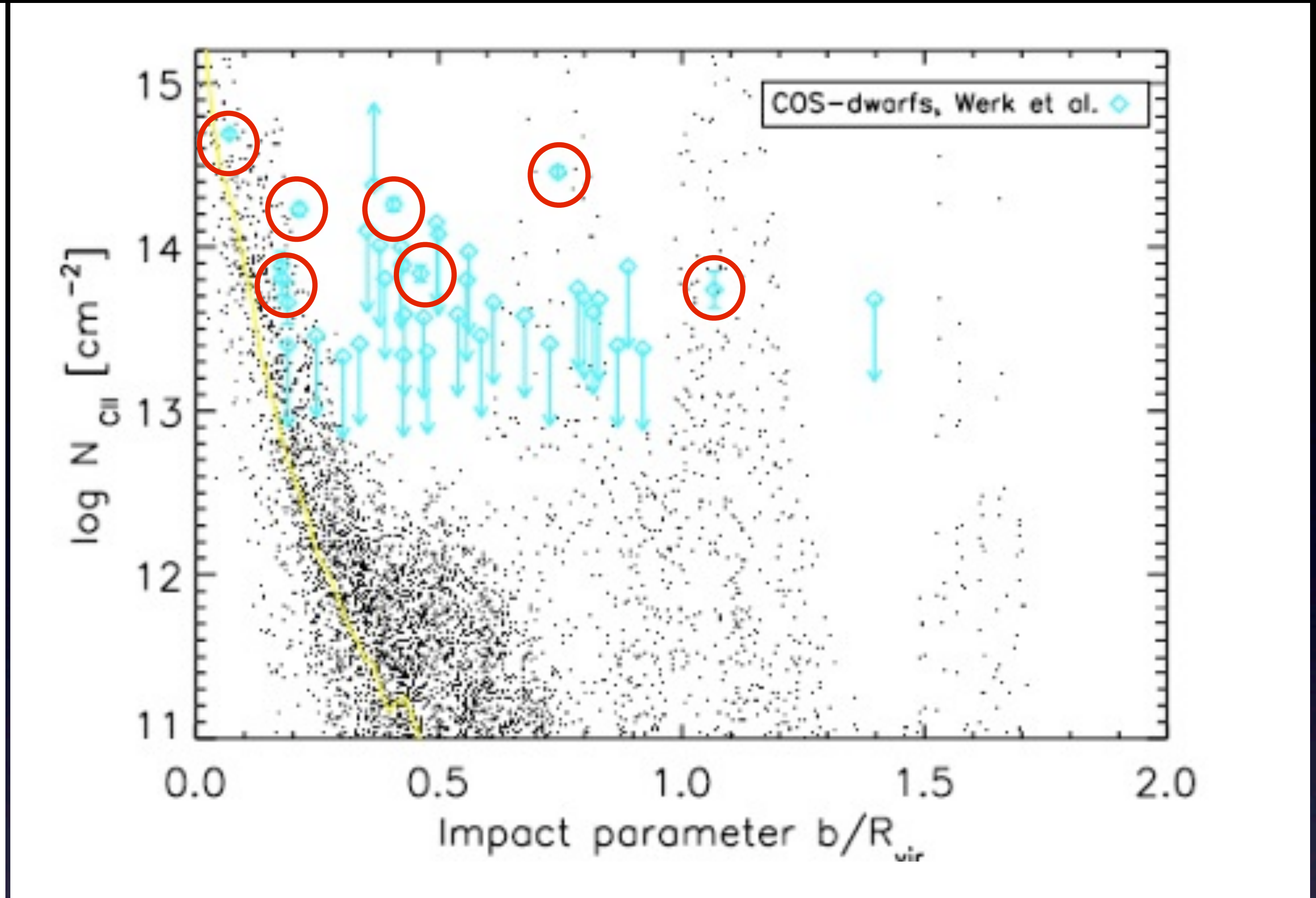

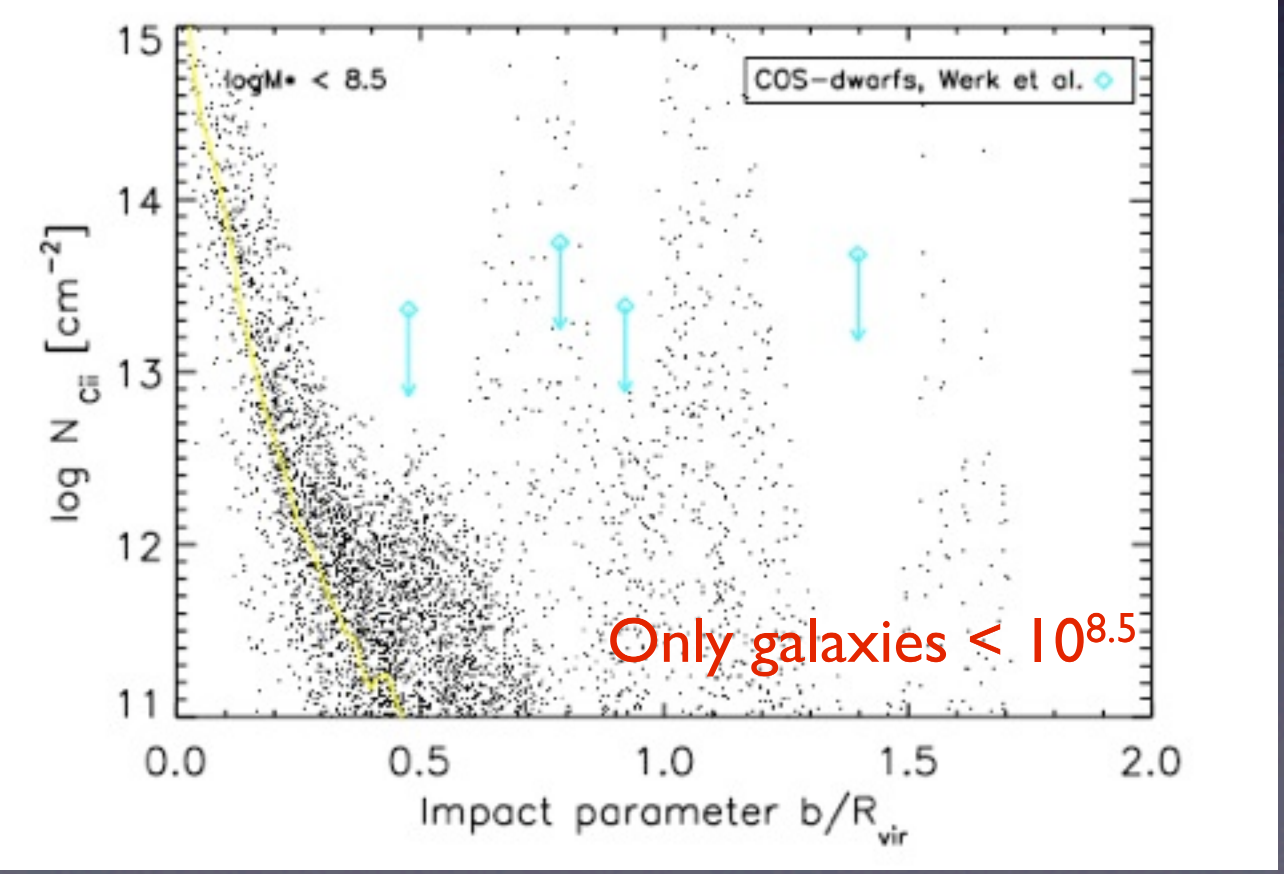

- COS-Dwarf Survey data from Werk et al. in prep;
- The most massive dwarf (Bashful) has M* = 1.5 x 10^8 Msun, rare in the COS-Dwarf Sample
- If choosing a cut of log M* < 8.5, then most metal signature are upper limits
- Needs simulations with different mass halos

Where are the metals?

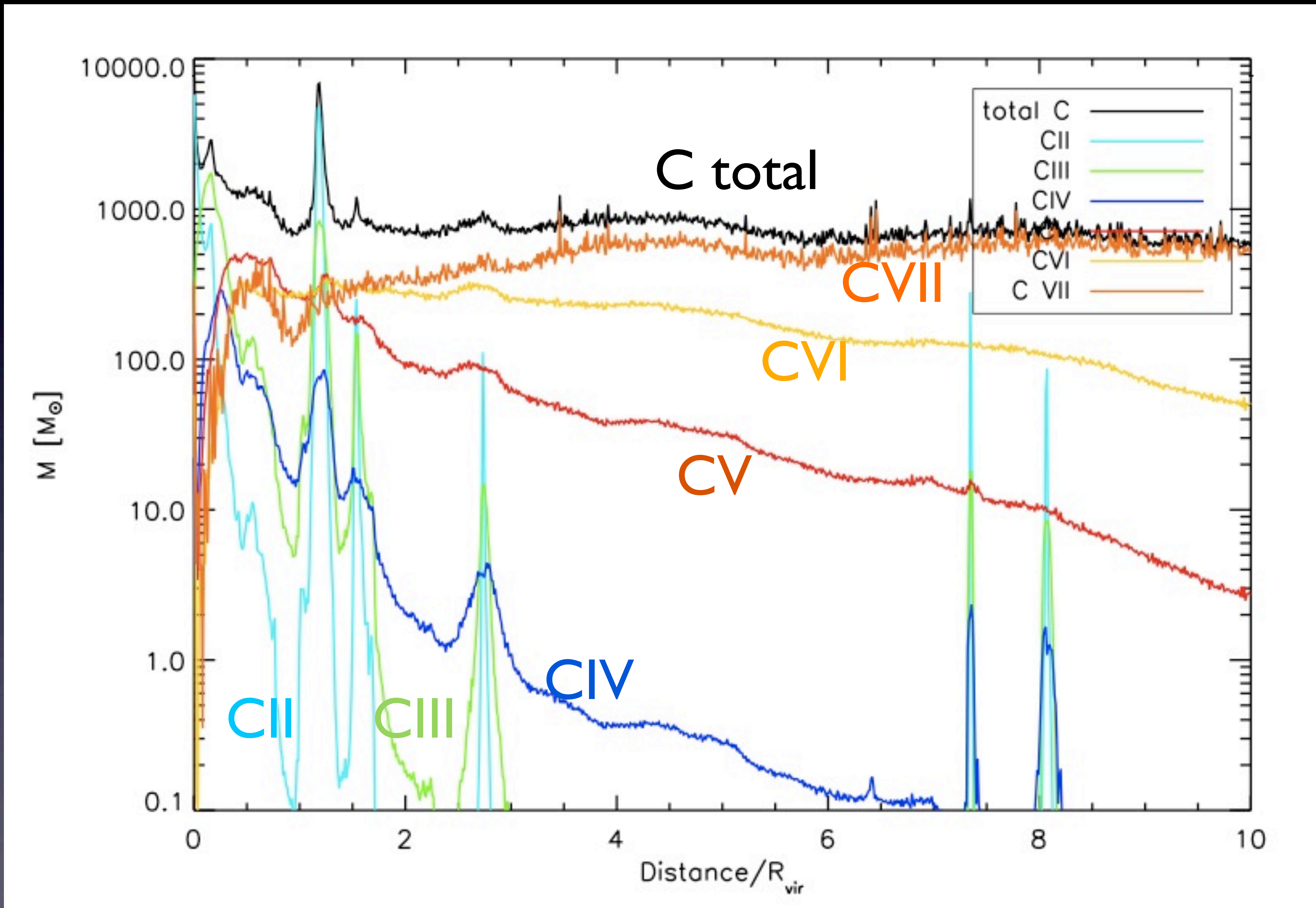

Summary II: CGM around Field Dwarf Galaxies

- For the same stellar feedback, galactic winds are more efficient in field dwarf galaxies, which leads to bursty SF and mass loading factor about few tens, much larger than large disk galaxies
- The dwarfs are very inefficient in turning gas into stars, and very metal poor, but still lies on the mass-metallicity relationship
- For the 2 biggest dwarfs, ~90% of metals ejected into the IGM. Mass loading factor (accumulative) varies from few tens to hundred
- Very extended enriched region (>15 R_{vir} at $z = 0$), much larger than disk galaxies. Dwarf galaxies probably the main polluters of the IGM
- The CGM of the dwarfs are not as clumpy and largely photoionized.

Clumpy CGM: Is that Real??

- Origin of the cold gas: entrained from the hot wind material
- But SPH cannot disrupt clumps easily... artificial surface tension that suppress KH instability

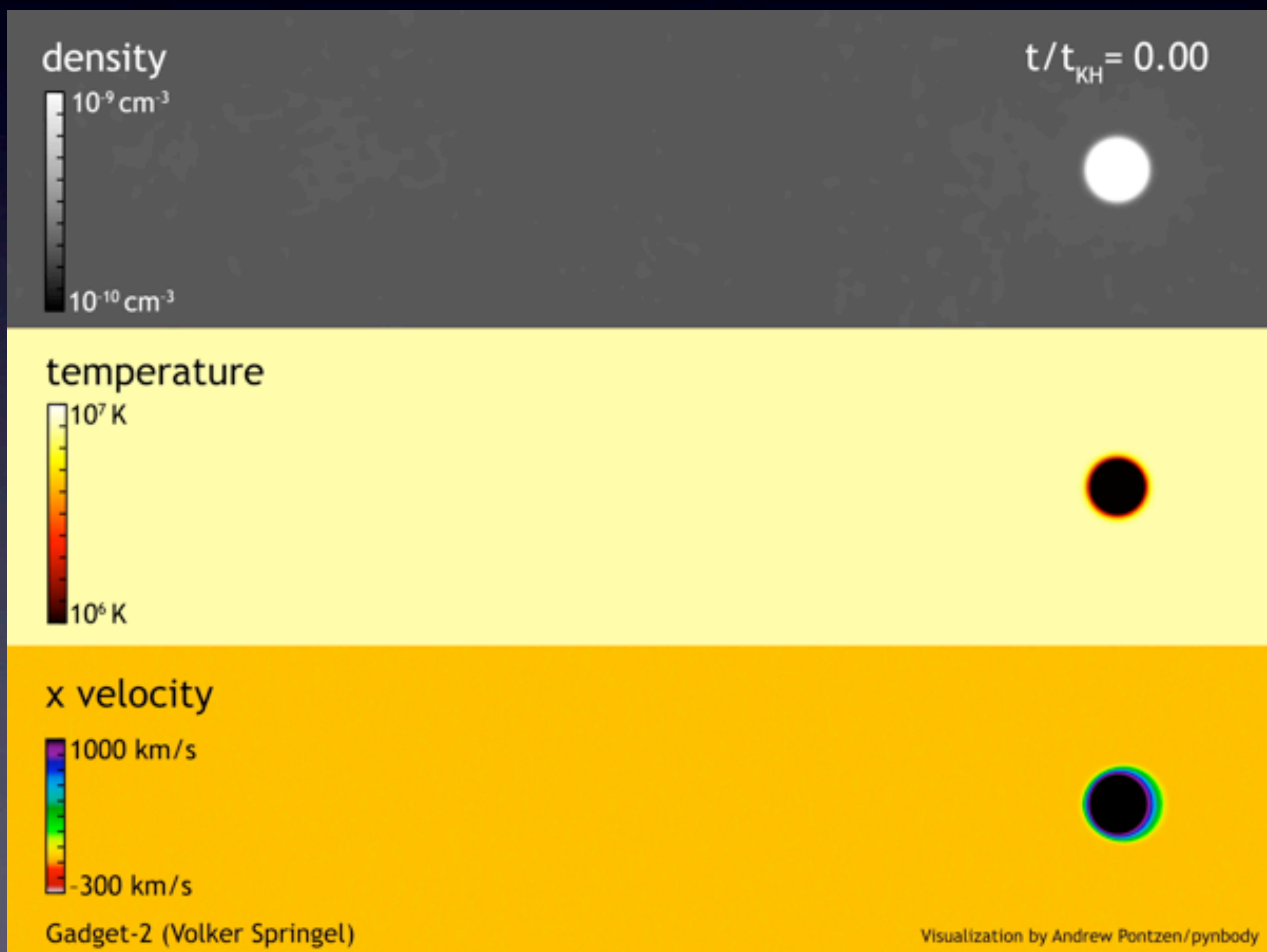

Gadget-2 Simulation Visualization by Andrew Pontzen

Clumpy CGM: Is that Real??

- New SPH in ChaNGa code (Quinn, Wadsley et al. in prep)

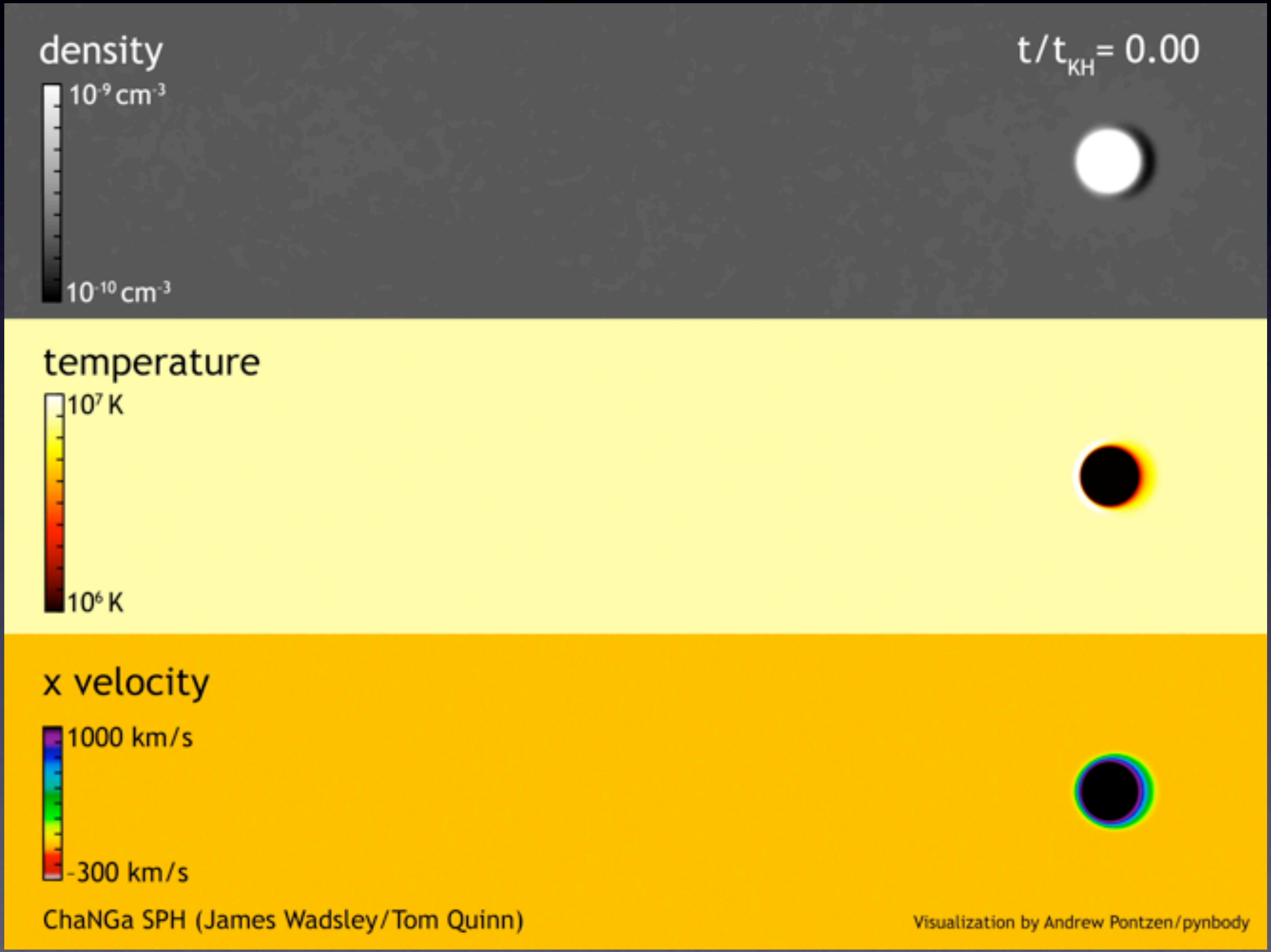

ChaNGa Simulation Visualization by Andrew Pontzen

Modified SPH in the Eris Simulation

New SPH | Old SPH

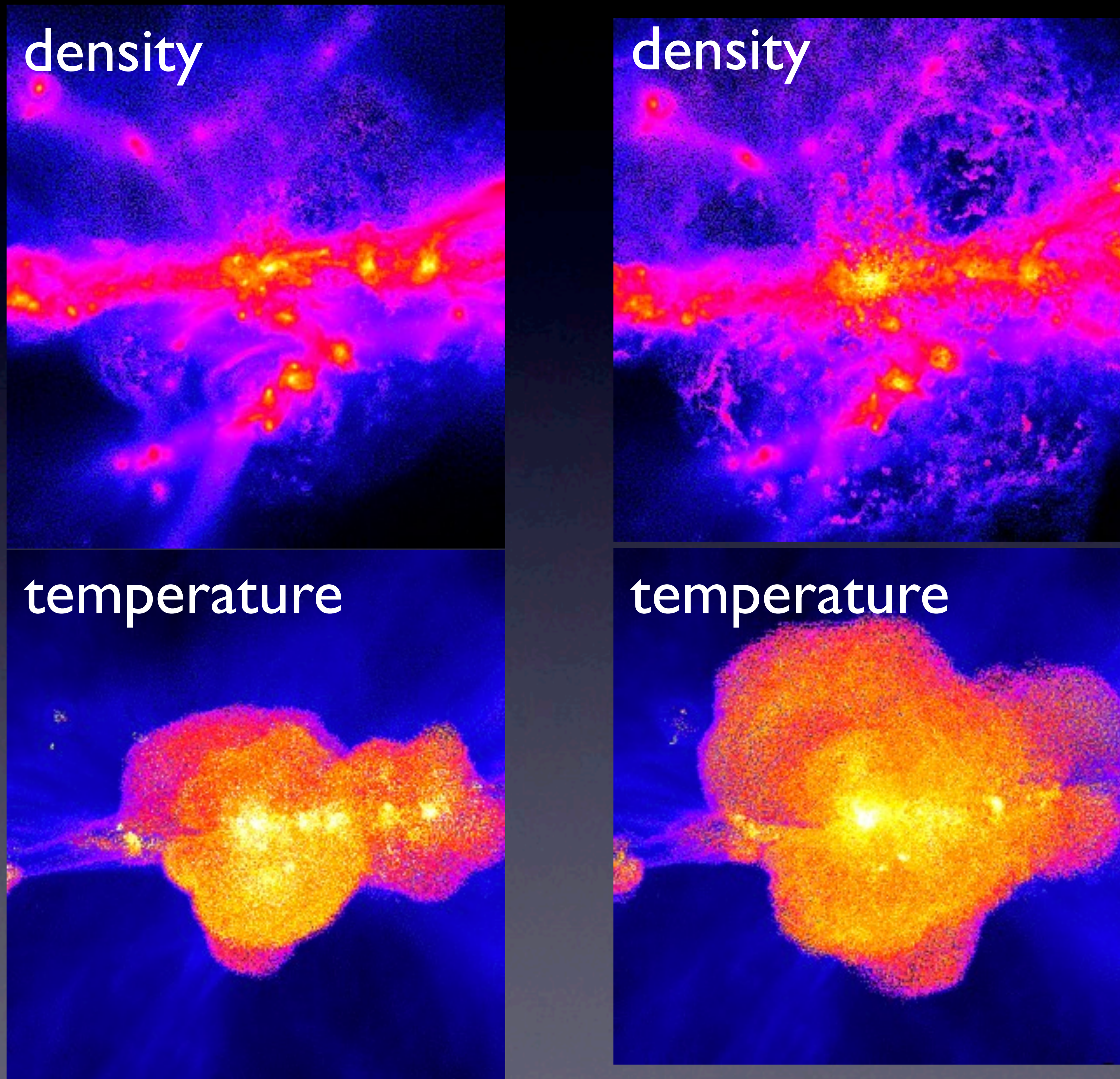

Smagorinsky Model of Turbulent Diffusion

Wadsley+ (2008); Shen+(2010)

- Most basic turbulent model: (κ_{Turb} has units of velocity × length)

$$\frac{\partial \bar{u}}{\partial t} + \bar{\mathrm{v}}.\nabla \bar{u} = -(\gamma - 1)\bar{u}(\nabla.\bar{\mathrm{v}}) + \nabla \kappa_{\mathrm{Turb}} \nabla \bar{u}$$

- Smagorinsky model (Mon. Weather Review 1963) -- Diffusion Coefficient determined by velocity Shear

$$\kappa_{Turb} = l_S{}^2 S, \;\; S = \sqrt{S_{ij} S_{ij}}$$

- S_{ij} = trace-free strain rate of resolved flow; l_s = Smagorinsky length. For incompressible grid models $l_s^2 \sim 0.02\ \Delta x^2$

- For SPH we use $\kappa_{Turb} = C\ |S_{ij}| h^2$ with $C \sim 0.05$ (Wadsley, Veeravalli & Couchman 2008; See also Scannapieco & Brüggen 2008, Grief et al 2009)

- After implementation of turbulent diffusion, SPH is able to produce the entropy profile similar to grid codes

The Effect of Metal and Thermal Diffusion - I

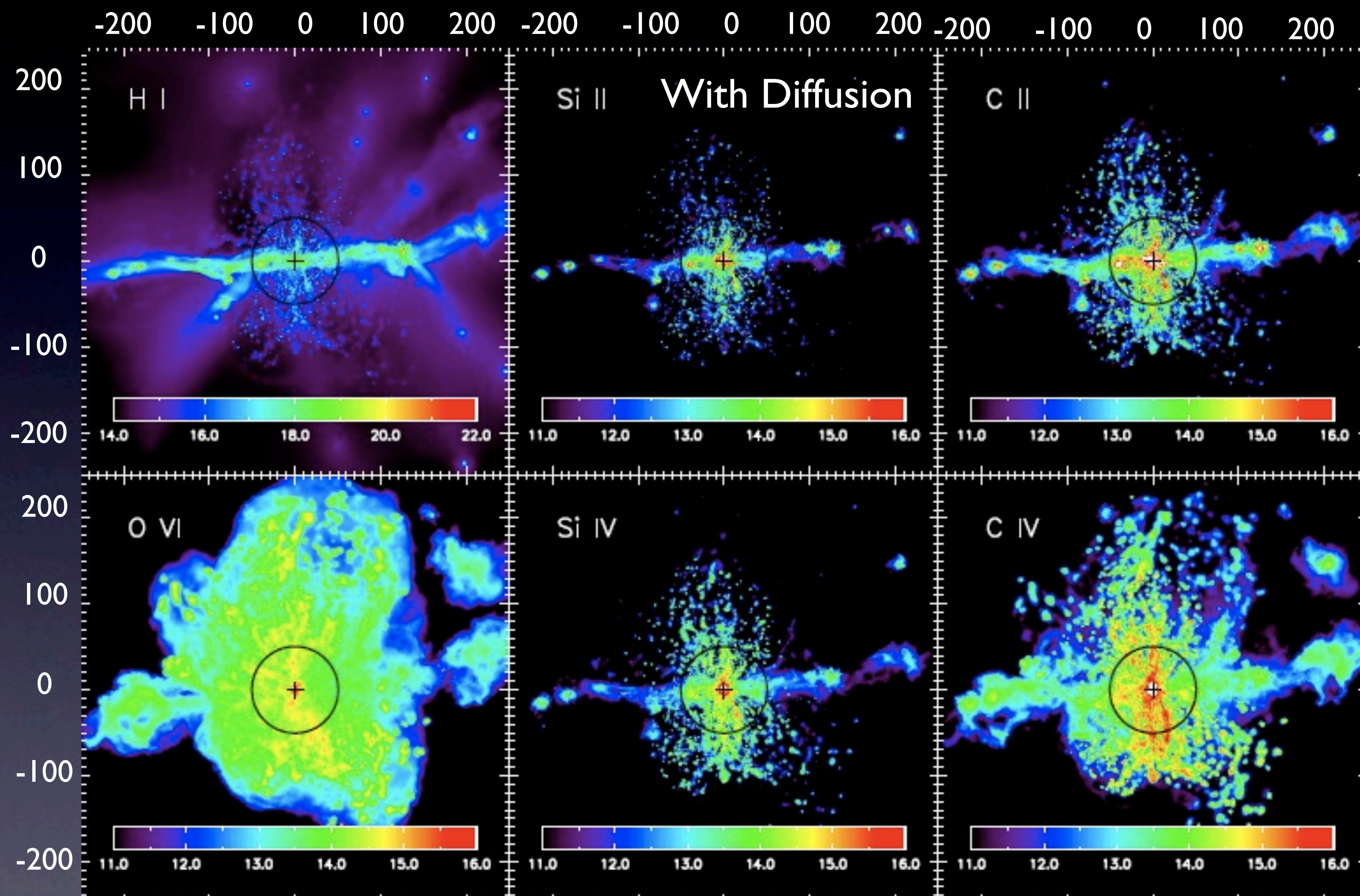

No turbulent mixing 1. Larger metal bubble (cf. Shen+ 2010);
2. "Clumpier" CGM due to higher Z and metal cooling;
3. Inflowing dwarfs are enriched, but less for the material in between

The Effect of Metal and Thermal Diffusion - I

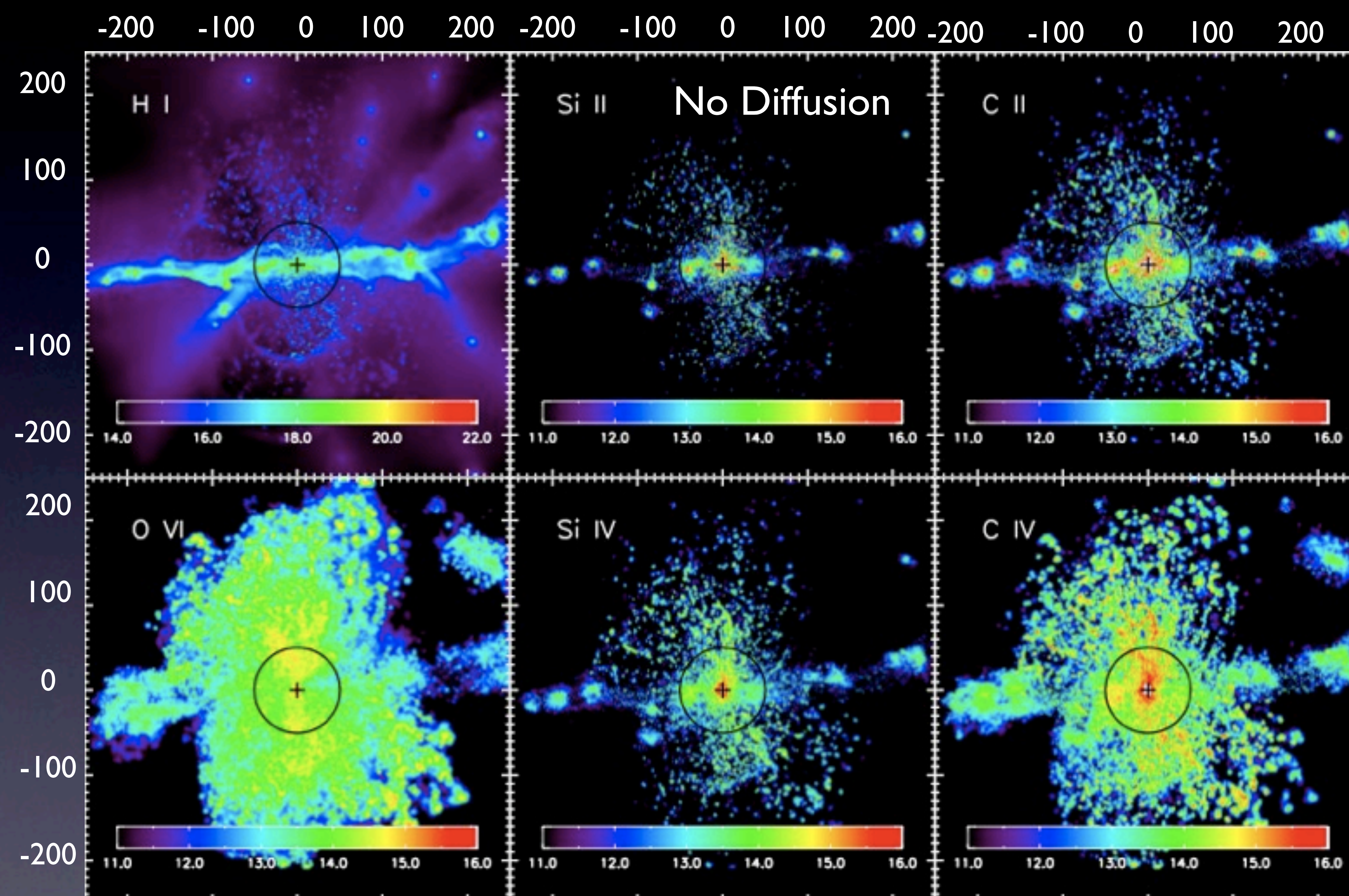

No turbulent mixing 1. Larger metal bubble (cf. Shen+ 2010);

2. "Clumpier" CGM due to higher Z and metal cooling;

3. Inflowing dwarfs are enriched, but less for the material in between

The Effect of Metal and Thermal Diffusion - II

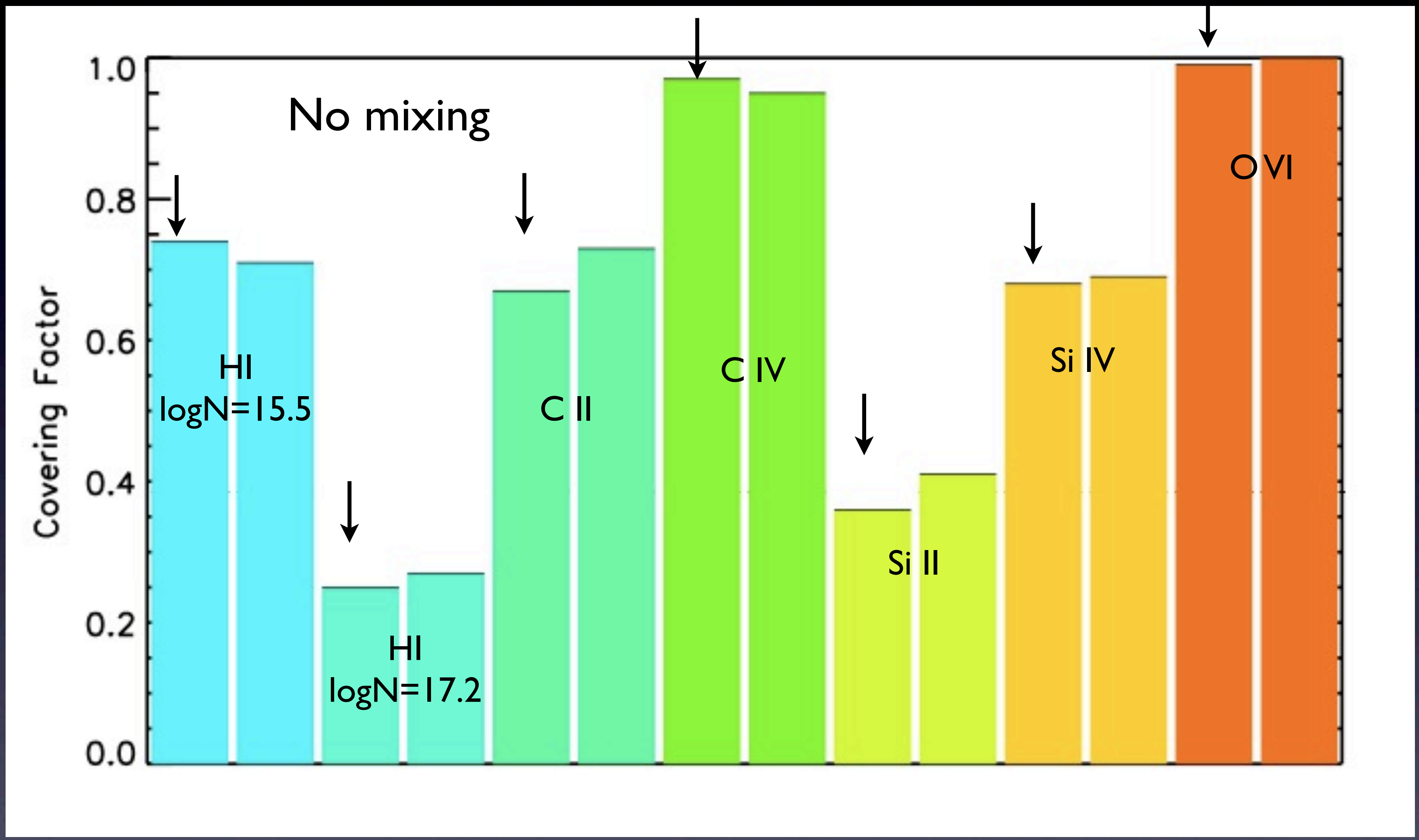

- The covering factor of metal ions at log N > 13 does not change significantly
- The covering factor of LLS H I, C II and Si II decreases because the CGM is clumpier
- Cf for more diffuse H I and C IV increases because of more efficient wind

The Effect of Metal and Thermal Diffusion III

With Metal Diffusion | No Metal Diffusion

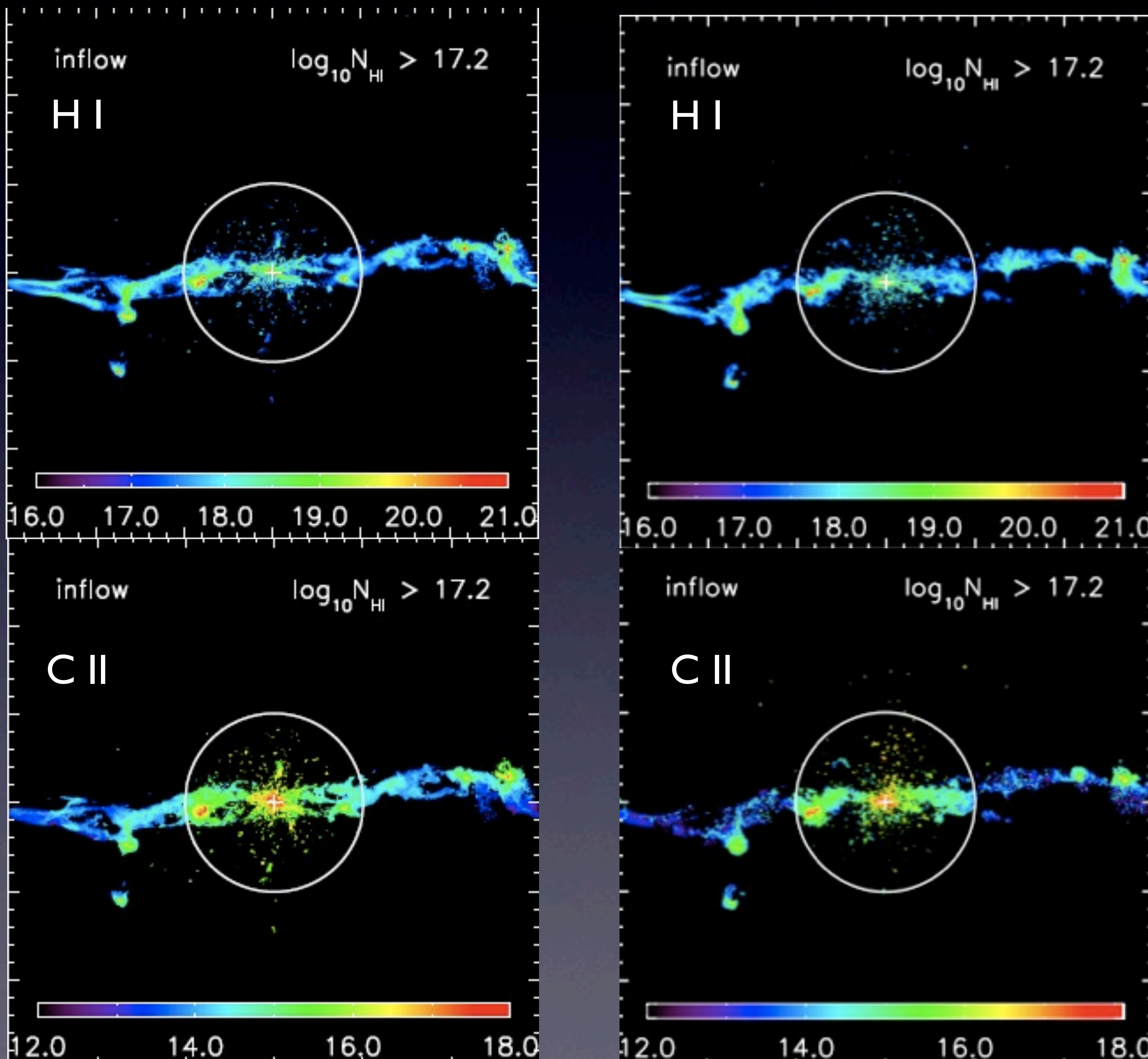

- Covering factor of both H I and low ions decreases
- Inflowing gas with $N_{HI} > 10^{17.2}$ cm^{-2} and $N_{CII} > 10^{13}$ cm-2 decreases from 22% to 16% in R_{vir} and from 10% to 5% in $2R_{vir}$

SPH & KH Instability

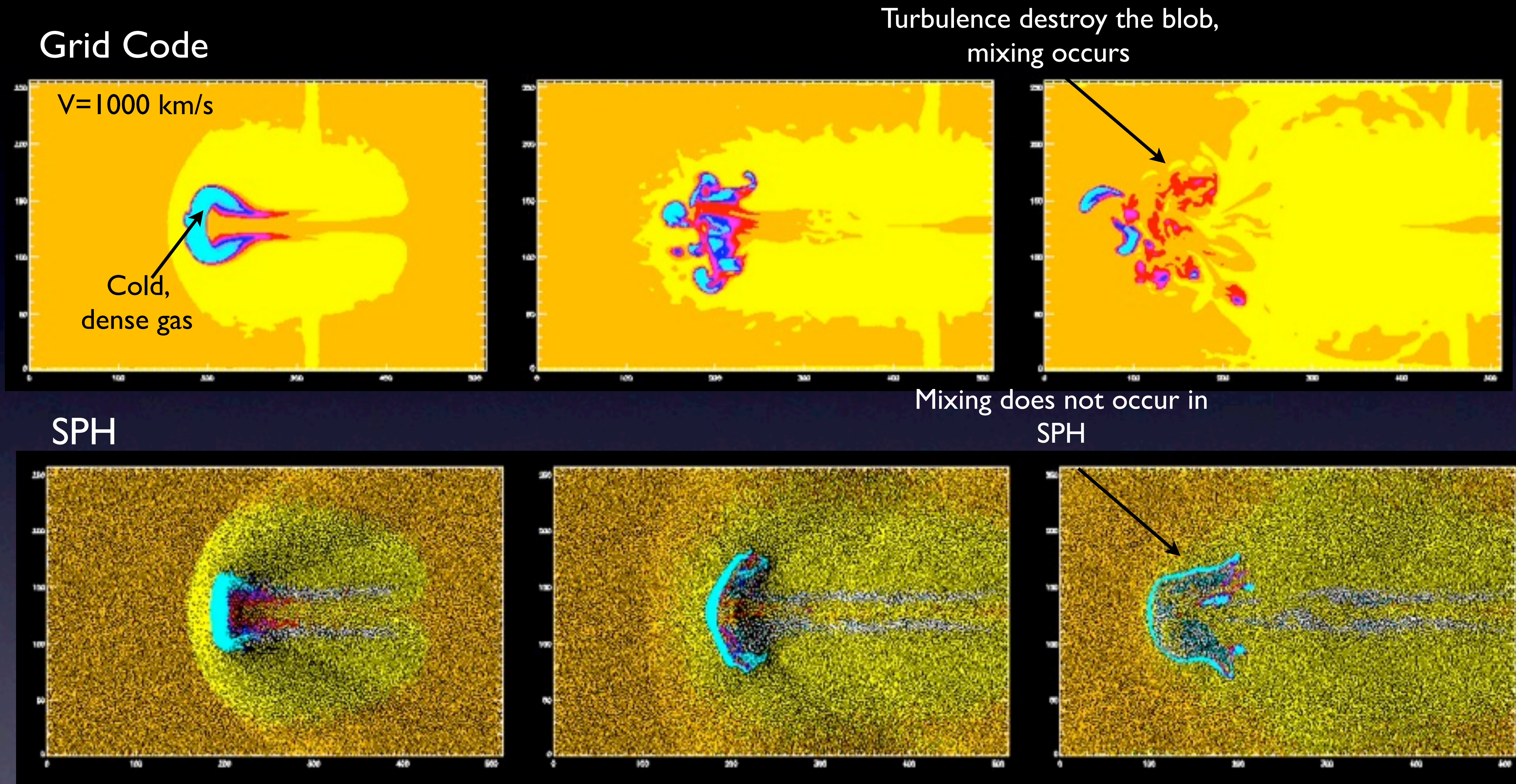

- Galactic outflows entrain cold ISM and metals when ejected to CGM (e.g., Veilleux 2005). Shearing between the outflow & surrounding gas induce KH instability and mixing (Klein+ 1994; Hartquist+ 1997; Williams & Dyson 2002)
- SPH conserves entropy along the streamline, mixing does not occur

SPH & KH Instability

Wadsley+ in prep.

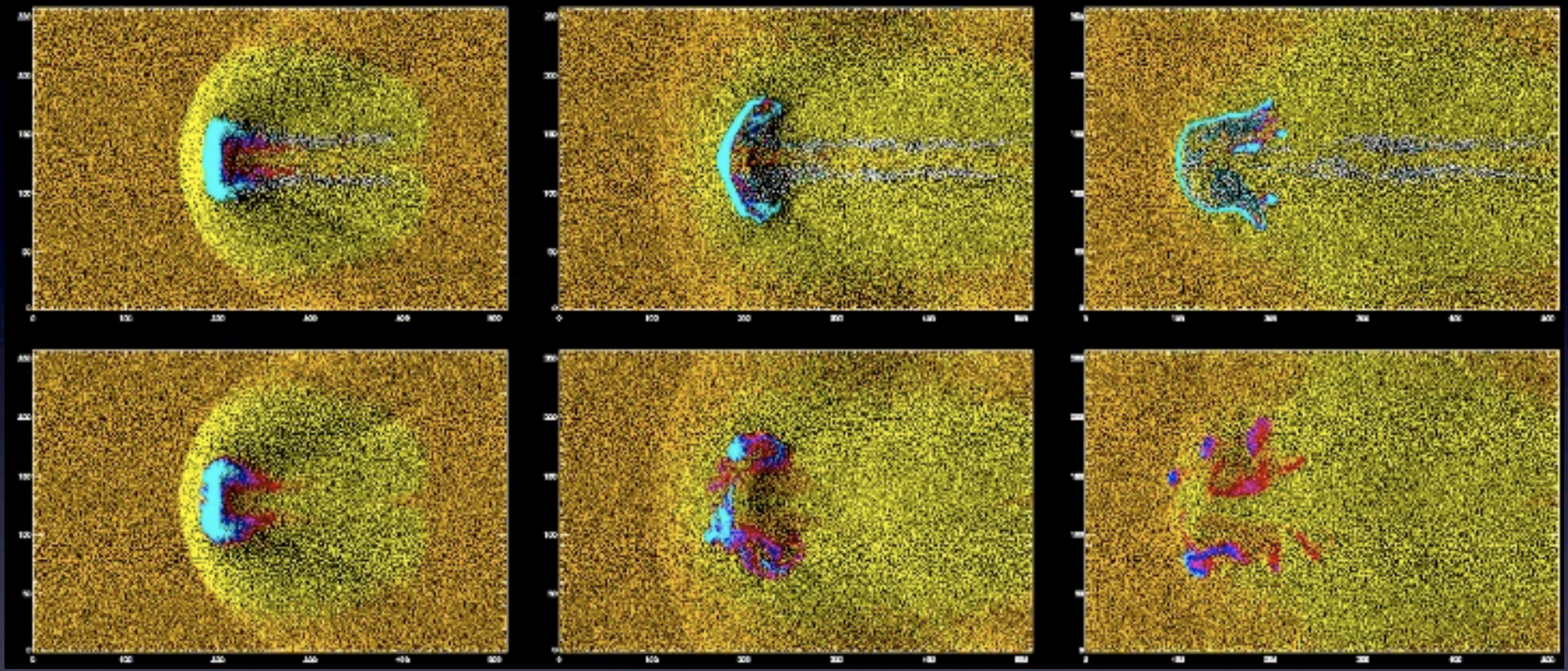

Old SPH

New SPH

Where are the metals?

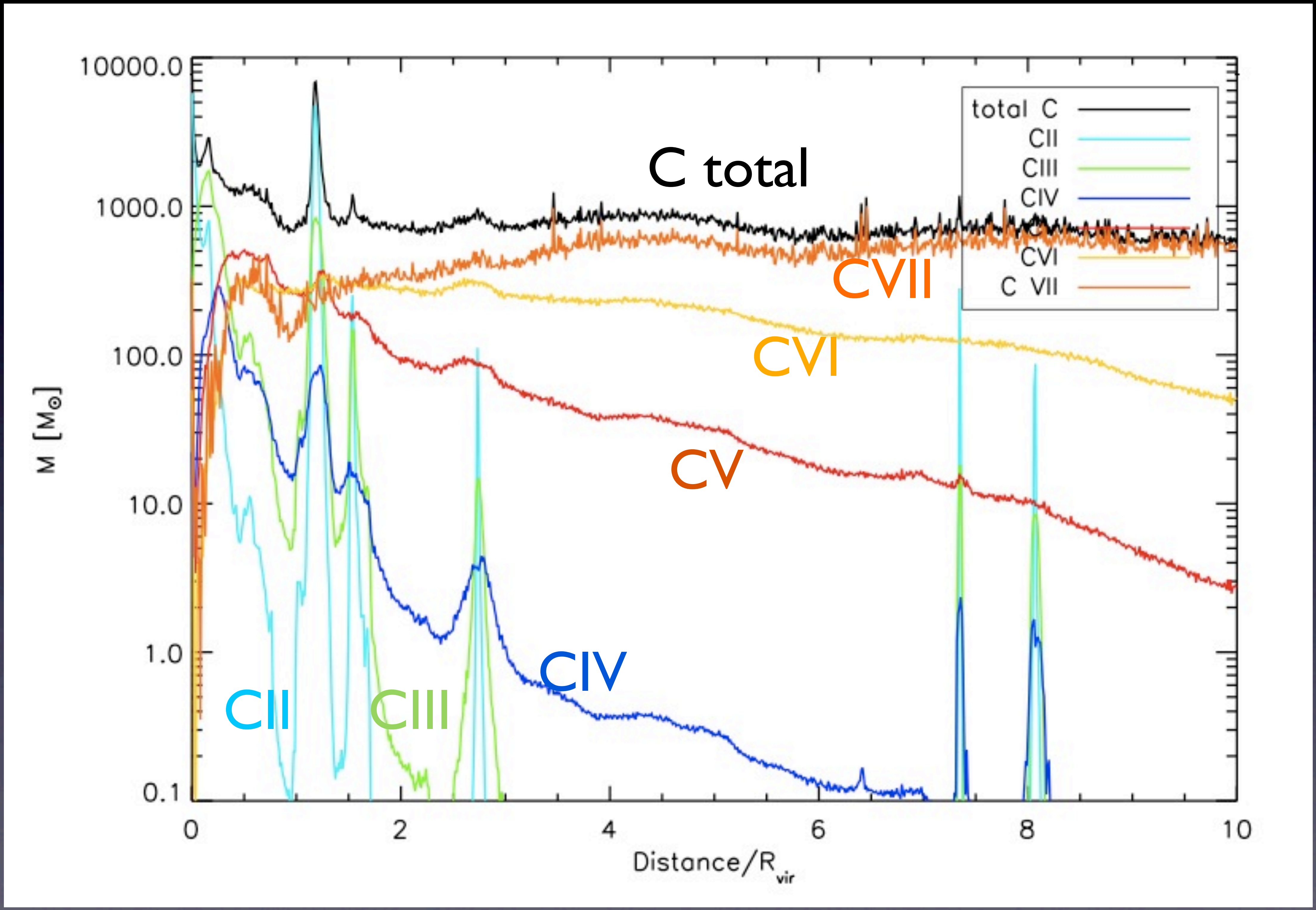

Distribution of Metals and Ions in ρ-T plane

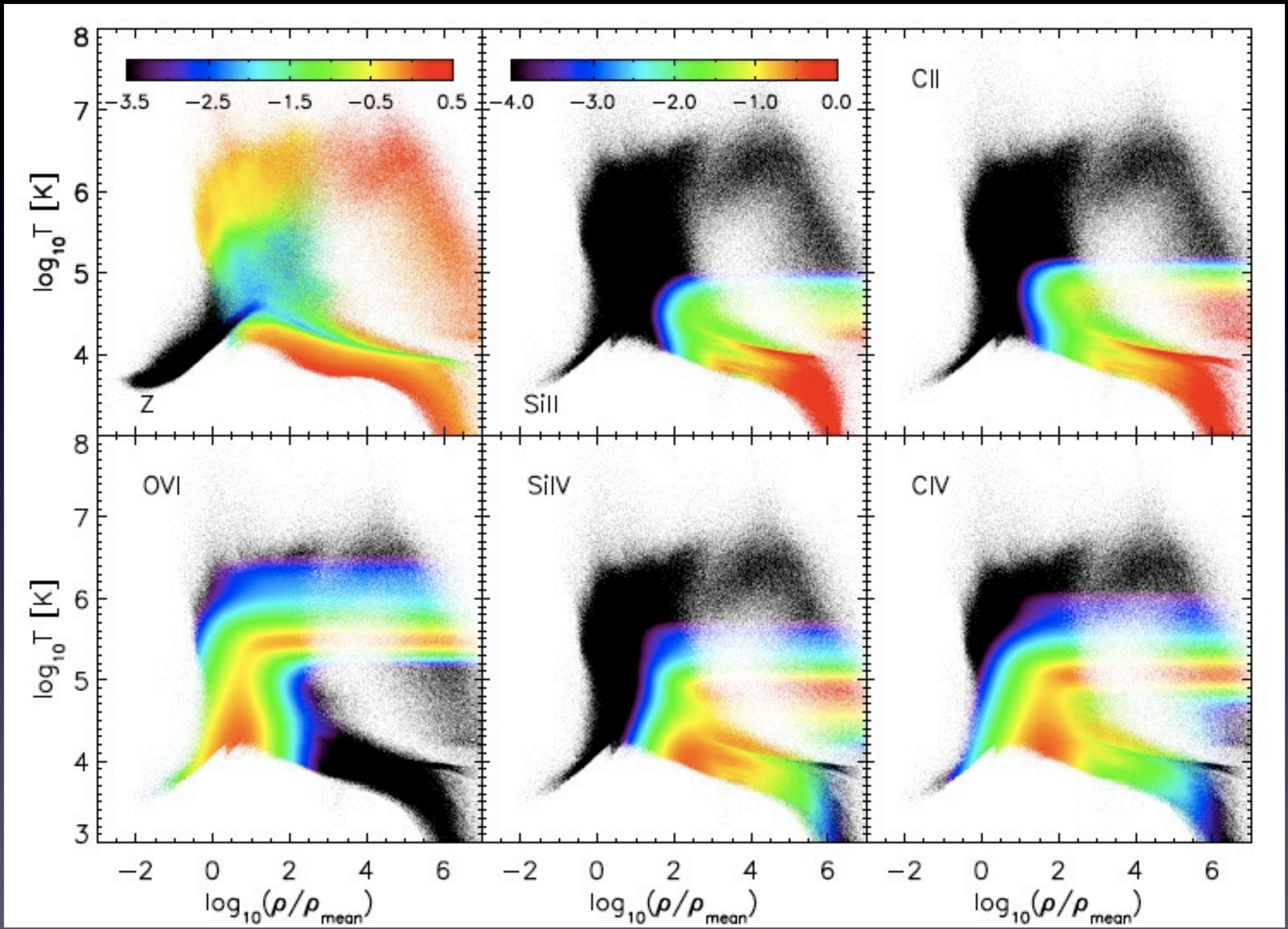

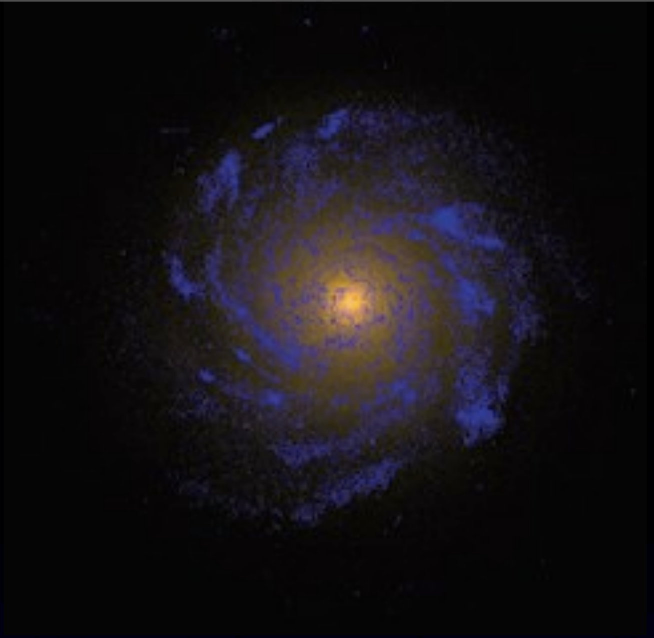

The Simulations

- TreeSPH code Gasoline (Wadsley et al. 2004)
- SF: $d\rho_*/dt = \varepsilon_{SF}\rho_{gas}/t_{dyn} \propto \rho_{gas}^{1.5}$ when gas has $n_H > n_{SF}$
- Blastwave feedback model for SN II (Stinson+ 2006): radiative cooling turned-off according to analytical solution from McKee & Ostriker (1977).
- Radiative cooling for H, He and metals: metal cooling computed using Cloudy (Ferland+ 1998), assuming ionization equilibrium under uniform UVB (Haardt & Madau 2012)
- Turbulent diffusion model for thermal energy, and metals (Wadsley+ 2008; Shen +2010) .

Galaxy	m_{DM} (Msun)	m_{SPH} (Msun)	ε_G (pc)	n_{SF} (cm^{-3})
Eris2 (Eris2h)	9.8×10^4	2×10^4	120	20.0
Dwarf	1.6×10^4	3.3×10^3	86	100.0

Why High Resolution?

- Resolve the clumpy SF behavior
- Allow gas density start to be able to form H_2

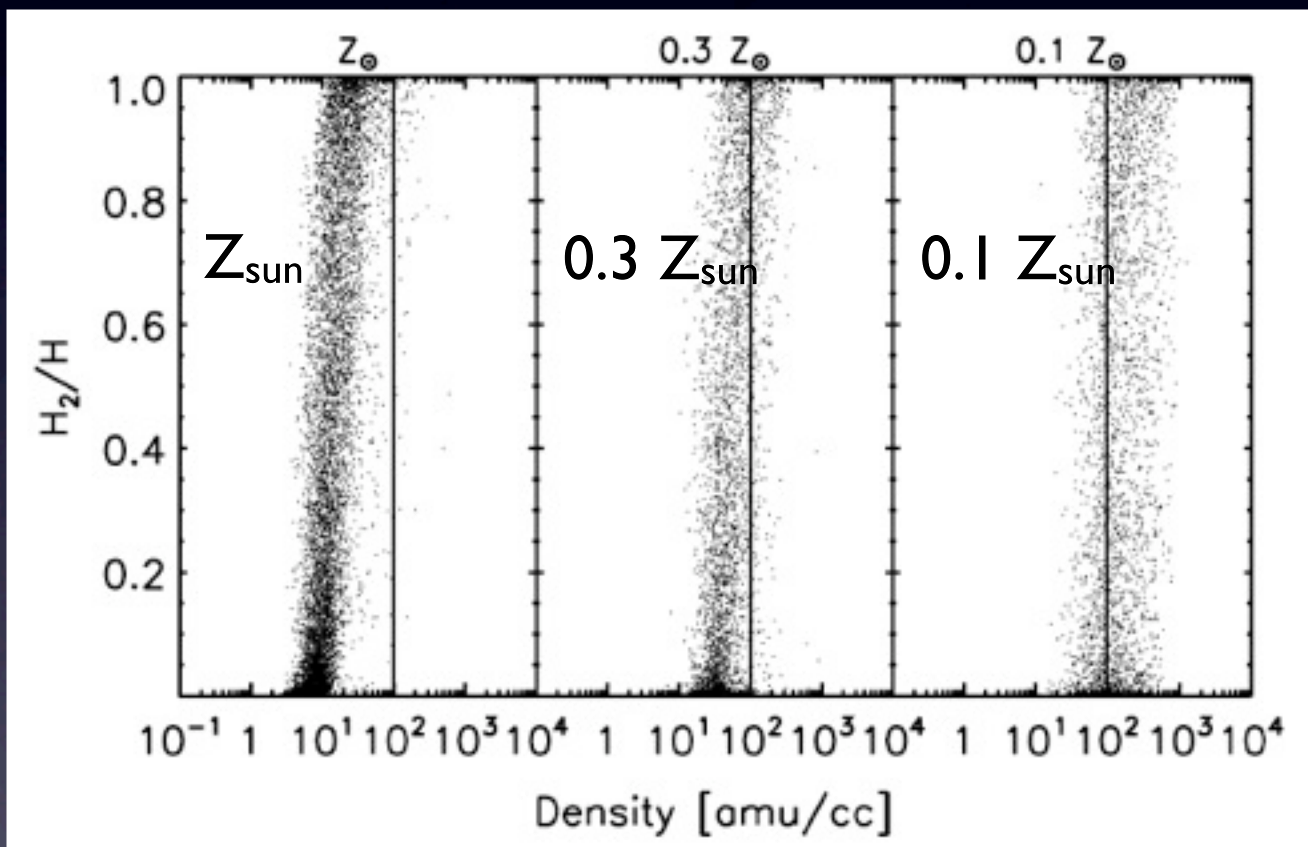

- Full model of gas phase and dust grain H2 formation with radiative transfer approximation (Christensen+ 2012).
- Similar behavior in analytical model from Krumholz+ 2009

- The blastwave model is NOT resolution independent; works better when gas more like the ISM
  - SN feedback (Stinson+2006): Based on explicit blastwave model of Chevalier (1974) and McKee & Ostriker (1977)
    - Hot, low density shell surviving time -- cooling shutoff time:

$$t_{\max} = 10^{6.85} E_{51}^{0.32} n_0^{0.34} P_{04}^{-0.7} yr$$

    - Maximum radius of a SN blastwave -- energy and metal distribution radius:

$$R_E = 10^{1.74} E_{51}^{0.32} n_0^{-0.16} P_{04}^{-0.20} pc$$

The Eris Simulation

Guedes+2011

- Eris has structural properties, mass budget and scaling relations all consistent with observations.

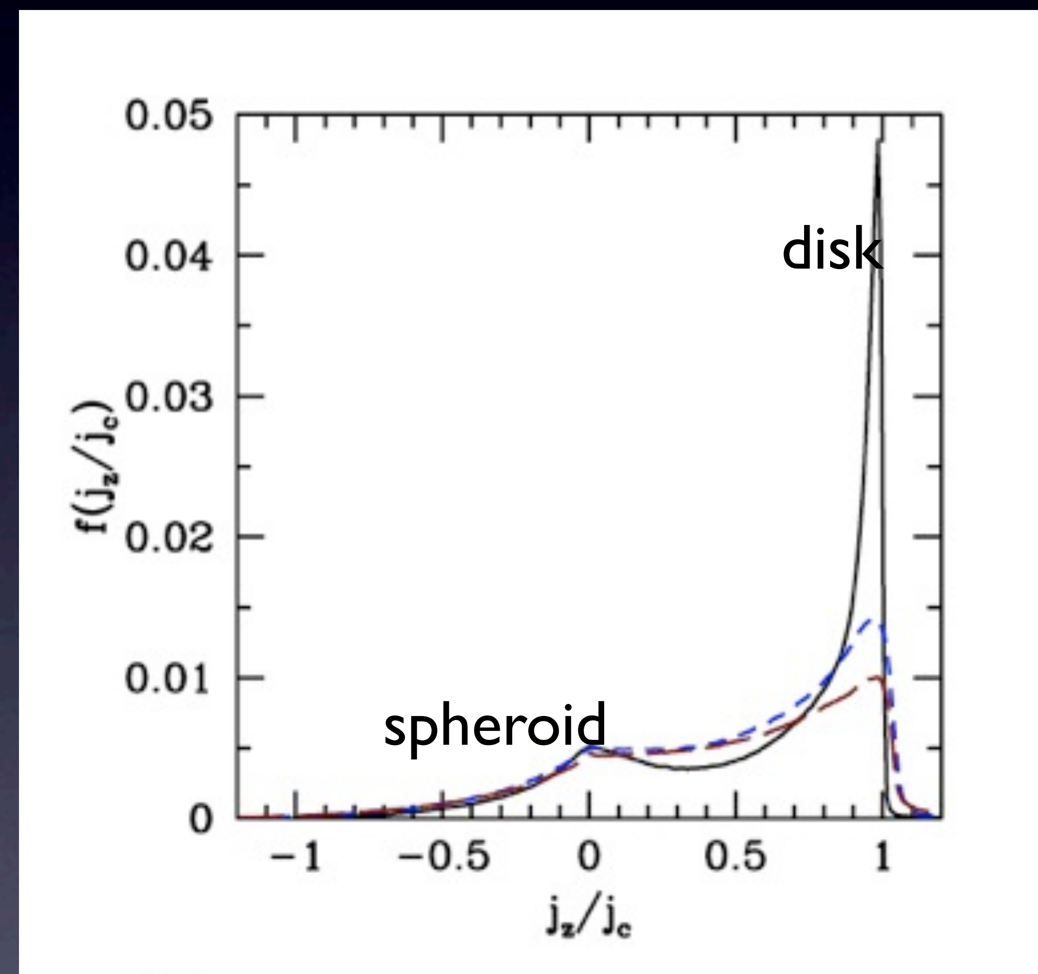

	M_{vir} [$10^{12}M_{sun}$]	V_{sun} [km/s]	M^* [$10^{10}M_{sun}$]	f_b	B/D	R_d [kpc]	M_i	SFR [M_{sun} yr^{-1}]
Eris	0.79	206	3.9	0.12	0.35	2.5	-21.7	1.1
MW	1±0.2	221±18	4.9-5.5	?	0.33	2.3±0.6	?	0.68-1.45

The Eris Simulation

Guedes+2011

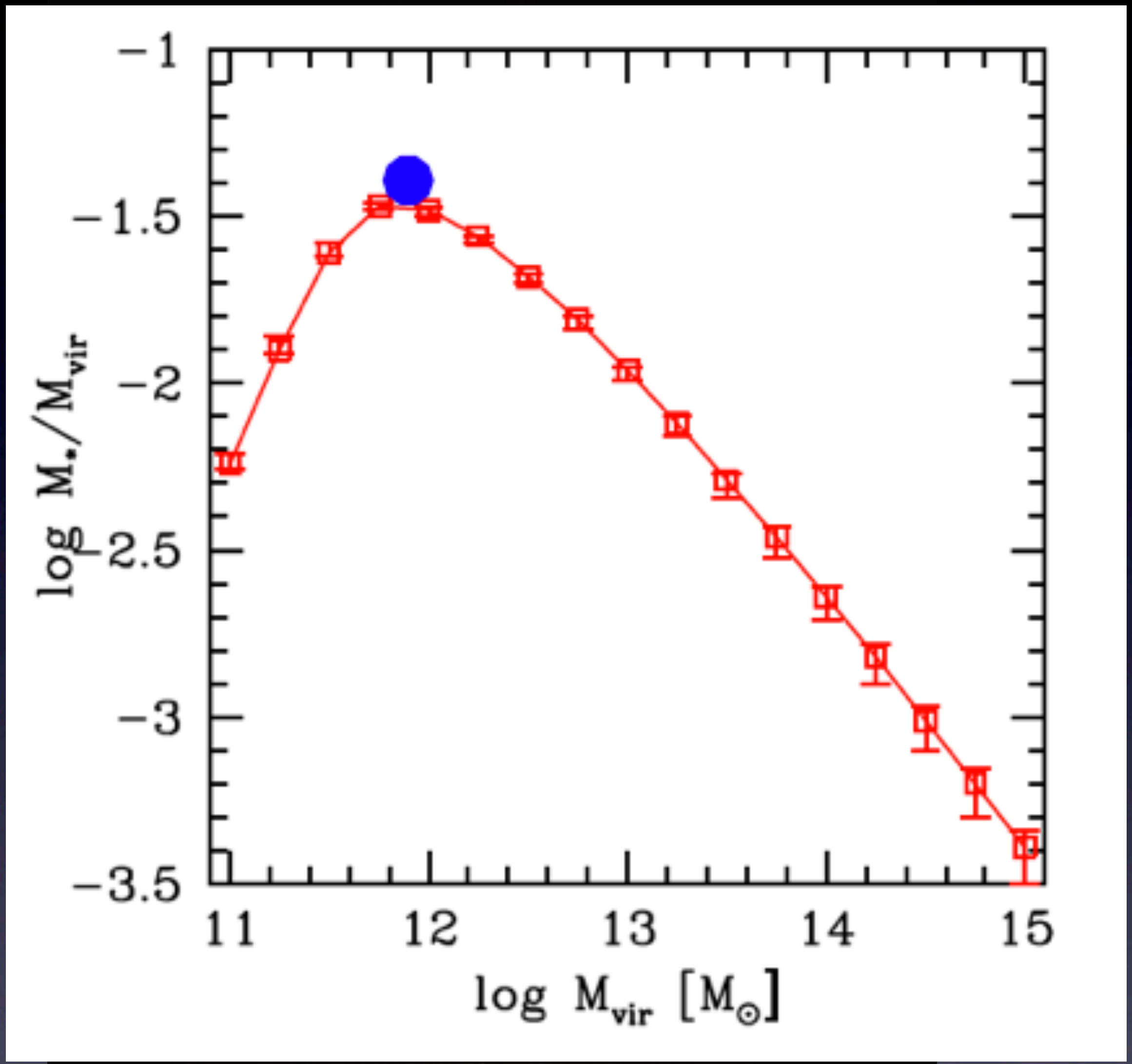

Observations from Behroozi et al. (2010)

- Eris has structural properties, mass budget and scaling relations all consistent with observations.

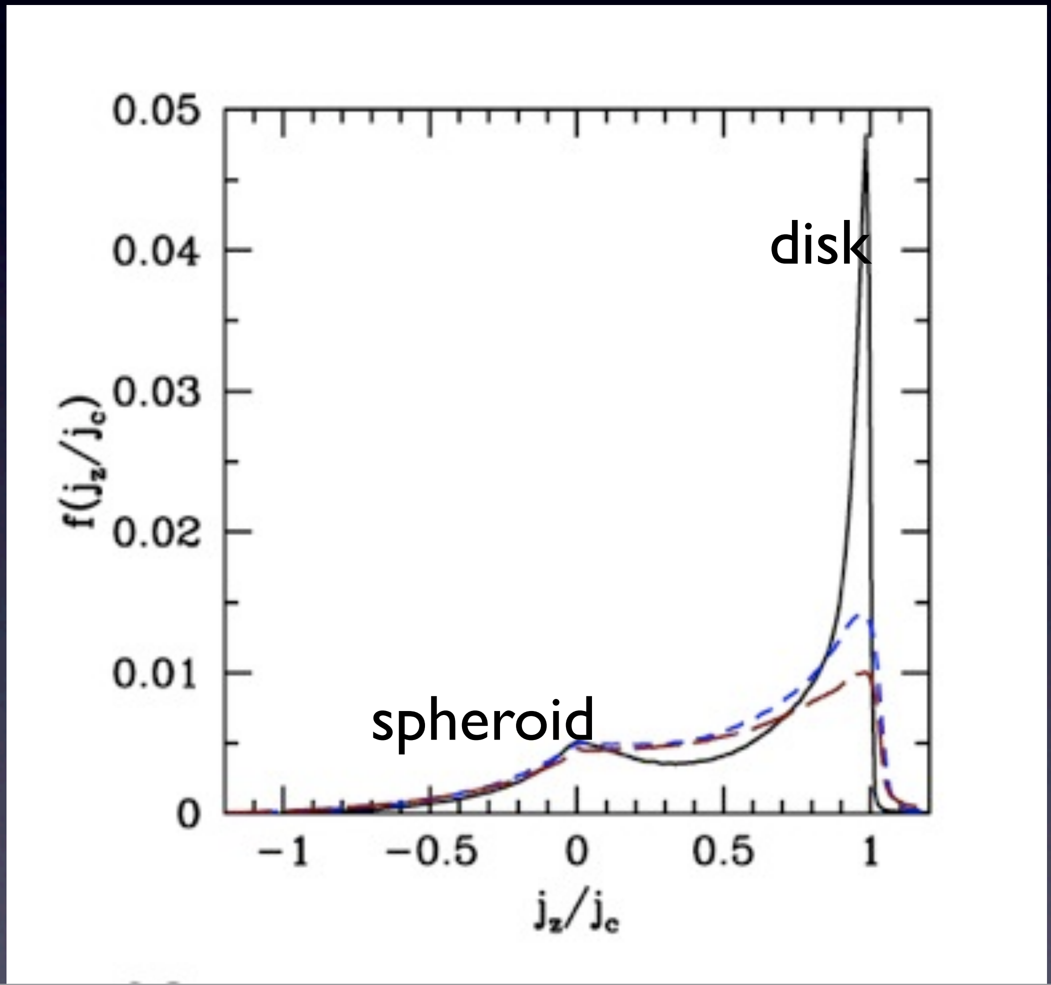

	M_{vir} [$10^{12}M_{sun}$]	V_{sun} [km/s]	M* [$10^{10}M_{sun}$]	f_b	B/D	R_d [kpc]	M_i	SFR [M_{sun} yr^{-1}]
Eris	0.79	206	3.9	0.12	0.35	2.5	-21.7	1.1
MW	1±0.2	221±18	4.9-5.5	?	0.33	2.3±0.6	?	0.68-1.45

The Eris2 and Eris2h Simulations

Eris2:

1) Incorporate metal cooling at $T > 10^4$ K (Shen+2010)
2) updated IMF (Kroupa+ 2001)
3) updated UV background (Haardt & Madau 2012)
4) allow metal to mix according to a turbulent diffusion model (Wadsley+2008; Shen+10)
5) higher SF threshold n_{th} = 20 atoms/cm^3 instead of 5 atoms/cm^3

Eris2h: increase eSN from 0.8 to 1.0

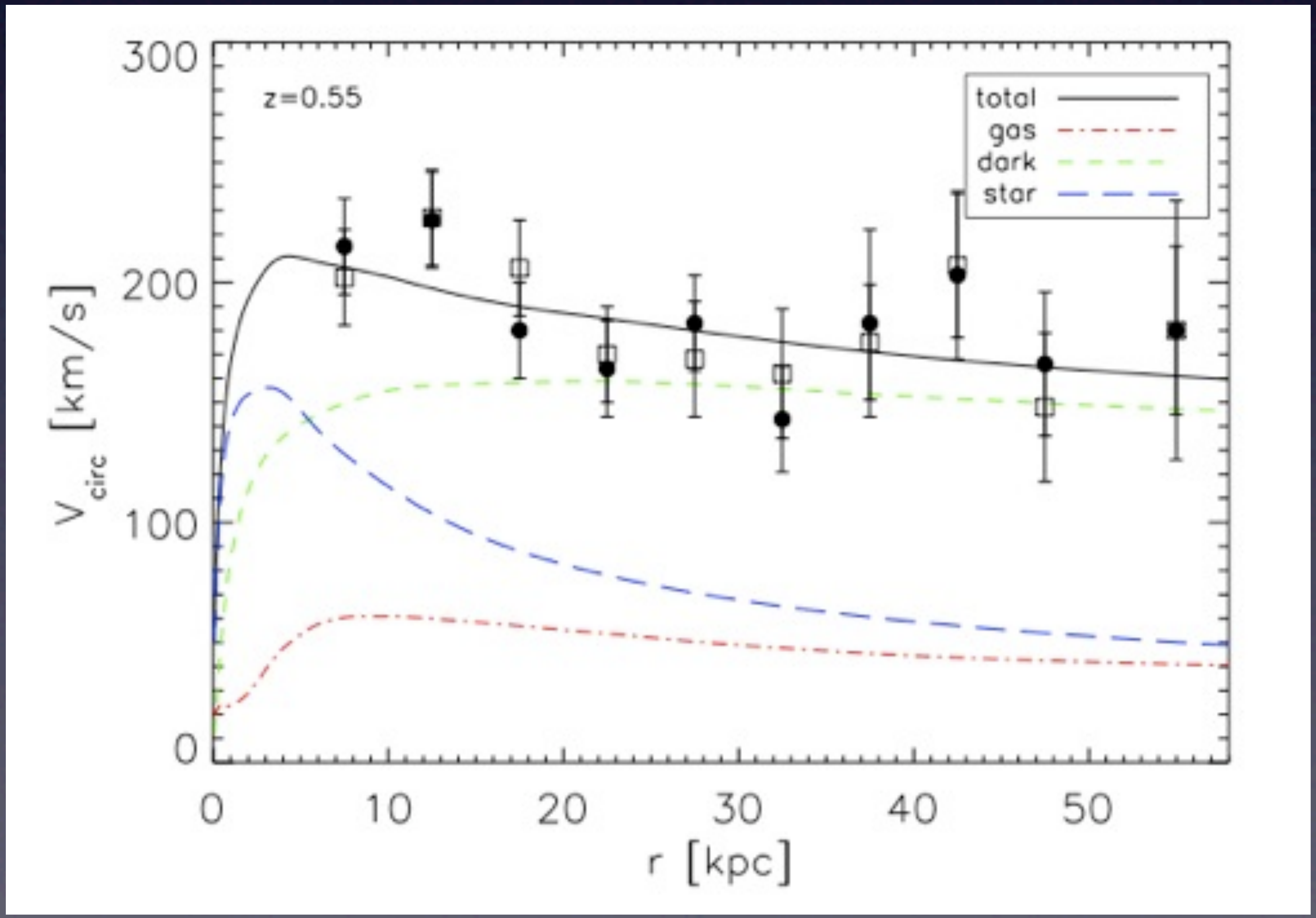

Stellar Mass - Halo mass relation follows the values predicted by abundance matching (Moster+ 2012, Behroozi+2012)